Simulated Influence of Electric Vehicles on Traffic Flow and Analysis of Energy Consumption Using the Example of the City of Duisburg

Von der Fakultät für Ingenieurwissenschaften, Abteilung Maschinenbau und Verfahrenstechnik der

Universität Duisburg-Essen

zur Erlangung des akademischen Grades

eines

Doktors der Ingenieurwissenschaften

Dr.-Ing.

genehmigte Dissertation

von

Xiaowei Hu
aus
Baotou, China

1. Gutachter: Prof. Dr.-Ing Dr. h.c. Dieter Schramm
2. Gutachter: Prof. Dr.-Ing Jian Zhao
Tag der mündlichen Prüfung: 23.02.2020
Tag der Einreichung: 12.01.2021

Abstract

Vehicles offer people many conveniences, but at the same time cause considerable problems, for example for the environment. Today, the electrification of the automobile is considered the best way to solve at least a large part of the environmental problems caused by motor vehicles. Apart from the fact that an electric powertrain produces no local emissions, it also differs from a conventional fossil-fuel powertrain in its propulsion dynamics. It is therefore also to be expected that electric vehicles will influence the flow of traffic due to their different dynamic properties. This thesis focuses on using microscopic traffic simulation to provide a first estimation of how the electrification of vehicles could change the traffic flow and to what extent different traffic situations would influence the fuel and energy consumption of vehicles.

In most microscopic traffic flow models, drivers and vehicles are modeled together by a combined model in one simulation object. By adjusting some parameter values, different combinations of driver and vehicle can be roughly distinguished. The values are determined on the basis of observational data of the traffic flow. However, the currently still small share of electric vehicles in road traffic and the fact that they look little different from combustion engine driven and hybrid vehicles make it difficult to collect data from electric vehicles in traffic flow, unless the data is collected in fleet tests. In this thesis, drivers and vehicles were modeled separately. The focus of this thesis is on the assessment of the influence of vehicle propulsion on traffic flow. Therefore, the model developed in this thesis was based on the physical capabilities of both the fossil-fuel powered and the electric powered vehicles. The driver model, which was also required, was created on the basis of data of human drivers, which were determined in an accompanying investigation of a driving simulator. Driver and vehicle model were combined again in the microscopic traffic simulation to a car-following model.

For observing the impact of electric vehicles on traffic flow and estimating energy consumption of vehicles, a traffic scenario of a part of the City of Duisburg was established. The effect of electric vehicles on traffic flow, as well as the effect of traffic density on fuel and energy consumption was studied based on this scenario.

The simulation results indicate that electric vehicles could raise the average speed of traffic flow to a certain degree, when traffic load and driving styles of the drivers remain the same. The increase of the share of electric vehicles has a positive effect on traffic efficiency. In situations with higher traffic density, energy consumption of electric vehicles is far superior to that of vehicles with internal combustion engine powertrains.

Kurzfassung

Kraftfahrzeuge bieten den Menschen viele Annehmlichkeiten, verursachen gleichzeitig aber auch erhebliche Probleme, zum Beispiel für Umwelt. Heute gilt die Elektrifizierung des Automobils als der beste Weg, zumindest einen Großteil der durch Kraftfahrzeuge verursachten Umweltprobleme zu vermeiden. Abgesehen davon, dass ein elektrischer Antriebsstrang keine lokalen Emissionen erzeugt, unterscheidet er sich von einem konventionellen Fossil-Kraftstoff-Antriebsstrang auch in seiner Antriebsdynamik. Es ist daher auch zu vermuten, dass Elektrofahrzeuge durch ihre abweichenden dynamischen Eigenschaften den Verkehrsfluss beeinflussen. Diese Arbeit konzentriert sich darauf, mit Hilfe mikroskopischer Verkehrssimulation eine erste Abschätzung abzugeben, wie die Elektrifizierung von Fahrzeugen den Verkehrsfluss verändern würde und in welchem Maße unterschiedliche Verkehrssituationen den Kraftstoff- und Energieverbrauch von Fahrzeugen mit beeinflussen.

In den meisten mikroskopischen Verkehrsflussmodellen werden Fahrer und Fahrzeug zusammengefasst und gemeinsam durch ein kombiniertes Modell in einer Einheit beschrieben. Durch Anpassung einiger Parameterwerte können so verschiedene Kombinationen von Fahrer und Fahrzeug grob unterschieden werden. Die Werte werden auf der Grundlage von Beobachtungsdaten des Verkehrsflusses bestimmt. Der derzeit noch geringe Anteil von Elektrofahrzeugen im Straßenverkehr und die Tatsache, dass sie sich äußerlich wenig von verbrennungsmotorisch angetriebenen und Hybridfahrzeugen unterscheiden, erschweren jedoch die Erfassung von Daten von Elektrofahrzeugen im Verkehrsfluss, es sei denn, die Daten werden in Flottenversuchen erhoben. In dieser Arbeit wurden Fahrer und Fahrzeuge getrennt modelliert. Der Fokus dieser Arbeit liegt auf der Beurteilung des Einflusses des Fahrzeugantriebs auf den Verkehrsfluss. Daher basierte das in der Arbeit entwickelte Modell auf den physischen Fähigkeiten sowohl konventioneller als auch elektrisch angetriebener Fahrzeuge. Das ebenfalls benötigte Fahrermodell wurde auf der Grundlage von Daten menschlicher Fahrer, die in einer begleitenden Untersuchung einem Fahrsimulator ermittelt wurden, erstellt. Fahrer- und Fahrzeugmodell wurden in der mikroskopischen Verkehrssimulation wieder zu einem Fahrzeugfolgemodell kombiniert.

Um die Auswirkung von Elektrofahrzeugen auf den Verkehrsfluss zu beobachten, wurde ein Verkehrsszenario eines Teils der Stadt Duisburg erstellt. Anhand dieses Szenarios wurden die Auswirkungen von Elektrofahrzeugen auf den Verkehrsfluss sowie die Auswirkungen der Verkehrsdichte auf den Kraftstoff- und Energieverbrauch untersucht.

Die Simulationsergebnisse zeigen, dass Elektrofahrzeuge die durchschnittliche Geschwindigkeit des Verkehrsflusses bis zu einem gewissen Grad erhöhen können, wenn der Verkehrsfluss und die Fahrstile des Fahrers gleichzeitig gleichbleiben. Die Erhöhung des Anteils von Elektrofahrzeugen wirkt sich positiv auf die Verkehrseffizienz aus. In Situationen mit höherer Verkehrsdichte ist der Energieverbrauch von Elektrofahrzeugen dem herkömmlichen Fahrzeuge deutlich überlegen.

Contents

List of Figures

List of Tables

Notation

Formula Symbols

Latin Letters

Symbols	Unit	Meaning
A_f	m^2	Projected frontal area of vehicle
a	$\mathrm{m} \cdot \mathrm{s}^{-2}$	Acceleration of vehicle
a_{max}	$\mathrm{m} \cdot \mathrm{s}^{-2}$	Maximum acceleration of vehicle
a_{typ}	$\mathrm{m} \cdot \mathrm{s}^{-2}$	Typical acceleration of a vehicle type
b	$\mathrm{m} \cdot \mathrm{s}^{-2}$	Deceleration of vehicle
b_{max}	$\mathrm{m} \cdot \mathrm{s}^{-2}$	Maximum deceleration of vehicle
C_d	-	Drag coefficient
E_{100km}	$\mathrm{kWh} \cdot 100km^{-1}$	Energy consumption per 100km
E_{fuel}	J	Chemical energy of consumed fuel
E_{total}	kWh	Total energy consumption during a trip
F_{acc}	N	Acceleration force on vehicle
F_b	N	Brake force on vehicle
F_f	N	Total rolling resistance on vehicle
$F_{f,F}$	N	Rolling resistance on front wheels
$F_{f,R}$	N	Rolling resistance on rear wheels
F_{grav}	N	Component of gravity along road surface
F_T	N	Traction force on vehicle
F_W	N	Wind drag
f	-	Rolling resistance coefficient
G	m	Distance gap between two vehicles
$G_{desired}$	m	Desired following gap
G_{min}	m	Minimum following gap
g	$\mathrm{m} \cdot \mathrm{s}^{-2}$	Gravitational acceleration
I_{RP}	kg	Inertias of the rotating parts in vehicle
i	-	Simulation step index
i_D	-	Transmission ratio of differential
i_G	-	Transmission ratio of gearbox
L	m	Vehicle length

l	-	Index of leading vehicle
m	kg	Mass of vehicle
n	-	Total steps of simulation
n_{motor}	rpm	Rotation speed of engine or motor
n_{wheel}	rpm	Rotation speed of wheel
$P_{at\ wheel}$	W	Power at wheels
P_{engine}	W	Output power of internal combustion engine
P_{max}	W	Maximal power of internal combustion engine
$P_{resistance}$	W	Power of driving resistances
q_{fuel}	$\mathrm{J \cdot kg^{-1}}$	Fuel calorific value
r_{dyn}	m	Dynamic radius of wheel
s	m	Moving distance of vehicle
$\dot{s}$	$\mathrm{m \cdot s^{-1}}$	Velocity of vehicle
$\ddot{s}$	$\mathrm{m \cdot s^{-1}}$	Acceleration of vehicle
T	s	Time step of simulation
T_{brake}	$\mathrm{N \cdot m}$	Braking torque of braking system
T_m	$\mathrm{N \cdot m}$	Torque of engine or motor
t	s	Simulation time
V_{100km}	$\mathrm{l} \cdot 100km^{-1}$	Fuel consumption per 100km
V_{fuel}	l	Volume of consumed fuel
V_{idling}	l	Idling fuel consumption in time T
v	$\mathrm{m \cdot s^{-1}}$	Velocity of vehicle
$\dot{v}$	$\mathrm{m \cdot s^{-1}}$	Acceleration of vehicle
Δv	$\mathrm{m \cdot s^{-1}}$	Speed difference between ego car and leading car
$v_{desired}$	$\mathrm{m \cdot s^{-1}}$	Desired speed of driver
$v_{difference}$	$\mathrm{m \cdot s^{-1}}$	Difference of desired speed minus current speed
v_{limit}	$\mathrm{m \cdot s^{-1}}$	Speed limit of road
v_{opt}	$\mathrm{m \cdot s^{-1}}$	Optimal speed
v_{safe}	$\mathrm{m \cdot s^{-1}}$	Safe speed in accident-free car-following model
$W_{at\ wheel}$	J	Energy at wheels
W_{output}	J	Discharged energy from battery
$W_{recycle}$	J	Charged energy into battery from regenerative braking
$W_{resistance}$	J	Work of driving resistances
x	m	Vehicle location on the road

Greek Letters

Symbols	Unit	Meaning
α	-	Index of driver-vehicle unit
δ	-	Acceleration exponent
ϵ	-	Noise amplitude
η_{charge}	-	Charging efficiency of battery when charging from electric grid
η_D	-	Mechanical transmission efficiency of differential
$\eta_{discharge}$	-	Discharging efficiency of battery
η_{engine}	-	Energy conversion efficiency of internal combustion engine
η_G	-	Mechanical transmission efficiency of gearbox
η_{motor}	-	Energy conversion efficiency of electric motor
$\eta_{powertrain}$	-	Mechanical transmission efficiency of powertrain
$\eta_{recycle}$	-	Efficiency of battery when charging from regenerative braking
θ	°	Slop of road
λ	-	Coefficient of acceleration resistance
ξ	-	A random number in [0,1]
ρ_{air}	$\mathrm{kg \cdot m^{-3}}$	Density of air
ρ_{fuel}	$\mathrm{kg \cdot L^{-3}}$	Density of fuel
τ	s	Reaction time of driver

Abbreviations

Abbreviation	Meaning
3D	Three-dimensional
AC	Alternating Current
ACC	Adaptive Cruise Control
ADAC	German Automobile Club (Allgemeiner Deutscher Automobil- Club e.V.)
ADAS	Advanced Driver Assistance Systems
ADVISOR	NREL's ADvanced VehIcle SimulatOR
AI	Artificial Intelligence
API	Application Programming Interface
BEV	Battery Electric Vehicle
CNG	Compressed Natural Gas
DIL	Driver in Loop
DLR	German Aerospace Centre

	(Deutsche Zentrum für Luft- und Raumfahrt e.V.)
DOHC	Double Overhead Camshaft
EV	Electric Vehicle
FCEV	Fuel Cell Electric Vehicle
GUI	Graphical User Interface
HBEFA	Handbook Emission Factors for Road Transport
HEV	Hybrid Electric Vehicle
ICE	Internal Combustion Engine
ICEV	Internal Combustion Engine Vehicle
IDM	Intelligent Driver Model
MC	Motor & Controller
NCAP	New Car Assessment Programme
NEDC	New European Driving Cycle
OD-Matrix	Origin-Destination Matrix
OSM	Open Street Map
PHEV	Plug-in Hybrid Electric Vehicle
PM	Permanent Magnet Motor
rpm	Round per minute
SOC	State of Charge
SUMO	Simulation of Urban MObility
TCP	Transmission Control Protocol
TraCI	Traffic Control Interface
WBD	Wirtschaftsbetriebe Duisburg (German)
WLTP	World Harmonized Light-duty Vehicles Test Procedure
XML	Extensible Markup Language
ZAIK	Center for Applied Informatics Cologne

1 Motivation and Structure of the Thesis

In this Chapter the motivation and the targets for the scientific investigations of the work is described and its structure is presented.

1.1 Motivation

No matter in personal life, public transit, or transportation, vehicles have already been an important part of the modern society since more than one century. However, the rapidly increasing number of vehicles also causes many problems. Exhaust and noise pollution increasingly threaten people's health and well-being. The more and more frequent traffic congestions also reduce the comfort of our life.

For solving these problems, many technologies have been developed. The electrification of vehicle has been one of the research hotspots for a long time. In the automotive market there are also already several mature and reliable products. The electric vehicles (EVs) provide a clean and quiet driving experience. As more and more countries have announced their plan of banning fossil fuel vehicles (Burch and Gilchrist 2018), the electrification of automobiles is an inevitable development direction of automotive technology. Reducing the use of non-renewable fossil energy is only one of the advantages of electric vehicles (Schramm and Koppers 2013). Thanks to the more extensive operating range of electric motors, the transmission structure of electric vehicles is also greatly simplified. During the acceleration of a conventional internal combustion engine vehicle (ICEV), not only does the torque converter waste a lot of kinetic energy, but the shift process also creates a loss of efficiency and for manually shifted vehicles, causes even power interruption. However, an electric vehicle does not have a torque converter nor normally even a gearbox with more than one shift step. This means that EVs have better energy efficiency along with a better acceleration performance. This acceleration behavior difference between EV and ICEV appears not to be significant for the traffic on highways. But in urban traffic, where vehicles always drive in stop&go conditions, the acceleration performance of vehicles could play a much more important role. It is a reasonable inference that increased acceleration performance of all vehicles on the road would help improve traffic efficiency.

However, the electric vehicles still possess many disadvantages compared to the ICEVs. Because of the limited energy density of the battery, the travelling distance of EV is obviously shorter than that of an ICEV in the same vehicle class, especially in low temperature environments (Schramm et al. 2017a; Schüller 2019). The lack of charging stations, especially fast charging stations, also brings feelings of insecurity to the drivers of EV. When driving they always have to mind the remaining battery capacity. The electric vehicles indeed have brought some excellent experiences in many aspects. However, the comprehensive experience is still worse than an ICEV for most of consumers. These aspects hindered largely the popularization of electric vehicles. Therefore, although the governments of many countries have implemented lots of incentive policies, the overall proportion of electric vehicle is still insignificant. According to the annual report of car ownership published by Federal Motor Transport Authority of Germany, until 1st January 2019, there are only 83,175 electric passenger cars registered in Germany (Kraftfahrt-Bundesamt), less than 0.18% of all registered passenger cars. Although the electrification of vehicles has still a long way to go, it is inevitable that fossil fuel-powered vehicles will be replaced.

When electric vehicles will be the main composition of traffic flows someday and are quite different with the ICEVs, it is worth to discuss and predict how the traffic flows will be affected by the special properties of electric vehicles. Studying the differences of energy consumption characters between ICEV and EV is also obviously a meaningful work.

Traffic simulation is in many cases the right and only way to predict future traffic. Traffic simulation is a technology that has been well developed in recent years. The macroscopic traffic simulation has been a powerful tool for transportation planning and traffic prediction. However, macroscopic traffic simulation can also be considered as a compromise on computing power (Nagel and Schreckenberg 1992). With the improvement of computer performance, microscopic traffic simulation is being more and more used, which can provide much more simulation details. This also makes it possible to be utilized in a wider range of research fields. The significance of microscopic traffic simulation is that it can provide a large and safe test environment. In this environment as many traffic elements as necessary can be added to reproduce the real traffic environment as realistic as possible. This is less

expensive and much safer than building a test site of the same size. With the help of traffic simulation, it is also easier to study the impact of automotive technology on traffic flow. Thus, microscopic traffic simulation was assuredly selected as the way of predicting the effect of electric vehicles on traffic flow and the tool of studying vehicle energy consumption.

Most of traffic simulation software packages were built mainly for transportation research like transportation planning or prediction of traffic congestions. Therefore, the models used in simulation focus more about the characteristics of the combination of driver and vehicle. And the willing of drivers is often more important than the physical abilities of vehicle in these models. Generally, the vehicles are also according to purpose roughly classified, like into passenger cars, trucks, transport vans, etc. On the other hand, the mathematical abstraction from collected traffic observation data is a typical modeling method and many traffic simulation models were also built in this way. However, the rare proportion of electric vehicles makes it difficult to collect enough data for modeling. In observation it is also difficult to distinguish electric from the ICEVs. The typical models and previous modeling methods seem not suitable for this study. Therefore, it is necessary to find a new modeling method for electric vehicles in the context of traffic simulation.

Because of the difficulty of collecting data of electric vehicles from real traffic flows, the electric vehicle was planned to be modeled based on the physical characteristics. In this way, the necessary data are the specification parameters of the vehicle, which are easier to obtain than the traffic counts data. In addition, a driver model is needed for controlling the vehicle model during simulation.

In summary, for studying the effect of electric vehicles on traffic flow, the existing microscopic models are not applicable directly. A model for microscopic traffic simulation, in which the different behavior of the EVs and the ICEVs are considered, is needed in this thesis. Then, the established models were implemented in a traffic scenario based on a real road network and real traffic data. The effect of electric vehicles was described based on the simulation results.

1.2 Targets of the Thesis

The purpose of this thesis is to explore the effect of electric vehicles on traffic flow. The comparison between fuel consumption of ICEV and energy consumption of EV in similar simulation are also investigated.

First, the mentioned vehicle model and driver model need to be established. In the vehicle model the dynamic characteristics of vehicles need to be considered and reflected in simulation. The vehicle model should also be based on the data and parameters, which can be obtained by means other than traffic observation. While the driver model should imitate the behaviors of real human drivers. Besides, the vehicle model and driver model should be able to be adjusted individually, so that the impact from drivers can be excluded when comparing simulations with different vehicle models. The vehicle model and driver model cooperate for controlling the vehicle during the simulation.

Then, a traffic scenario needs to be built for implementing the simulation with the established models. In this thesis, a scenario of the center of the City of Duisburg was used as the basis for the simulation (Ma et al. 2020). The road network was exported from OSM (Open Street Map). The traffic demand was generated from real traffic counts data. Further refinements of this scenario have been made in this study based on the real traffic data.

The simulations of the scenario based on vehicle models with dedicated power trains were implemented. With the help of traffic simulation software, the key parameters of traffic flows could be monitored during simulation, including the number of vehicles in each time interval, mean speed of the vehicles, and road occupancy. By analyzing the change of the collected data of traffic flows, the effect of electric vehicles on traffic flow could be estimated. It also can be predicted based on the simulations, whether traffic efficiency can be improved with the increasing share of electrification of vehicles.

Finally, the calculation method of fuel and energy consumption was proposed. The variation of traffic density was realized by adjusting the traffic demand in the established traffic scenario. The variation of fuel and energy consumption of ICEV and EV in different traffic density was observed and compared.

1.3 Structure of the Thesis

The thesis consists of 10 Chapters.

In Chapter 2 the basics and states of actual research are explained. The basic knowledge about traffic simulation and some research projects based on traffic simulation are introduced. Then the existing modeling methods of drivers and vehicles are discussed.

Chapter 3 describes the general structure of the proposed car-following model. This model consists of a driver part and a vehicle part. The driver model and the vehicle model are introduced in Chapter 4 and Chapter 5, respectively. A driver model based on fuzzy control has been used in this thesis and is described and parameterized in Chapter 4. Three sizes of ICEVs and also three sizes of EVs, as well as their components are modeled in Chapter 5. After calibrating the driver model for the corresponding vehicle models, the acceleration process of the vehicle was compared using a commonly used car-following model and the proposed model.

A traffic scenario of the center part of the City of Duisburg has been used for simulating with the car-following models. In Chapter 6 first the establishing method of the traffic scenario is introduced. Based on real traffic data and street views of the roads, the road network and the traffic demand in this scenario are then calibrated. This simulation scenario serves as a basis for the following research work.

Chapter 7 describes the implementation of the proposed car-following model in the traffic scenario. The proposed car-following model is established in MATLAB and is then linked to the traffic simulation software. The main program and the vehicle type assigning method are also introduced. The proposed car-following model is validated by comparing the average speed of the vehicular flow.

The traffic scenario is then simulated after replacing the ICEV models with the EV models. The simulation results are then analyzed and summarized in Chapter 8.

Chapter 9 introduces the calculation method of fuel and energy consumption in simulation. The energy consumption of the ICEVs and EVs in the 24-hour simulation is calculated and compared. A 2-hour traffic demand is then extracted

and enlarged for studying the energy saving potential of the EVs in different traffic conditions.

Chapter 10 contains the conclusion and a summary of the thesis.

2 Basics and State of Research

In this Chapter, the basics, and related research about modeling of traffic flow, vehicles and drivers are introduced. The typical car-following models and the traffic simulation software are introduced and reviewed. After introducing the structure of the powertrains of ICEVs and EVs, the commonly used vehicle and driver models, as well as the fuel and energy consumption models, are also explained. In the end of the Chapter, research methods that have been used in this thesis are concluded.

2.1 Traffic Flow and Modeling

The simulation of the traffic flow is a fundamental part of the work necessary for the achievement of the scientific results within the scope of the thesis. Traffic flow describes the movement of individual traffic participants and their interactions, including pedestrians, cyclists, and vehicles. Since this thesis focuses on the effect of electric vehicles on traffic flow, hereafter the term traffic flow refers to vehicular flow. The study of traffic flow is difficult, as the precise prediction about the behaviors of driver or vehicle trajectories is impossible. Nevertheless, the behavior of the majority of drivers can be described mathematically to a certain extent. Therefore, the real behavior can be predicted despite the individual differences.

The traffic flow modeling aims to find out the regularities of the traffic flows and express it with mathematical methods. The theory study and modeling of traffic flow started already in the 1930s (Greenshields et al. 1935). Until the 1990s this area was strongly affected and developed due to the increasing traffic volume as well as the spread and rapidly increasing performance of computers. Depending on the level of aggregation of traffic flow models, they can be divided into macroscopic, microscopic and mesoscopic models (Treiber and Kesting 2013).

Macroscopic traffic flow models have the highest aggregation level. They describe the traffic similarly to the description of the flowing motion of fluids. In macroscopic models, also called hydrodynamic models sometimes, the dynamic variables are aggregated to the observation locations (Leutzbach 1988). The local traffic conditions are described with variables such as traffic density, flow, and mean speed.

The Nagel-Schreckenberg Model (Nagel and Schreckenberg 1992) is one of the popular macroscopic traffic flow models, which is also a kind of cell automaton. It uses a completely discrete way to describe the traffic flow. Macroscopic models determine the interaction of traffic flows in neighboring observation sites, i.e., the way in which the dynamic variables are transferred between neighboring road sections. Therefore, macroscopic models describe the relationship between vehicle aggregations. The influence of individual vehicles is greatly erased in a macroscopic traffic simulation. Therefore, macroscopic models are not applicable in some research areas, e.g., studying the microscopic behaviors like lane-changing, or when there are several types of drivers and vehicles in simulation. Even though, this modeling method still has its unique advantages. Modeling allows for a relatively efficient calculation. When there are no extra requirements for considering the behaviors of individual vehicles but strict requirements for computing speed, or when a quite large-scaled scenario needs to be simulated, the macroscopic traffic simulation is suitable. However, due to the lack of possibilities to consider individual vehicle characteristics in a simulation, it is not applicable in this work.

With the rapid development of computer performance, microscopic traffic simulation has become a powerful tool. The microscopic traffic flow describes the interactions between individual drivers and their vehicles. In a microscopic traffic simulation, the basic element becomes the driver-vehicle unit. During simulation, the velocity profile, travelling routes, and many other information of each vehicle can be tracked and recorded. Therefore, this type of model contains much more details in simulation and is more intuitive than macroscopic traffic simulation. These features also broaden the application fields of microscopic traffic simulation.

Another kind of traffic flow model is the mesoscopic model (Burghout 2004). It combines the macroscopic model and microscopic model. Through aggregation and disaggregation, the traffic flow can be switched between macroscopic and microscopic models. The traffic flow is usually described with a macroscopic model. While in some locations macroscopic models are not applicable, especially at intersections, the traffic flow is disaggregated into individual drivers and vehicles. When vehicles move out of these locations, they are aggregated into macroscopic traffic flow again.

As the different types of vehicles need to be distinguished in simulation, microscopic modeling is the method of choice for this study. The microscopic traffic flow modeling and several models are further introduced in following.

2.1.1 Microscopic Traffic Flow Modeling

The microscopic model describes the microscopic behaviors of each driver-vehicle unit, including acceleration, velocity, position, etc. As this thesis studies the effect of the vehicle type, especially the type of powertrain, on traffic flow, the microscopic models are the preferred method.

Different from the abstract description of macroscopic traffic flow models, microscopic models describe directly the behavior of each vehicle. The acceleration, velocity, precise position in the road network, yaw angle, and even travelling trajectory of vehicle can be studied in a microscopic simulation.

The motion of vehicles in a microscopic model is determined by two aspects, i.e. the controlling behavior of the driver and the physical abilities of vehicle (Chowdhury et al. 2000). The physical abilities of a vehicle are usually roughly expressed by variables such as maximum acceleration, maximum deceleration, etc. While the controlling behavior in microscopic traffic flow could be approximately classified as car-following and lane changing. There are also corresponding models describing the car-following and lane changing behavior.

Car-following models describe the behavior of a driver-vehicle unit in longitudinal direction, i.e., the direction along the lane. They determine how a driver behaves when he follows another vehicle. Compared to the car-following situation, lane changing is a quite more complicated situation. It is related to physiological psychology of driver, decision strategy (Rehder et al. 2016; Rehder 2020) and vehicle steering dynamics (Moser et al. 2019; Moser 2020). The lane change model describes the decision process of the driver when he is ready to change lanes.

As the research focus in this thesis is the impact of electric vehicles on traffic flow, the longitudinal dynamics of vehicle will be paid more attention. The reason is that the main differences between EVs and ICEVs are the different powertrain behavior and especially the different dynamics of powertrain. The steering systems

of EVs and ICEVs on the other hand are very similar. Therefore, car-following models are the main study object in this thesis.

2.1.2 Car-Following Models

Basics of Car-Following Models

Although car-following behavior appears to be easier to describe than lane changing, it is still determined by various factors. Drivers and their vehicles are obviously influenced by other traffic. The other influence factors can be categorized to individual differences and situation factors (Ranney 1999). The relative constant factors belong to the individual differences, such as age and gender of driver, driving skills and driving styles, type of vehicle and vehicle dynamics. The situation factors are also classified into two categories, environment factors and individual factors. Time, day of week, weather, and other factors determined by other influences than driver and vehicle belong to the environment factors. While individual, but always varying, factors contain those determined by the driver, such as travel hurrying, fatigue, concentration level, etc. the weights of these factors also vary in different traffic flows. In free flow, the individual differences and situation factors have greater impact on the car-following behavior. While in a congested flow, the car-following behavior is more determined by other traffic.

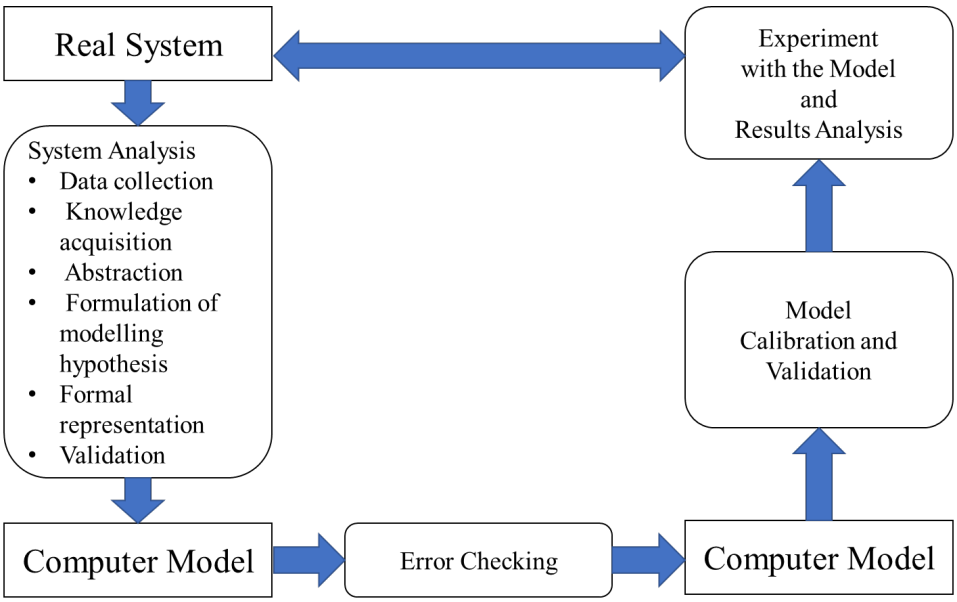

Figure 2.1 Methodological steps of model-building process

The car-following behavior is also influenced by lane-changing behavior. According to the description in oversaturated freeway flow algorithms (Yeo et al. 2008),

except a common and base car-following model, the car-following behaviors need also to be described with before lane changing car-following model, during lane changing car-following model, after lane changing car-following, emergency lane changing car-following model and some other car-following model for corresponding driving situations.

It is therefore not just a matter of using a single model that simulates the behavior of the car in all driving situations. In modeling of car-following behavior, the model designer has to make some assumptions and simplifications according to the research purposes. When building a model, the analysis of the real system is the first step. System analysis usually contains data collection, knowledge acquisition, abstraction, formulation of modeling hypothesis, formal representation, and validation. Then, the obtained computer model needs calibration and validation. Finally, experiments with the model could be implemented. These steps above are the methodological steps of the model-building process (Barceló 2010). In the various modeling methods about car-following behavior, these basic steps should be followed.

Generally, the driver-vehicle unit is the basic element in microscopic traffic simulation, also the describing object of car-following model. A combination of a certain type of driver and a certain type of vehicle is described by a kind of car-following model and a unique set of parameters. Car-following models describe the motion of each individual driver-vehicle unit. Then, the whole traffic flow consists of these individual motions. Some typical and widely used car-following models are introduced in following.

The earliest car-following models have been proposed by Reuschel (Reuschel 1950) and Pipes (Pipes 1953) over sixty years ago. In these two models, a basic idea of modern car-following models has been proposed: the minimum or safety distance gap between two vehicles increases with the growth of vehicle speed. There is a proportional relationship between these two variables.

After years of development, various car-following model have been developed (Brackstone and McDonald 1999). A car-following model always describes the relationship between several key parameters. The basic description variables of a driver-vehicle unit α in microscopic traffic simulation are location $x_\alpha(t)$, speed $v_\alpha(t)$ and vehicle length L_α. Location $x_\alpha(t)$ indicates the position of vehicle α's

front bumper on the road. Here it is defined that the vehicle index α decreases along the driving direction, i.e., the vehicle $\alpha - 1$ is the leading vehicle of vehicle α, shown as in Figure 2.2. For the sake of simplicity, the leading vehicle is also indicated with symbol l.

Distance gap between two vehicles, the distance from front bumper of vehicle α to leading vehicle's rear bumper, can be represented by their locations and lengths

$$G_\alpha = x_{\alpha-1} - L_{\alpha-1} - x_\alpha = x_l - L_l - x_\alpha \tag{2.1}$$

Depending on the models, sometimes additional variables might be needed, for instance, vehicle α's acceleration $\dot{v}_\alpha = \mathrm{d}v/\mathrm{d}t$. But the variables mentioned above could already compose the minimal models, which can represent the human drivers' behavior to a certain extent through a function of G_α, v_α and v_l.

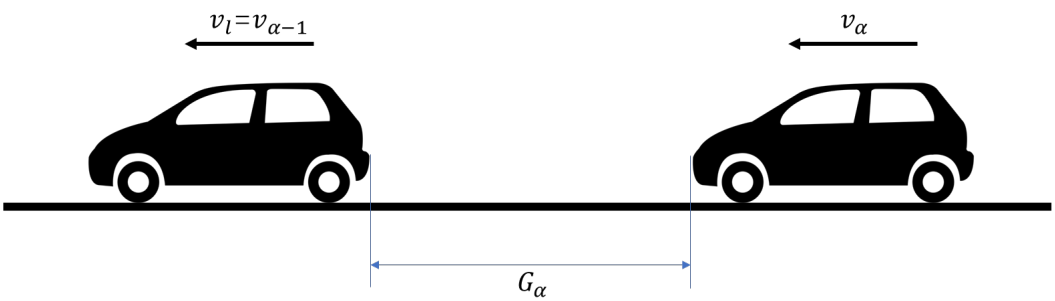

Figure 2.2 State variables defining for car-following models

Newell's Car-Following Model

Newell's car-following model (Newell 2002) is a very simple kind of time-discrete model. Its mathematical representation is:

$$v(t+T) = v_{opt}\big(G(t)\big), \tag{2.2}$$

$$v_{opt}(G) = \min\left(v_{limit}, \frac{G}{T}\right), \tag{2.3}$$

where v_{opt} is the optimal speed, v_{limit} is the limit speed of road, t is time in simulation, $G(t)$ is the current following gap at time t.

Newell's model has expressed the relationship between vehicle speed and following gap in a simple way. However, many other factors in the car-following behavior have also been ignored. The following gap G can be seen as the influence from other

traffic, v_{limit} acts as the influence from environment factor. The other influence factors are not considered. In simulation, vehicles with Newell's model will always drive at the possible highest speed. There is also no acceleration process like in a real vehicle. The vehicle just immediately reaches the highest speed.

Therefore, as it is a quite simple model, Newell's model has not considered the physical abilities of vehicles. In simulation, the vehicle types cannot be distinguished, either. As the model dynamics differ from real vehicles, the simulation results would also quite probably deviate from reality. Because the lack of factors describing individual differences, when the model deviates far from real traffic flow, the calibration of model is also not possible. In addition, the parameters in the Newell's model need to be adjusted precisely, otherwise it can produce accidents.

Gipps' Model

Gipps' model (Gipps 1981) is also a simple but accident-free model. The Gipps' model introduced here has been simplified. Its concept nevertheless remains the same (Treiber and Kesting 2013). The Gipps' model is described by

$$v(t+\tau) = min\left[v + a_{max}\tau,\ v_{limit},\ v_{safe}(g, v_l)\right], \tag{2.4}$$

where τ is the reaction time of the driver, a_{max} is the maximum acceleration of the vehicle that is determined by the type of vehicle, v_l is the speed of leading vehicle.

In the Gipps' model, the concept of safe speed was introduced for avoiding accidents. The safe speed v_{safe} is determined by following gap and the speed of the leading vehicle using

$$v_{safe}(G, v_l) = -b\tau + \sqrt{b^2\tau^2 + {v_l}^2 + 2b(G - G_{min})}, \tag{2.5}$$

where b is the deceleration and G_{min} is the minimum following gap.

Equation (2.5) is based on two assumptions. The vehicle always decelerates with a constant deceleration b. And the reaction time τ is also constant.

Compared with Newell's model, in the Gipps' model more influence factors have been considered, such as acceleration, deceleration and minimum distance gap. And the introduce of save speed can avoid unnecessary accidents in simulation. After

calibration of a model with traffic observation data, with the Gipps' model it is able to distinguish several vehicle types in simulation. However, the collection and analysis of traffic data are the basic steps.

Intelligent Driver Model

The Intelligent Driver Model (IDM) (Treiber et al. 2000) is one of the simplest complete models, which is free from accidents and can provide acceleration profiles in all single-lane traffic situations. The acceleration profiles are obtained by

$$a = a_{typ}\left[1 - \left(\frac{v}{v_{desired}}\right)^{\delta} - \left(\frac{G_{desire}(v, \Delta v)}{G}\right)^{2}\right], \tag{2.6}$$

where a is the vehicle acceleration, a_{typ} is the typical acceleration of the corresponding vehicle type, v is the current speed of ego vehicle, Δv is the speed difference from the leading vehicle, δ is the acceleration exponent, and $G_{desired}$ is desired gap. $G_{desired}$ is obtained from

$$G_{desired}(v, \Delta v) = G_{min} + \max\left(0, vT + \frac{v\Delta v}{2\sqrt{a_{typ}b}}\right). \tag{2.7}$$

IDM can provide a detailed acceleration process description of vehicle both in free flow and congested flow. The generated acceleration profile of IDM is closer to an adaptive cruise control (ACC). If the imitation of human driver behavior is envisaged, the IDM needs to be extended by considering the characteristics of a human driver, such as operation imperfection, reaction time, etc.

Wiedemann's Car-Following Model

The three car-following models introduced all use a single equation or a single set of equations describing the car-following model in all situations. While in the Wiedemann model, there are four discrete driving situations. In each situation there is a associated function determining the acceleration of vehicle.

The driving simulations are categorized by free-flow, approaching slower vehicles, car-following near steady-state equilibrium, and critical situations requiring higher deceleration. These four situations are distributed in a 3-dimensional space,

which consists of the state variables G, v, and Δv. The area of each situation is defined by corresponding nonlinear equations.

The distribution of the driving situations is shown in Figure 2.3.

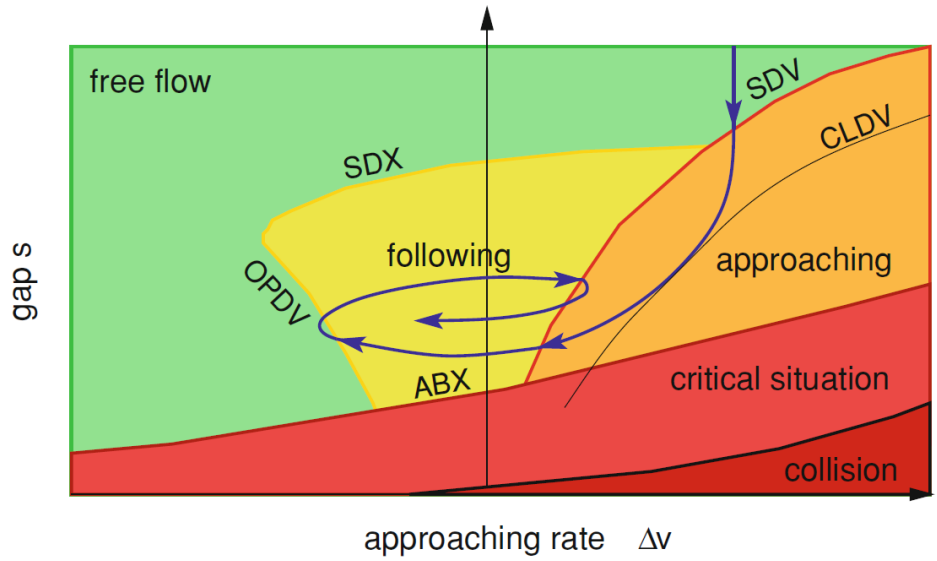

Figure 2.3 Schematic of Wiedemann car-following model (Wiedemann 1974; Treiber and Kesting 2013)

By defining the distribution of different driving situations, the local traffic conditions can be reflected in the Wiedemann model. The psycho-physiological properties of the human driver are also considered in this model. However, as many influence factors of car-following behavior have been considered, the calibration of this model is more complicated and needs more kinds of data.

Krauß Model

The Krauß model (Krauß et al. 1997) is a variant of Gipps' model. The main improvement of Krauß model compared to the Gipps' model is that it considers the impact of imperfection. Operating errors and irregularities in driving style are common among human drivers. By introducing some noise into the driver's action, e.g., acceleration, this impact could be reflected in the car-following model.

As a variant of Gipps' model, a similar equation was used in the Krauß model for determining the desired speed:

$$v_{desired} = min[v + a_{max}\tau,\ v_{limit},\ v_{safe}]. \tag{2.8}$$

Then, the desired speed $v_{desired}$ is added to a noise and the result is the speed of vehicle:

$$v = max(0, v_{desired} - \epsilon a_{max}\xi), \tag{2.9}$$

where ϵ is the noise amplitude, ξ is a random number in [0,1].

Similarly, by varying acceleration and deceleration, different vehicle types can also be distinguished in the Krauß model (Krauß 1998).

In modeling methods and principles of several typical car-following models, it can be noticed that driver and vehicle are described with one equation at a time. By calibrating the values of several key parameters, the different vehicles and drivers can be distinguished. However, this also means that a set of values corresponds only to one combination of a certain driver and a certain vehicle.

2.2 Traffic Simulation Software

A traffic flow model determines the motion characteristics of vehicles. However, there are far more essential elements in a traffic system, such as shape and connection of roads, traffic light logics, traffic demand, etc. The traffic simulation software is quite helpful for integrating the corresponding data into a traffic scenario.

There are many traffic simulation software tools that have been widely used in many projects. These software tools were developed with individual application purposes. Therefore, their functions and simulation abilities have their own focuses. In this Section some popular traffic simulation tools and some relative research projects are introduced.

PTV Vissim is today perhaps the most widely used commercial microscopic traffic simulation software. The name Vissim relates from “Verkehr in Städten – Simulationsmodell”, which is German for “Traffic in cities – Simulation model”. In Vissim, vehicles including cars, buses and trucks, public transport, cyclists, pedestrians can be simulated and interact. Vissim provides microscopic and discrete traffic simulation, in which the position of each vehicle can be updated every 0.1-1 s based on several traffic flow models.

As a successful commercial software tool, ease of use is not the only advantage of Vissim. Vissim contains a large number of 3D computer models for traffic and infrastructures. Based on these 3D models, the simulation can be visualized with a 3D view in Vissim. Figure 2.4 is an official demonstration of a complex intersection with a 3D-view in Vissim. Not only traffic including vehicles and pedestrians, but also traffic infrastructure and buildings nearby are all visualized with a high level of details.

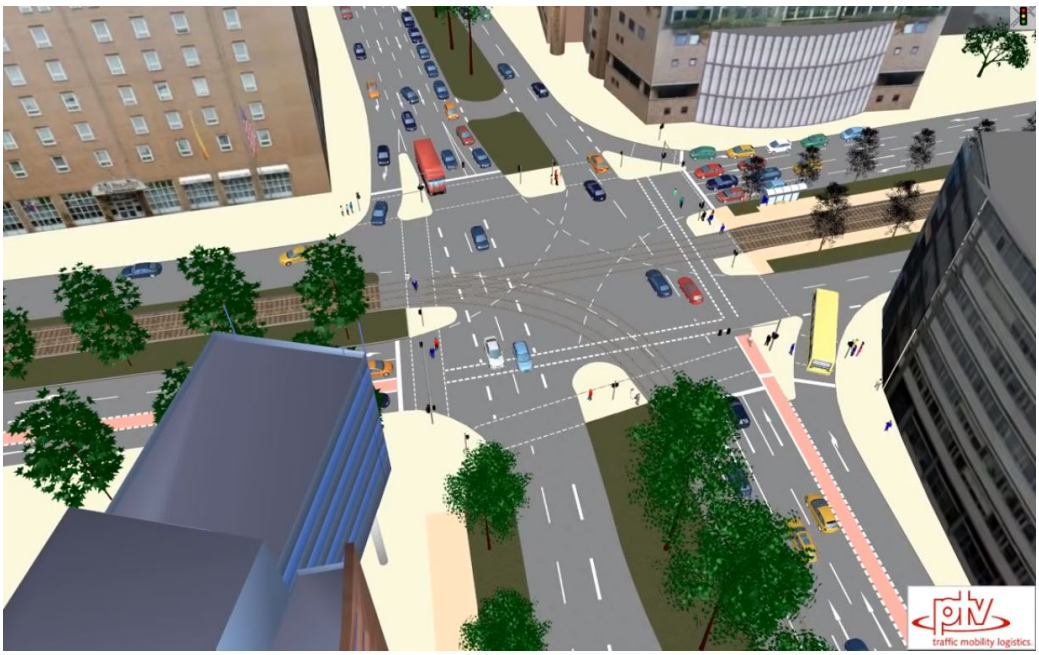

Figure 2.4 Official demonstration of a complex intersection in Vissim (PTV-Group 2020)

Vissim has been applied in many research projects, e.g. assessing the influence of adverse weather on traffic flow (Chen et al. 2019), estimating project-level vehicle emissions (Xu et al. 2016), etc. Many works have also been done about the calibration and validation the models in Vissim, such as junction parameter calibration for mesoscopic simulation in Vissim (Ehlert et al. 2017), calibrating car-following parameters in VISSIM with video-based approach (Lu et al. 2016).

As a commercial product, the property of a ready-to-use black-box provides much convenience for the users of Vissim and other commercial simulation software packages. However, from the viewpoint of researchers, this availability may cause problems in some applications (Krajzewicz et al. 2002). For trade secrets, data protection, program stabilities or other reasons, the functions, interfaces, internal principles of commercial software packages are always limited or blocked in a certain range.

Hence there will be many difficulties when the users want to extend or modify the applications of the software by themselves. In this situation, an open-source software package can is to be preferred.

SUMO is currently perhaps the most popular open-source software package, which can provide microscopic traffic simulation. “SUMO” is derived from “Simulation of Urban MObility”. The development of SUMO started in 2000 by the Center for Applied Informatics Cologne (ZAIK) and German Aerospace Centre (DLR). After 2004 only DLR continues the developing work on SUMO, also with help from external organizations or individuals.

As an open source, highly portable, microscopic traffic simulation software package, SUMO can provide time-discrete, space-continuous vehicle motion, different vehicle types, different right-of-way rules, and traffic lights in simulation. Streets with multi lanes can be simulated with lane changing. A traffic scenario in SUMO consists at least of road network and demands. The road network can be manually established. The existed network in formats of VISUM, Vissim, etc. can also be converted for use. Most input and output files of SUMO are in XML-format (Extensible Markup Language), which is a widely used common format. Therefore, the input and output files can be read and edited in other software for data exchange, data analysis or other purpose.

As an open-source software package with superior expandability, SUMO has been more and more applicated in many recent research projects, including many hot topics such as vehicular communication, route choice and dynamic navigation, traffic light algorithms, evaluation of traffic surveillance systems (Krajzewicz et al. 2012).

In the study on traffic behavior of emergency vehicles (Bieker-Walz et al. 2018), a modeling method of emergency vehicles including ambulances, police cars and fire engines was introduced. An emergency lane for emergency vehicles could be temporary established in the simulation, as shown in Figure 2.5.

One of the design purposes of SUMO is to handle large networks. In project LuST (Codeca et al. 2015; Codecá et al. 2017), a 24-hour scenario of City Luxembourg was built in SUMO, as shown in Figure 2.6. This scenario was built as a common

basis for evaluations about technologies related to vehicular traffic congestion, intelligent transportation systems, and mobility patterns.

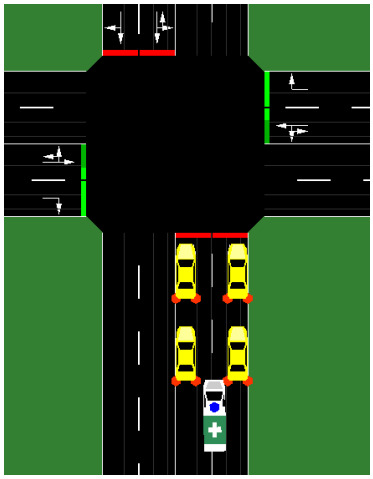

Figure 2.5 Emergency lane for emergency vehicles in SUMO (Bieker-Walz et al. 2018)

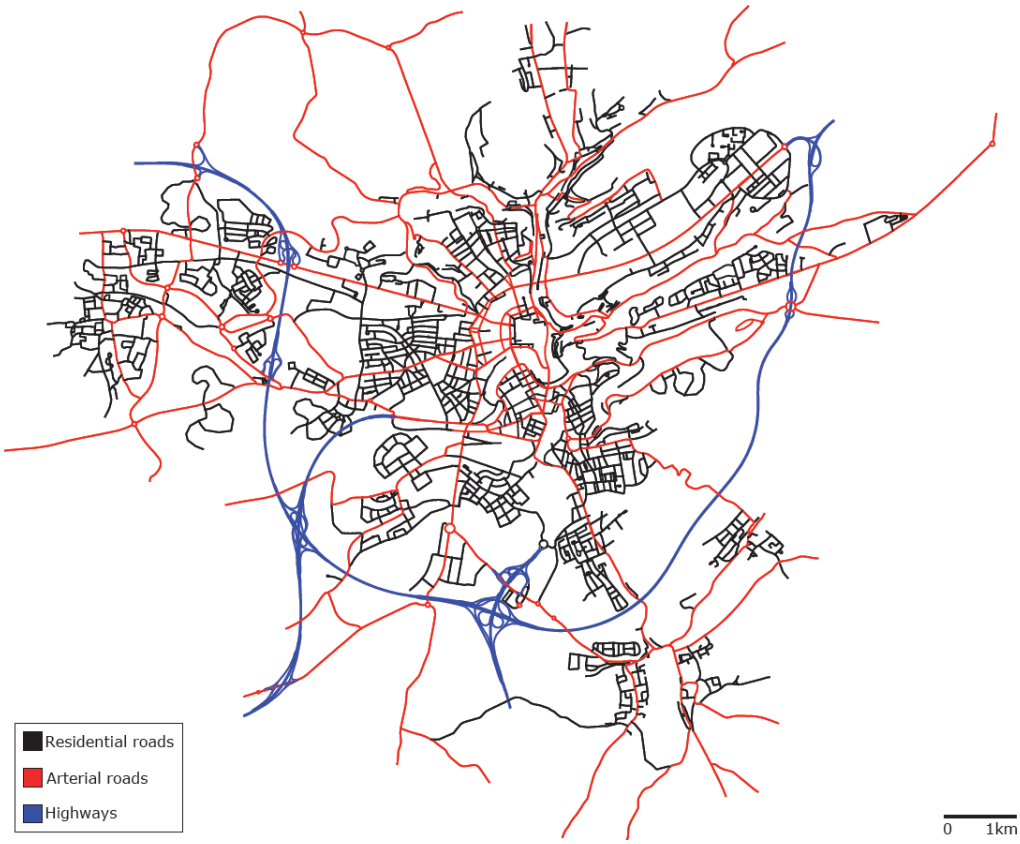

Figure 2.6 LuST: traffic scenario of City Luxembourg (Codeca et al. 2015)

SUMO also provides an interoperability with other applications during simulation. This makes some works possible through the cooperation of SUMO and other software. Based on the integration work completed by rFpro and SUMO, a complete

real-time simulation of urban environments for DIL (Driver in Loop), ADAS (Advanced Driver Assistance Systems) and autonomous testing was created (Cottignies et al. 2017). The high-resolution 3D models from rFpro were combined with traffic scenario in SUMO. In Figure 2.7, the black vehicle was controlled by human driver, while other vehicles were controlled by SUMO.

Figure 2.7 rFpro & SUMO (Cottignies et al. 2017)

2.3 Powertrains of ICEVs and EVs

It is well known that in 1885 German inventor Karl Benz built the first automobile in Mannheim, Germany. With Benz Patent-Motorwagen was patented in 1886, this year is also regarded as the birth year of the modern car. After the advent of assembly line cars by Ford, the internal combustion engine has always been the dominant propulsion method for ground vehicles.

The use of an internal combustion engine requires many peripheral components (Koppers 2019). Figure 2.8 shows a typical topology of an ICEV, the arrows indicate the direction of energy flow. Through the combustion of fossil fuel in the combustion chamber, pistons are pushed for turning the crankshaft by the high-pressure gases after combustion. Then part of the chemical energy is transformed into useful work, while the rest energy leaves engine into the environment in the form of heat (Schramm et al. 2020). Gearbox is a necessary component in an internal combustion engine powertrain. The power from engine must be transferred to gearbox first. A vehicle needs very high torque for starting to move, while at low rotation speeds the

ICE cannot reach the highest torque (Schramm et al. 2017b). Therefore, when a vehicle is starting and moving at low speeds, the gearbox needs to amplify the torque from engine. On the contrary, a lower transmission ratio is needed when vehicle needs to reach higher speed.

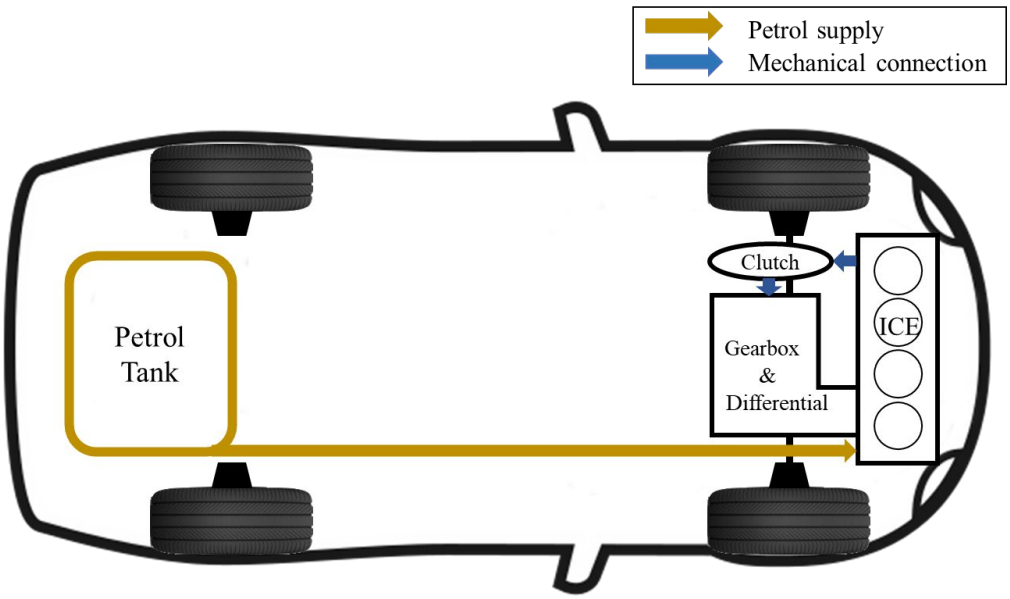

Figure 2.8 Topology of a conventional internal combustion engine vehicle

With the rapid increase in the number of motorized vehicles, travel comfort increased on the one hand; on the other hand, more and more problems became apparent. The negative impact of vehicle emission on the environment is one of the main problems. Although many fuel-efficient technologies have been developed and applied into ICEVs, such as lean-burn systems, variable valve lift, turbocharging, etc., the maximum thermal efficiency of ICE is still around 35%. Therefore, the researchers, manufactures, governments have in recent years turned their attention from improving efficiency of ICE to develop electric vehicles.

The development of electric vehicles also has a long history of over one hundred years (Lixin Situ 2009). However, due to the limitations of energy storage technologies at that time, electric propulsion was abandoned for a long time in applicating in ground vehicles. Due to many factors, electric vehicles have returned to people's vision in the last few decades. Electric vehicles can be basically categorized into several types, including pure-electric vehicle or battery electric vehicle (BEV), plug-in electric vehicle (PHEV), and hybrid electric vehicle (HEV) (Karle 2020).

A pure-electric vehicle has the simplest structure amongst electric vehicles. Figure 2.9 indicates the topology of pure-electric vehicle. There is an obvious difference with ICEV in EV that the energy flow can be two-way, because of the recuperation capability of the electric powertrain (Schramm et al. 2017b). This is a feature of the electric motor. When the rotation direction and torque direction are same, the electric motor can provide traction for vehicle. However, when the rotation direction and torque direction are reverse, electric motor can work as a generator. Through this process a part of vehicle kinetic energy can be reconverted into electric energy. The efficiency of an electric powertrain can be over 90% (Karle 2020). Moreover, an electric motor can smoothly operate in a wider speed interval than an ICE. Therefore, the gearbox as well as clutch is no more necessary. As well as electric motor usually use grease for lubrication, the manufacturing cost and maintenance cost of electric motor are quite lower than ICE.

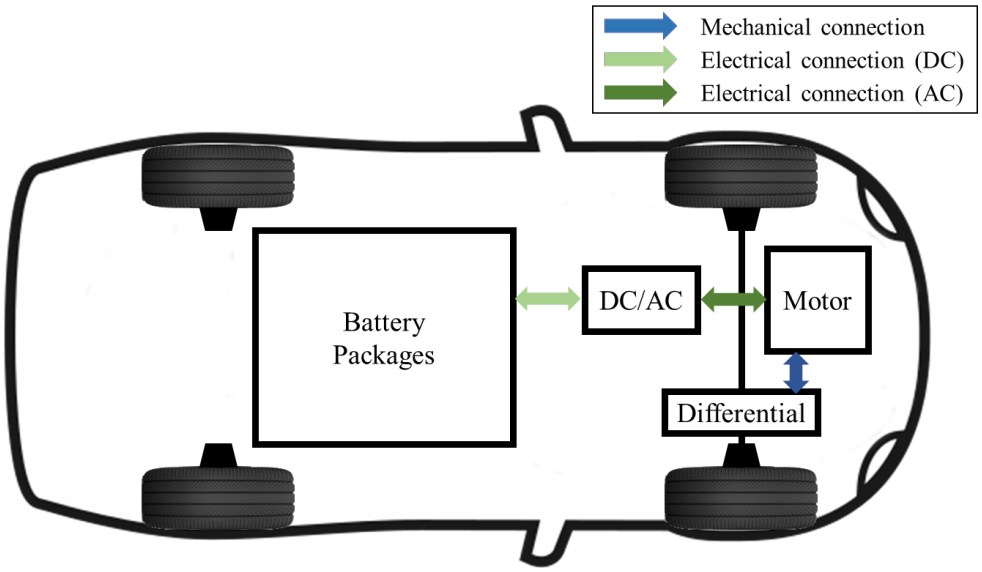

Figure 2.9 Topology of a pure-electric vehicle

However, the development and popularization of electric vehicles have been for a long time limited by the battery. Hence hybrid electric vehicles have been put on the market earlier than BEV and already for over twenty years. Toyota Prius could be the successful example of HEVs, which has been manufactured since 1997 (Taylor III et al. 2006). Prius is a kind of series-parallel HEV, its topology is shown in Figure 2.10.

The energy saving principle of HEV is to allow the ICE operating in the high efficiency interval through the intervention of the electric motor. In Figure 2.10, the power splitter, usually is a planetary gear unit, distributes the engine torque to generator for charging battery and wheels for driving vehicle according to required torque and battery SOC (State of Charge). When possible, the engine can also be turned off for an electric driving. With the decrease of manufacturing cost of batteries and the increase of battery energy density, some HEVs are equipped with a higher capacity battery and can be recharged from external source of electricity. This is the so-called PHEV. PHEV has a longer pure-electric travelling distance like 70km. In this range PHEV operates like a pure-electric vehicle. For longer travel, the fossil fuel can be an alternative energy source. Compared with HEV, the ability of externally charging further reduces the fossil fuel consumption of PHEV. However, the structure of HEVs and PHEVs is quite complicated. They are generally regarded as the transitional products before the breakthrough of battery technologies. Governments like China have excluded HEVs from new energy vehicle subsidy policy. HEVs were also not further discussed in this thesis.

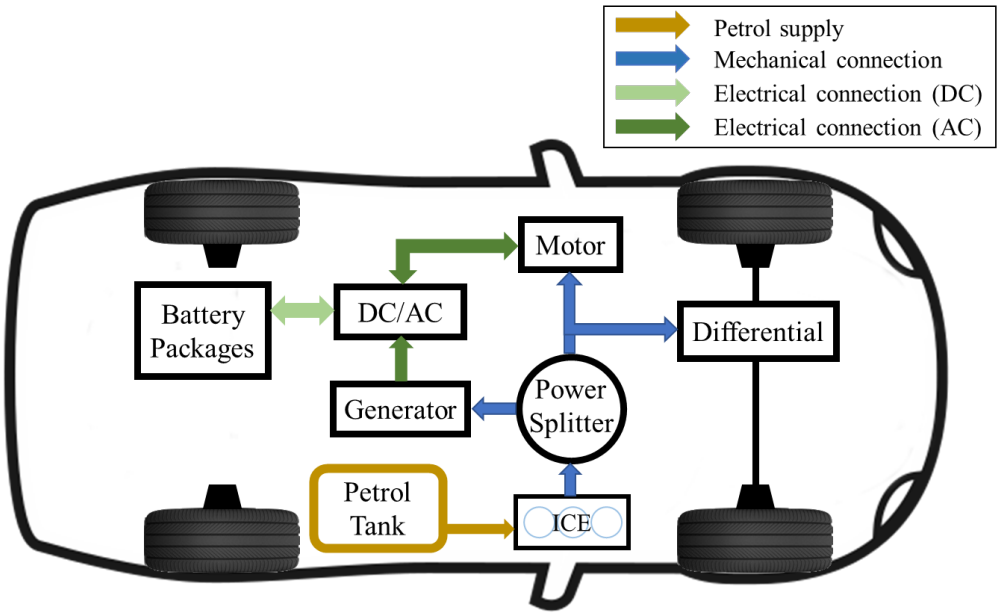

Figure 2.10 Topology of a series-parallel hybrid electric vehicle

Fuel cell electric vehicles (FCEV) belong to the HEVs and are considered by the market as one of the promising forms of EVs in the future (Karle 2020). They use compressed hydrogen as the energy source. Figure 2.11 indicates the topology. It is likely a pure-electric vehicle equipped with fuel cell system. However, the battery

capacity is much smaller. As the high manufacturing cost of fuel cell and rare hydrogen fueling stations, fuel cell electric vehicles are not produced in volumes.

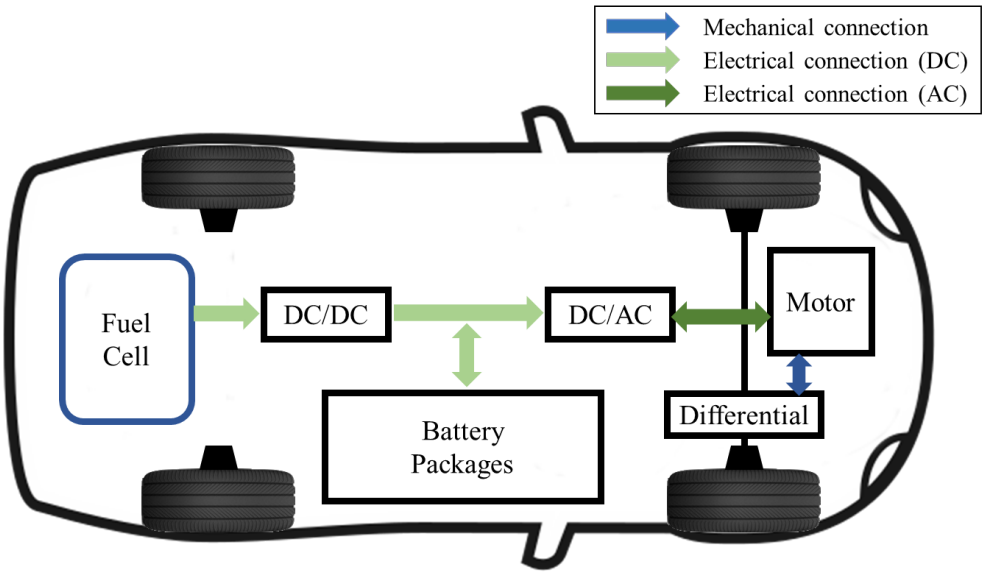

Figure 2.11 Topology of fuel cell electric vehicle

The structure and principle of several types of EVs have been explained. The term electric vehicle refers to the vehicles driven by the electric motors, i.e., HEVs and PHEVs in hybrid mode are not discussed. No matter for BEV, FCEV, or PHEV in pure-electric mode, the electric motor is the only propulsion component. This also means that they have the similar dynamic characteristics. Therefore, in the following simulations, electric vehicles used basically the same model, the specific types of electric vehicles were not distinguished.

2.4 Driver and Vehicle Modeling

The car-following models have provided the simplest methods of describing the behaviors of combinations of driver and vehicle. However, both the driver and the vehicle are already very complex systems in their own respects. There are also many complex models describing drivers and vehicles.

A complete vehicle model consists of several subsystems, including vehicle structure, powertrain, wheel suspension, wheels, brakes, and steering system (Schramm et al. 2018). Each subsystem can provide corresponding details in simulation. Depending on the requirement and target of research, the component models can also be ignored for simplifying the whole model and shorten the computation time.

The common vehicle models include single-track models, twin-track models, and complex multibody system models (Schramm et al. 2018). The more complicated models have usually more degrees of freedom. More degrees of freedom can provide a higher level of detail about the motion of each component in simulation. This is of varying importance in different research areas. As an example, a model with one degree of freedom might be sufficient for studying the longitudinal movement of vehicle. When researching the lateral characteristics of vehicle, a single-track model with 2 degrees of freedom is the minimum requirement. The twin-track model and more complex models are suitable for the research with higher requirements about the level of detail or research about specific components.

Unlike vehicles, the human driver is a more complicated system, which is quite nonlinear and hard to predict. The complete driving task can be described with three levels, i.e. strategic level, tactical level, and control level (Panou et al. 2007). The general planning of a trip like routes choosing belongs to the strategic level. The tactical level determines the local behaviors such as maneuvers, keeping a following gap. The control level contains the basic actions including operating pedals, steering wheel, and changing the gear. Due to the complexity of driving task and unpredictability of human behavior, there is not a generally accepted driver model for the complete driving task.

Similar with vehicle models, there are also simple driver models like linear models, nonlinear models and complex models based on artificial intelligence (AI) principles. The Newell's car-following model can also be seen as a simple linear driver model, since it describes more about the car-following logic of a driver, but less about the characteristics of the vehicle. The nonlinear behaviors of a driver can be described or predicted using statistical methods, e.g. by a Markov chain (Pentland and Liu 1999) or a Gaussian mixture model (Miyajima et al. 2007). The AI models can be used for describing more complicated human behaviors, e.g. using deep learning modeling driver risk perception (Ping et al. 2018). The modeling of driver should also depend on the researching demands choosing a suitable kind of modeling method.

2.5 Modeling of Fuel and Energy Consumption

Fuel economy is one of the most important characters for vehicles. Many driving cycles have been built for studying and evaluating the fuel economy of ICEV (Esteves-Booth et al. 2002). The actual fuel or energy consumption of a vehicle is however related to the driving condition. As a driving cycle can only represent several typical driving conditions, studying the fuel or energy consumption of vehicles in traffic simulation is more meaningful. It is also possible to observe the effect of traffic condition on fuel/energy consumption of vehicles.

In simulation, related models are needed for calculating the fuel or energy consumption of each simulated vehicle. The modeling methods can be classified into two kinds, i.e., forward analysis, and backward analysis. Forward consumption modeling is based on the fuel consumption characteristics of engine or the energy consumption characteristics of electric motor. As an example, ADVISOR (NREL's ADvanced VehIcle SimulatOR) is a vehicle simulation software package using forward models (Markel et al. 2002). For each engine, a fuel use map in gram per second can be generated and indexed by engine speed and torque. By accumulating the fuel consumption in each simulation step, which can be directly obtained from the fuel use map according to engine speed and torque, the total fuel consumption during the simulation and average fuel consumption can be calculated.

Generally, the fuel use map of an engine is obtained from calibration experiments about engine fuel consumption. The fuel use map can provide precise analysis results, while itself is however not easy to obtain. Therefore, backward analysis is more commonly used in fuel/energy consumption calculation. As an example, SUMO provides the calculation of emission and fuel consumption based on HBEFA (Handbook Emission Factors for Road Transport), which can be seen as a quite simple backward model. HBEFA provides the emission and fuel consumption factors according to the vehicle categories (Matzer et al. 2019). Table 2.1 is an example of emission factors of passenger vehicle in Germany in 2020, exported from HBEFA 4.1. With the fuel consumption factors of corresponding category and the driving distance of vehicle, the total fuel consumption of vehicle can be calculated.

Whether ICEVs or BEVs, in any case they are complicated systems. The fuel/energy consumption is not a constant parameter and varies with the driving condition. Therefore, with the emission and fuel consumption factor, only a rough calculation or estimate about the fuel consumption of vehicles can be obtained. If the more precise results are needed, the more precise models can fulfil the requirements.

The speed profiles of vehicle, which are not difficult to obtain both in simulation and from real cars equipped with data loggers, are normally the input data of a backward consumption model. Using speed profiles and necessary parameters of vehicles, some information of the vehicle during driving can be obtained, such as acceleration profile, consumed work and power against driving resistances, etc. Based on the total work consumed by driving resistances and a series of efficiency models of components in powertrain, the input energy of vehicle system can be backwards calculated. The detailed modeling and calculating methods will also be introduced in following Chapters.

Table 2.1 Emission factors of passenger cars in Germany in HBEFA 4.1 (hbefa.net)

Year	Country	Vehicle Category	Pollutant	Emission Category	Technology	Emission Factor	Unit
2020	Germany	Passenger Car	CO_2	Warm	CNG	144.639	g/Vehkm
					Diesel	179.188	
					Petrol	173.119	
				Start	CNG	0.317	
					Diesel	5.991	
					Petrol	7.24	
			Fuel Consumption	Warm	CNG	49.562	
					Diesel	57.461	
					Petrol	56.729	
				Start	CNG	0.104	
					Diesel	1.921	
					Petrol	2.372	

2.6 Research Method of the Thesis

Some basics of traffic flow modeling and electric vehicles have been introduced in this Chapter. This thesis focuses on the effect of electric vehicles on traffic flow and the fuel/energy consumption of vehicles using microscopic traffic simulation. Therefore, the microscopic traffic simulation is the main studying method in this thesis. As the main difference between EVs and ICEVs is the different powertrain and corresponding longitudinal dynamics, the car-following behavior was mainly considered in modeling.

There are several requirements for the models implemented in the simulation. Firstly, the car-following model should imitate the real car-following behaviors in traffic flow.

Secondly, different vehicle types, especially EVs and ICEVs, should be clearly distinguished in simulation. The real physical abilities of vehicle should be considered and individually adjusted. Thus, the dynamics of traffic flow can be closer to reality. And the impact of driver can also be excluded when comparing the electric vehicular flow and conventional vehicular flow. Therefore, it is a better choice to build driver model and vehicle model separately. Then, the car-following behavior is described by the combination of driver model and vehicle model.

Thirdly, the modeling for different types of vehicle, especially for EVs, cannot yet be based on the traffic observation data. As this is a predictive study, some necessary data cannot be obtained at present. In the introduced car-following models, different types of vehicles are distinguished by adjusting the values of corresponding variables. The values are determined by traffic observation data of corresponding vehicles. However, the widely used induction loop detectors distinguish vehicle types based on the length of detected vehicle (Clark 1986). The detected vehicles can only be roughly categorized into motorcycle, passenger car, delivery truck, heavy truck, etc. Obviously, the induction loop observations cannot distinguish the EVs from the ICEVs. Because of the slight difference in appearance of EVs and ICEVs, it is also difficult for camera traffic counters in traffic data collection. On the other hand, the number of EVs is still trifling. It is also difficult to collect enough

samples for determining the values in car-following model. Therefore, the modeling of electric vehicles should consider the data that can be obtained with practical ways.

Fourthly, the computation speed of a model should be considered. In a traffic simulation there are generally at least thousands of vehicles to simulate. While there are also always hundreds of vehicles simultaneously in the scenario. Therefore, unnecessary component models can greatly increase the computation time. As the study focuses on the longitudinal dynamics of vehicles, a vehicle model with one degree of freedom is sufficient. In microscopic traffic simulations, the route of each vehicle is usually fixed. Hence, the driver model does not refer to the strategic level. A driver model considering only control level and part of tactical level, i.e., car-following behavior, is sufficient in this simulation.

In addition, a traffic scenario also needs to be established, in which the above-mentioned models can be simulated. Since an electric powertrain is more different from a conventional powertrain at lower speeds, it is expected that the electric vehicle flow in urban traffic will show more differences compared to the ICEV flow. An urban traffic scenario should therefore serve as a basis for answering the research questions in this thesis. The research about the fuel/energy consumption of vehicles should also be based on this urban traffic scenario.

3 Car-following Modeling

The modeling of car-following behavior is an important fundament of this thesis. In this Chapter first the necessary modeling assumptions and implementation conditions are explained. Then the overall structure and the data flow of the car-following model used in this thesis are illustrated.

3.1 Model Requirements

Generally, the "car-driver-unit" is the basic element in microscopic traffic simulation. Driver and vehicle are treated as one unit in most of the car-following and lane changing models. The main difference between the EVs and the ICEVs is function and structure of the powertrain. The dynamic characteristics of an electric powertrain influence mainly the longitudinal dynamics of vehicle, which is in traffic simulation described by the car-following model. Hence, this thesis focuses on car-following behavior modeling.

In simulation, the car-following model could be considered as the "black box" shown in Figure 3.1. The input variables can be any of the environmental parameters and important driver character parameters that are chosen from the car-following model designer, generally including current speed, leading speed, current gap, maximum acceleration, maxi-mum deceleration, comfort acceleration, desired speed, desired gap, etc. The output variables describe the state of the vehicle and are usually vehicle speed or acceleration. The main function of the car-following model is to calculate the output variables with its unique algorithm.

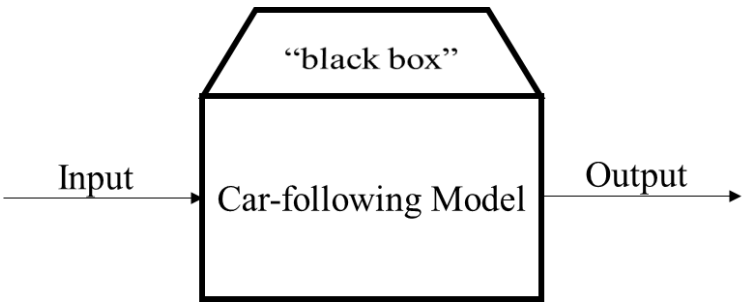

Figure 3.1 "black box" – Car-following model

As mentioned in Chapter 2, the mathematical abstraction from traffic observation data is a typical modeling method. Obviously, traffic data extraction and analysis

for specific vehicle types are the necessary basis of this method. However, this modeling approach is not suitable in this thesis due to its many restrictions. On one hand, for traffic counter devices, the electric passenger cars have no obvious distinguish from the ICEVs. This means that it is quite difficult to find out which traffic data belong to electric vehicles. On the other hand, although the proportion of electric vehicles increases every year, the total amount in current traffic is still quite few. Even if the data of electric vehicles could be found out, the number of samples seem to be too few to generate a representative model.

Therefore, the following modeling method was used in this thesis: The driver and vehicle were separately modeled. Such a model makes it possible to replace the fossil fuel vehicle model by an electric vehicle model, while the driver model part remains unchanged. In this way, the effect of electric vehicles on traffic flow could be better embodied in the simulation.

The main functions of a car-driver divided car-following model are not changed compared to a combined model. The difference is that there is a further segmentation in the "black box" in Figure 3.1. The driver model converts the input variables to drive/brake pedal position, instead of vehicle state. The vehicle state is calculated by the vehicle model based on drive/brake pedal position, vehicle physical abilities, and the speed in last simulation step. The combination of driver and vehicle part realizes a function similar to Figure 3.1.

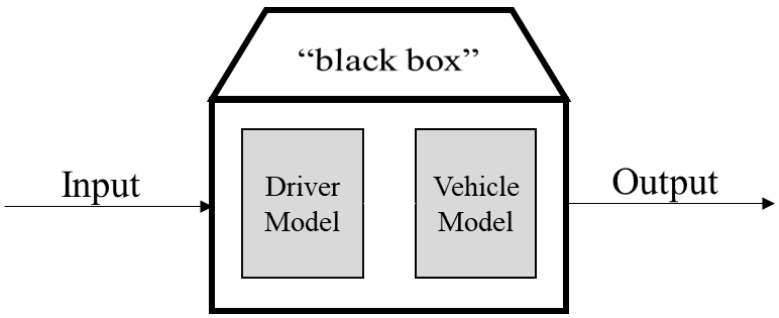

Figure 3.2 A car-driver divided car-following model

Altogether the following properties are necessary for the auto-successor model in this thesis:

- Driving in longitudinal direction like a car with a human driver.

- Realization of the same physical properties and capabilities as a combustion engine powered vehicle or an electric vehicle when using the respective applicable component models.

3.2 Modeling Assumptions and Conditions

In traffic simulation usually thousands of vehicles are simulated, the states of all vehicles need to be updated in every simulation step, which is a tight task for the computer processor. A simple but effective model can greatly shorten the simulation time. However, when driving in real traffic flow, the driver may encounter varied situations and in the same situation different drivers may have different driving strategies and habits. The behavior of human drivers is hard to completely predict and imitate, especially with a simple model. Therefore, the modeling must ignore ambiguous properties and details of the real circumstances, which have no significant influence on the simulation results. In this Section some of the assumptions underlying the modeling are explained. In particular, it is clarified under which conditions the car-following model can be implemented.

- The car motion in SUMO is space-continuous and time-discrete. The state of the simulated vehicle in each simulation step is described by position, yaw angle, and speed.
- In this thesis, only the car-following behavior of passenger cars is considered, as the main difference between fossil fuel vehicles and electric vehicles is the structure and performance of the powertrain. The influence of the lateral movement on the traffic flow, characterized by steering and lane changes, caused by the different behavior of the two vehicle types is significantly lower. In SUMO, the lane change process is realized by the intrinsic lane change model. The car-following model only determines the longitudinal speed of vehicle. When there is a leading car, the car-following model determines the speed depending on the relative velocity and distance to the leading car. If there is no leading vehicle, the vehicle accelerates gradually up to the speed limit prescribed for the respective road.
- Geometrically, a vehicle in simulation is represented by a planar rectangular, as the road network and simulation in SUMO is two-dimensional. Yaw direction is automatically calculated by SUMO and is always the

same with tangential direction along the traffic lane, which also means as a consequence that vehicle steering is not considered in car-following model.

- The car-following model outputs the speed of each vehicle in each step. The position is automatically updated by SUMO based on vehicle speed and previous position. As the vehicle position in SUMO is defined as the distance between the vehicle's current position and lane starting point along the lane, the vehicle movement can also be considered as a one-dimensional movement along the lane.
- Since the vehicle motion can be described one-dimensionally, the physically simulated vehicle is simply regarded as a particle that moves one-dimensionally on the roadway and is subject to driving forces and resistances. The acceleration and speed of vehicle in each step can be calculated with this physical model.

The simplification process and in-simulation representation of vehicles in this thesis can be graphically expressed as shown in Figure 3.3.

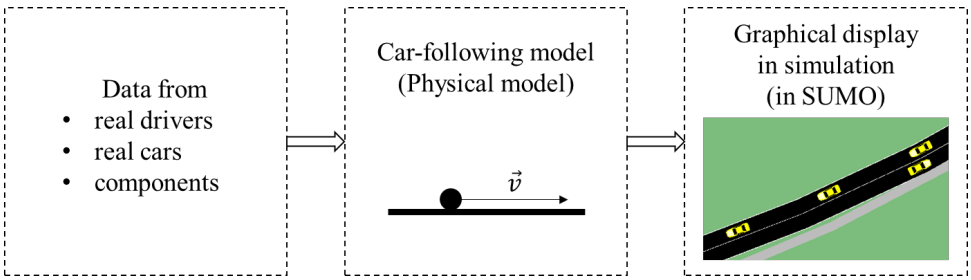

Figure 3.3 Simplification and in-simulation representation of vehicles

3.3 Overall Structure of the Car-following Model

After clarification of the necessary modeling assumptions and implementation conditions, the car-following model used in this thesis is presented in this Section in an overview.

The main function of a car-following model in simulation, is to control the vehicle speed, in order to maintain a relatively safe distance to the leading car, i.e., the car-following gap. In other words, vehicle speed is the immediate output of the car-following model.

3.3 Overall Structure of the Car-following Model

For maintaining a safe gap to the leading vehicle, the car-following model needs to consider several variables about the leading car and the ego car. In this thesis, the variables taken into consideration are current speed, speed of the leading car, speed limit of the road, maximum acceleration and deceleration, reaction time of the driver, and the following gap. These variables describe the properties of driver and vehicle as well as the relationship between leading car and ego car and aim to imitate the behavior of real drivers and vehicles in car-following situations.

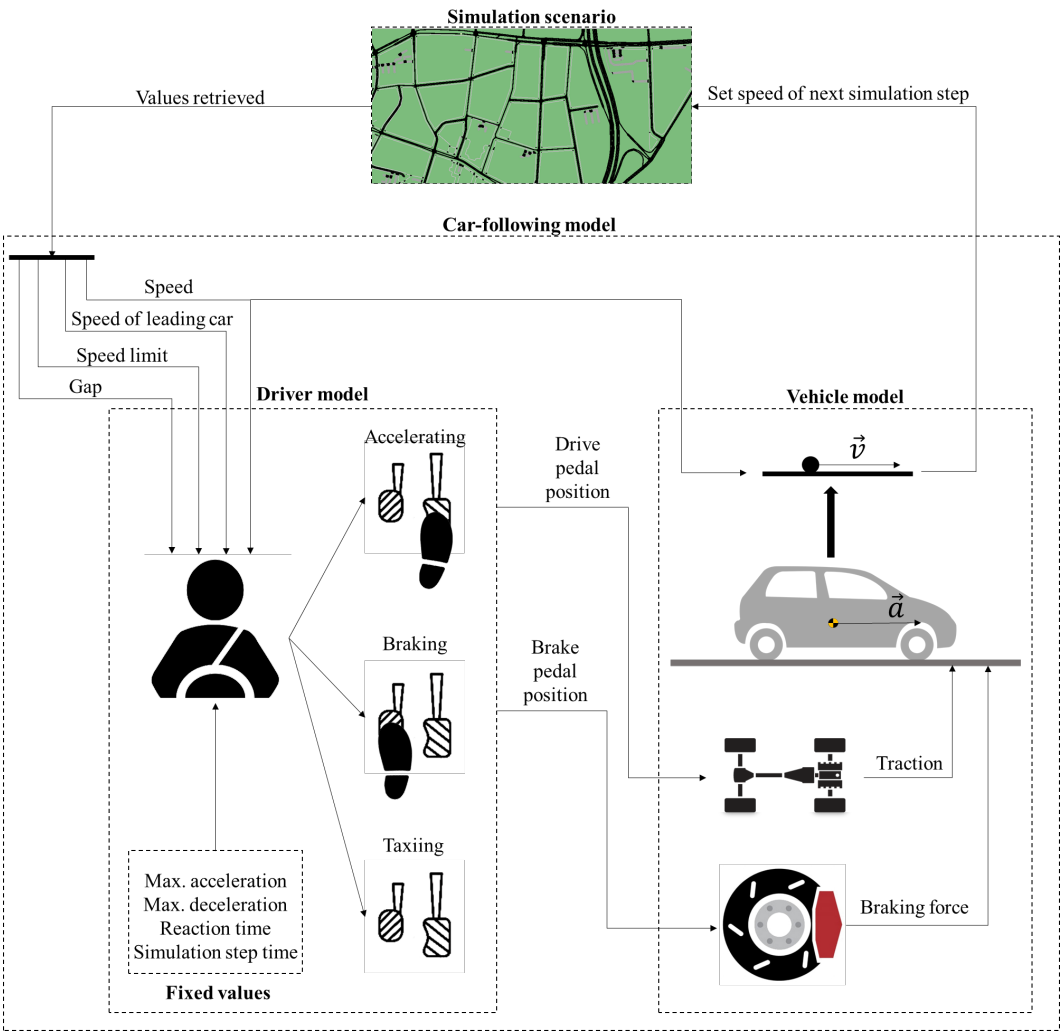

Figure 3.4 Architecture and data flow of the proposed car-following model

As mentioned earlier in this Chapter, the car-following model consists of a driver part and a vehicle part. If lane change and steering are not considered, the driver's remaining task when operating the vehicle is to actuate the drive and brake pedals. The position of the accelerator and brake pedal determined by the driver is first converted into the driving or braking force in the vehicle part of the car-following model.

The vehicle part model then calculates the vehicle speed in the next simulation step depending on the driving force and the current driving state of the vehicle.

The overall architecture of car-following model is illustrated in Figure 3.4. The detailed modeling progress of driver and vehicle is in introduced in following Chapters.

4 Driver Part of the Car-Following Model

In this Chapter first the necessary modeling assumptions and implementation conditions of the driver model are clarified. A driver model based on fuzzy logic and a driving experiment has been used in this thesis. The structure and the parameterization of this driver model are then introduced.

4.1 Modeling Assumptions and Conditions

Firstly, some more detailed modeling assumptions and implementation conditions by driver modeling are further clarified:

- The driver model in this thesis describes only the car-following behavior in a single lane. More precisely, the driver model imitates the human driver's operation of the drive pedal and braking pedal. The pedal position is the only output variable of the model. Actuation of the steering wheel is not considered.
- The driver model is time discrete. Therefore, the output of the driver model is only based on the values of corresponding parameters during the last simulation step.

When driving a car in real world, the behaviors of human drivers are quite different from a machine. Drivers have different driving experiences and driving habits. In some driving conditions, the intuition can also influence the drivers' operation. All these factors make it quite difficult to imitate the drivers' behaviors using classical control theory when we think of the human driver as a control system. Human drivers' behavior is quite nonlinear, which means it is hard to numerically describe this behavior (Ivanov 2015). As mentioned in Section 3.3, the driver model needs to process several input variables at the same time, which raise the modeling difficulty extremely no matter using mathematical methods or classical control theory.

For the modeling of a nonlinear system with multiple inputs, the artificial intelligence seems to be quite suitable. AI model can indeed imitate the drivers' behavior. However, an AI model is normally very complex and will put much computation

load to the computer. As the large number of vehicles in simulation need to be processed in each step, the complexity and computing speed of the model have also to be taken into consideration. For a long-term traffic simulation, i.e., 24 hours, the simulation time step is usually set to 1 second. Therefore, it can be considered to implement a model into simulation, which can roughly imitate the drivers' behavior, whilst not putting too much computation load to the computer. Finally, the fuzzy control system was selected as the main part of driver model. Fuzzy logic is one of the computational intelligence methods and has been used in various automotive engineering applications (Ivanov 2015). In the 1980s the fuzzy sets have been applied for the representation of perception characteristics of the driver (Kramer and Rohr 1982; Kramer 1985). Since it will not put too much computation load to the computer, a fuzzy model is quite suitable for simulating a large scenario.

4.2 Description and Parameterization of the Used Driver Models

In this thesis, a driver model based on fuzzy logic (Ma et al. 2021) has been used. The overall structure of the driver model is illustrated in Figure 4.1.

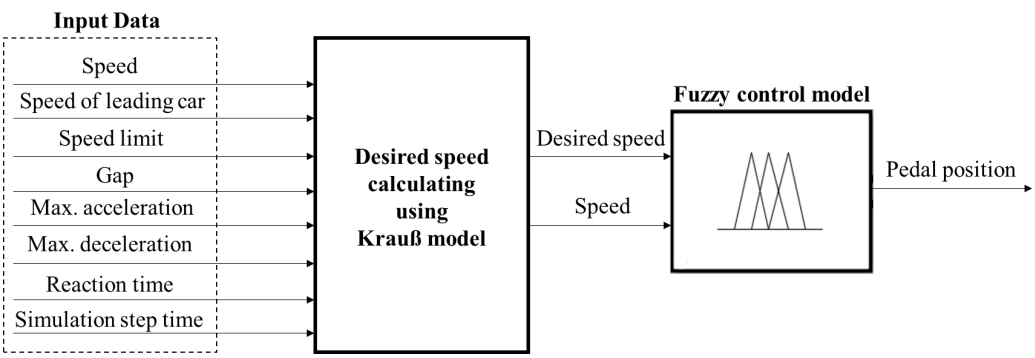

Figure 4.1 Architecture and data flow of the driver model (Ma et al. 2021)

Figure 4.1 shows that the input data are firstly processed with the Krauß model, in order to reduce the complexity of the fuzzy control model (Ma et al. 2021). The complexity of the fuzzy control model is determined by the number of fuzzy rules and related to the number of input variables. Here a fuzzy control system with double input variables and single output variable is taken as an example. When each input variable is described by 10 membership functions, there will be at least 10^2, i.e., 100 fuzzy rules to describe the relationship between input and output variables. If the number of input variables becomes 3, the minimal number of rules rises to 10^3.

As presented in Figure 3.4 the driver model needs to process 8 different input variables, which results in a quite complicated model. For decreasing the modeling difficulty, these 8 input variables need to be integrated and pre-processed. When driving a real car, drivers cannot intuitively get the values of all these variables. Many values are obtained by estimating, e.g., speed of leading car, gap, current maximal acceleration, and deceleration of vehicle, while desired speed and current speed are two quite intuitive variables. Therefore, current speed v and driver's desired speed $v_{desired}$ were used as the input variables of the fuzzy control model. These two variables can on the one hand from both, objective and subjective sides, determine the action of driver model. On the other hand, these two variables are very intuitive and controllable, which helps to simplify the following human driver experiment.

This chosen driver model still differs from real driving. In real driving all related variables directly determine the operations initiated by the driver. But in this driver model, the desired speed was used as an intermediate variable, through which other variables can just affect the driver's operation. However, in terms of the relationship between input and output variables, this driver model is closer to real human driver behavior than typical car-following models or classical control models.

4.2.1 Model for Driver Desired Speed

Like in the models by Gipps and the model by Krauß presented in Chapter 2, the following functions were used for calculating the desired speed in the driver model (Hu et al. 2020):

$$v_{desired} = \min\left[v_{safe}, v_{max}, v(i) + a_{max}T\right], \tag{4.1}$$

$$v_{safe} = -\tau b_{max} + \sqrt{(\tau b_{max})^2 + v_l(i)^2 + 2b_{max}G(i)}, \tag{4.2}$$

where v_{safe} is the safe speed, v_{max} is the speed limit of the road, $v(i)$ is current ego speed in step i, a_{max} is the maximum acceleration, T is the simulation time step, b_{max} is the maximum deceleration, τ is driver's reaction time, $v_l(i)$ is the speed of the leading vehicle, $G(i)$ is the following gap.

Table 4.1 lists the values of the variables in the desired speed model. The recommended values of τ and T in (Krauß et al. 1997) have been used. In the default passenger car-following model in SUMO, a_{max} and b_{max} are set to 2.6 m/s^2 and 4.5

m/s^2, respectively. However, these values of a_{max} and b_{max} are greatly higher than the acceleration and deceleration in daily driving. Therefore, the speed profiles of the NEDC (New European Driving Cycle) and the WLTP (world harmonized light-duty vehicles test procedure) were analyzed for finding out the suitable values of a_{max} and b_{max}.

NEDC has been widely used in Europe for accessing fuel economy of passenger cars for years. It consists of four repeated urban driving cycles and an extra-urban driving cycle. However, the NEDC was designed many years ago and last updated in 1997. Criticisms about NEDC also came out with the passage of time, e.g., it cannot represent the real-life driving, so that the actual fuel consumption of the vehicle is always different from the NEDC-test result (Schüller et al. 2016). WLTP is developed as the successor of NEDC and developed to better match the test estimates of fuel economy with measures of real-life driving condition (UNECE). The maximum and minimum acceleration in the entire NEDC is 1.06 m/s^2 and -1.39 m/s^2, respectively, while in the WLTP it is 1.75 m/s^2 and -1.5 m/s^2. The maximum and minimum acceleration in the NEDC and the WLTP was used for setting a_{max} and b_{max} in the desire speed model.

a_{max} and b_{max} belong to the parameters of the desired speed model. They impact but do not limit the actual acceleration of the car-following model. When necessary, e.g., in emergency situations, the vehicle can also brake with higher acceleration than b_{max}.

Table 4.1 Fixed values in the desired speed model

Variable name	Symbol	Value
Maximum acceleration /$m \cdot s^{-2}$	a_{max}	1.75
Maximum deceleration /$m \cdot s^{-2}$	b_{max}	1.5
Driver's reaction time /s	τ	1
Time step /s	T	1

4.2.2 Fuzzy Control Model of the Drive/Brake Pedal Position

After pre-processing, the input variables of the driver model can be represented by two variables, vehicle speed and driver desired speed. The transfer process from

vehicle speed and desired speed to pedal position was completed by a fuzzy control model (Ma et al. 2021).

The fuzzy control system is a control system based on fuzzy logic (Hájek 2013). It is a kind of intelligent control system. In a fuzzy control system, the analogue variables are firstly converted to fuzzy variables, which are continuous variables between 0 and 1 and differ from the digital discrete variables. This process is called fuzzification. Through a set of linguistic rules, which are established by designer, a connection between input and output fuzzy variables is built. The output variable can be converted through defuzzification back to analogue values for a precise control.

Fuzzy control can greatly simplify the design of a control system, especially suitable for systems with nonlinear, time-varying, and incomplete models. The complete mathematical model for the controlled objects is no more necessary using fuzzy control. The linguistic design method is quite friendly for system designing by non-professionals. And for non-professionals it is also possible to establish a control system with good robustness and fault-tolerance.

Figure 4.1 shows that the drive/brake pedal position is finally output by fuzzy control model. The fuzzy control model was established based on a driving test in a driving simulator with 34 subjects (Ma et al. 2021).

For ease of understanding, the desired speed was replaced with the difference between desired speed and current speed $v_{difference}$ as one of the input variables of the fuzzy model. The other input variable remains current speed. Figure 4.2, Figure 4.3, and Figure 4.4 show the fuzzy sets of input and output variables used in the driver model.

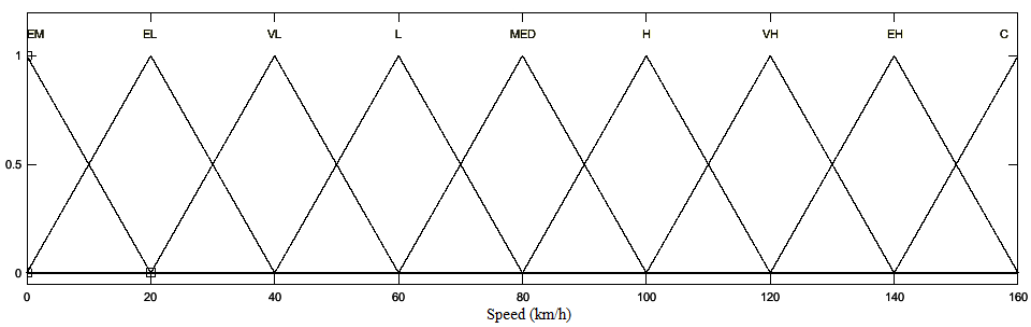

Figure 4.2 Fuzzy set of current speed (Ma et al. 2021)

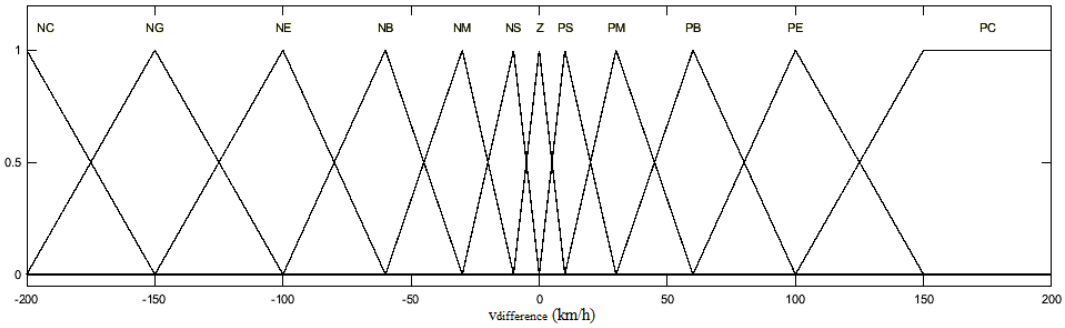

Figure 4.3 Fuzzy set of speed difference (Ma et al. 2021)

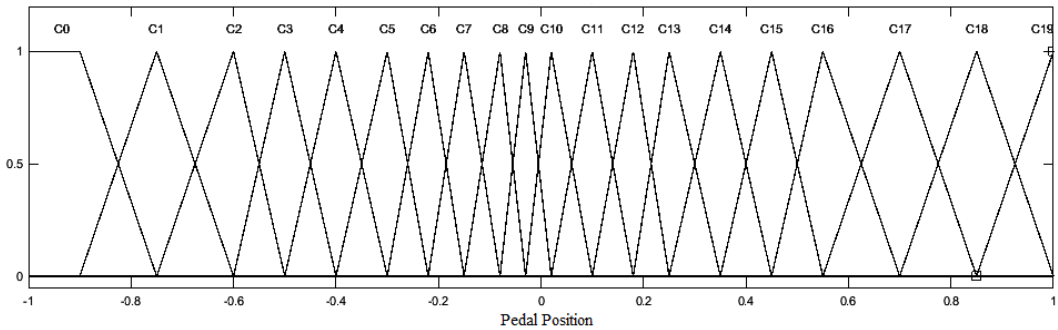

Figure 4.4 Fuzzy set of pedal position (Ma et al. 2021)

Based on the collected data from the human drivers in the driving simulator, a set of fuzzy rules was generated. The final fuzzy rule set is listed in Table 4.2. The cells in grey were manually added. They correspond to the situations that will never happen in real driving, e.g., when the current speed is 0 km/h while the desired speed is -200 km/h. The other fuzzy rules were based on the driving simulator test results (Ma et al. 2021).

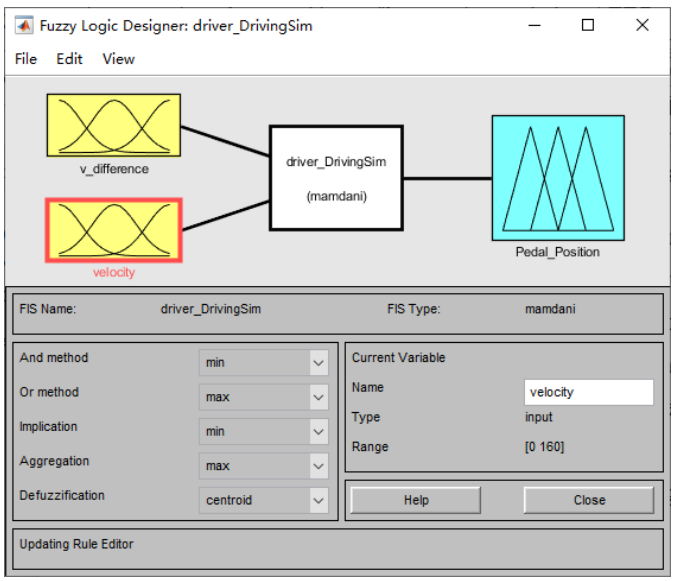

Figure 4.5 Fuzzy model using Fuzzy Logic Toolbox in MATALB

Table 4.2 Fuzzy rule set of the fuzzy model (Ma et al. 2021)

$v_{difference}$ \ v	EM	EL	VL	L	MED	H	VH	EH	C
NC	C0	C0	C0	C0	C0	C0	C0	C0	C0
NG	C1	C1	C1	C1	C1	C1	C1	C1	C1
NE	C2	C2	C2	C2	C2	C2	C1	C2	C1
NB	C3	C3	C3	C1	C2	C2	C2	C2	C2
NM	C5	C5	C3	C2	C2	C2	C3	C3	C3
NS	C6	C4	C3	C3	C3	C4	C4	C4	C5
Z	C2	C10	C11	C11	C11	C12	C13	C13	C14
PS	C14	C14	C14	C14	C14	C14	C15	C15	C15
PM	C17	C14	C15	C16	C16	C16	C16	C16	C16
PB	C17	C17	C17	C16	C17	C17	C17	C17	C17
PE	C18	C18	C18	C18	C17	C17	C17	C17	C18
PC	C18	C18	C18	C18	C18	C18	C19	C19	C19

MATLAB provides a tool for fuzzy control system design and use, the Fuzzy Logic Toolbox. The fuzzy control part of the driver model was also based on it. The fuzzy model built in MATLAB is shown in Figure 4.5. Thus, the driver desired speed model and fuzzy model together constitute the complete driver model in this thesis.

The fuzzy rules in Table 4.2 were generated based on the driving behaviors of drivers in the driving simulator. Therefore, the rules may be inapplicable when the dynamic features of the vehicle have been changed. The drive model needs to be further calibrated when implemented with other vehicle models. The calibration of the driver model is introduced in the next Chapter after that the vehicle models have been established.

5 Vehicle Modeling of the Car-Following Model

In this Chapter the modeling process of the conventional and the electric vehicles is introduced. Firstly, the modeling assumptions are clarified. Then the physical model of the entire vehicle and its components are introduced. The driver model is also calibrated with different vehicle models. This concludes the modeling of the car-following behavior in this thesis.

5.1 Modeling Assumptions

The function of the vehicle part in the car-following model is to determine the vehicle speed for the next simulation step depending on the operation input from driver and the external force on the vehicle. Similarly, some modeling assumptions and implementation conditions are clarified.

- In this thesis, only passenger cars are considered. The passenger cars are hereby roughly divided into three categories: small cars, mid-sized cars, and large cars.
- Geometrically, each vehicle in the simulation is represented by a two-dimensional, planar rectangular.
- Physically, the vehicle is simplified by a particle, which moves one-dimensionally along the lane and is subject to driving resistance and traction force.
- As the traffic simulation is time-discrete, static component models were used for the analysis of the forces acting on the vehicle. For the same reason, the clutch and gear shifting process of fossil fuel-powered vehicles are difficult to simulate. Thus, clutch and gear shifting process are ignored in the vehicle model. Engine torque is 100% transmitted to the gearbox at any time. And in each simulation step the gear is only selected depending on the current speed and independent of the gear selection of the previous step.

- For simplifying the model and improving computation speed, wheels and tires are reduced to rigid bodies, i.e., tire deformation and tire slip are not considered.
- The regenerative braking function of electric vehicles in this Chapter, when calculating the velocity and the acceleration of the vehicle, is not considered.

5.2 Physical Model of Vehicle

The purpose of the physical model is to obtain the speed and acceleration of the vehicle through mechanical analysis of the entire vehicle. Generally, the force on the vehicle can be represented as shown in Figure 5.1.

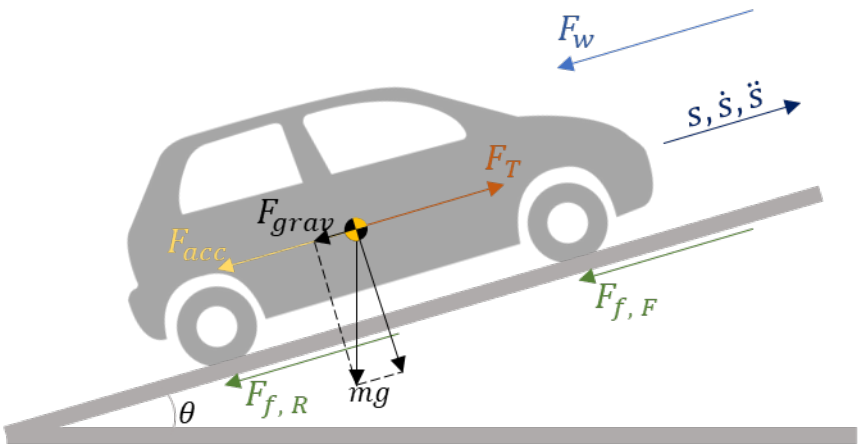

Figure 5.1 Force analysis of a vehicle

In Figure 5.1, m is the vehicle mass, g is acceleration of gravity, θ is the slope of the road, F_T is the traction force on the vehicle, $F_{f,F}$ is rolling resistance on the front wheel, $F_{f,R}$ is rolling resistance on the rear wheel, F_{acc} is the acceleration resistance caused by inertia, F_{grav} is the component of gravity, F_w is wind drag, s is the displacement of the vehicle, $\dot{s}$ is the vehicle speed, i.e. v, and $\ddot{s}$ is the acceleration of vehicle, i.e. a.

As mentioned before, the road network of this traffic simulation is two-dimensional, i.e., θ is always 0. As $F_{grav} = mgsin\theta$, F_{grav} is also 0. When the vehicle is simplified into a particle, the force on vehicle can be illustrated by Figure 5.2.

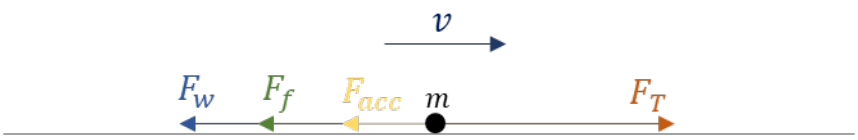

Figure 5.2 Force analysis of simplified vehicle model when accelerating

F_f is the total rolling resistance.

According to Newton's second law, Figure 5.2 can also be expressed by the equation

$$F_T - F_f - F_w - F_{acc} = ma. \tag{5.1}$$

Here all variables are scalar. When the brake pedal is actuated, the force analysis can be illustrated by Figure 5.3. F_b is the braking force on vehicle.

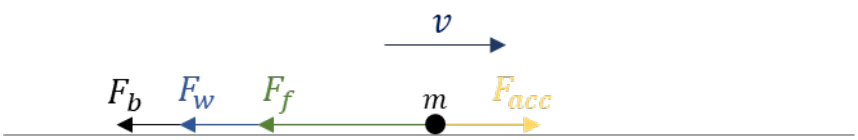

Figure 5.3 Force analysis of simplified vehicle model when braking

In Figure 5.3, the vehicle moves from left to right. The wind drag F_w and the rolling resistance F_f are always opposite to the direction of vehicle movement, and they keep the same direction as in Figure 5.2. However, F_{acc} is caused by the inertia of vehicle itself and the rotating parts such as engine crankshaft and flywheel. F_{acc} always keeps the vehicle moving at a constant speed. When braking as in Figure 5.3, the acceleration of vehicle is leftward. Therefore, the direction of F_{acc} has changed in Figure 5.3.

Altogether Figure 5.3 can be represented by

$$-F_b - F_f - F_w + F_{acc} = ma. \tag{5.2}$$

In simulation, the speed of the vehicle can be calculated by

$$v_{i+1} = v_i + aT, \tag{5.3}$$

where i is the number of simulation step, v_i is vehicle speed in step i, T is time step.

The driving resistances are expressed by

$$F_f = mgf, \tag{5.4}$$

$$F_w = \frac{1}{2} C_d \, \rho_{air} \, A_f \, v^2, \tag{5.5}$$

$$F_{acc} = (m + I_{RP}) \, a = \lambda m a, \tag{5.6}$$

where f is the rolling resistance coefficient, C_d is the drag coefficient, ρ_{air} is the air density, A_f the projected frontal area of the vehicle, I_{RP} represents the rotational inertia of the rotating parts. For calculation convenience, the coefficient λ was used here for determining the acceleration resistance.

The calculation method of F_T and F_b are explained in the following component modeling parts.

5.3 Components Modeling for Fossil Fuel-powered Passenger Vehicles

As mentioned in Section 5.1, there are three categories of passenger vehicles to simulate. According to the classification from European NCAP (New Car Assessment Programme), small car, mid-sized car and large car simulation models in this thesis correspond to Supermini-class, small family car and large family car, respectively. These three classes of cars were equipped with suitable conventional and electric powertrains, respectively. Thus, there are up to 6 kinds of vehicles in a single simulation. In this Section, the modeling for ICEVs is introduced.

The power transmission process is illustrated in Figure 5.4. When accelerating, the driving torque is directly transmitted to the gearbox without clutch. This torque is then transmitted by the gearbox and the final drive to the wheel.

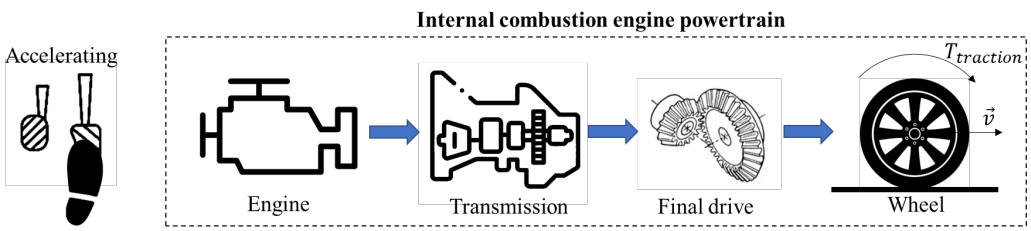

Figure 5.4 Internal combustion engine powertrain model

Some ADVISOR models are used for vehicle modeling. ADVISOR is an expansion pack for use with MATLAB and Simulink, including a set of models, data, and

script files about vehicle dynamics. Its main usage is to analyze dynamic performance and energy consumption of fossil fuel-powered, electric, and hybrid vehicles. ADVISOR provides some example models and the corresponding data. Figure 5.5 shows the graphical user interface (GUI) of ADVISOR, where the configuration of the vehicle data can be set. On the right side of this interface, many component models for different kinds of vehicle can be loaded here. The vehicle modeling in this thesis is also based on these models and data.

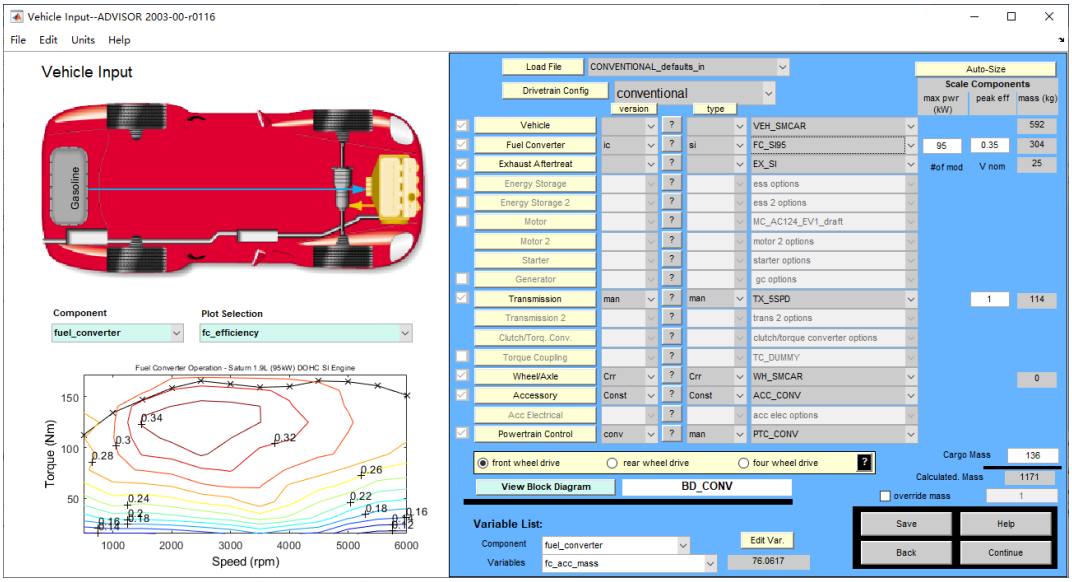

Figure 5.5 GUI of ADVISOR with an example conventional passenger vehicle

5.3.1 Internal Combustion Engine Model

In Figure 5.4, the internal combustion engine model firstly converts the drive pedal position to engine torque. The ICE model essentially describes the static relationship between drive pedal position, speed and output torque. Here, petrol engine model FC_SI95 and FC_SI102 from ADVISOR have been used as the engine for small car and mid-sized car, respectively. FC is the abbreviation for fuel converter, while SI means spark ignition. FC_SI95 was based on Saturn 1.9L 95-kW DOHC Engine (Reilly et al. 1991) and is the recommended engine model for small cars in ADVISOR. FC_SI102 was based on 1991 Dodge Caravan 3.0L (102-kW) Engine and used here for mid-sized car. The maximum torque of the FC_SI102 engine model is however always lower than the FC_SI95 model under 2500 rpm. ADVISOR has indicated an acceptable accuracy in the file of FC_SI95, while in the file of FC_SI102 there is no description about the data confidence level. Therefore, the

FC_SI102 model has been modified based on the original data in FC_SI102, as well as the data of FC_SI95.

As in ADVISOR there is not a suitable engine model for large car, the dyno test result of an Audi A6 (C7) 3.0 TFSI (Dyno-ChiptuningFiles.com) was used. Since in the dyno test the engine torque between 500 rpm and 1500 rpm was not tested, the corresponding data were manually added.

Maximum engine torque corresponds to the working point of 100% drive pedal position. When the drive pedal is at 0% position, i.e., the throttle is closed, the engine torque is negative because of the frictions inside the engine. According to the calculation method of the closed throttle torque in ADVISOR engine models, the closed throttle torque of engine is related to the rotating speed and the engine displacement. The curves of the maximum torque of the three sizes of internal combustion engine are illustrated in Figure 5.6. The engine torque at drive pedal position between 0 to 100% was linear mapped between the maximum torque curve and the closed throttle torque curve.

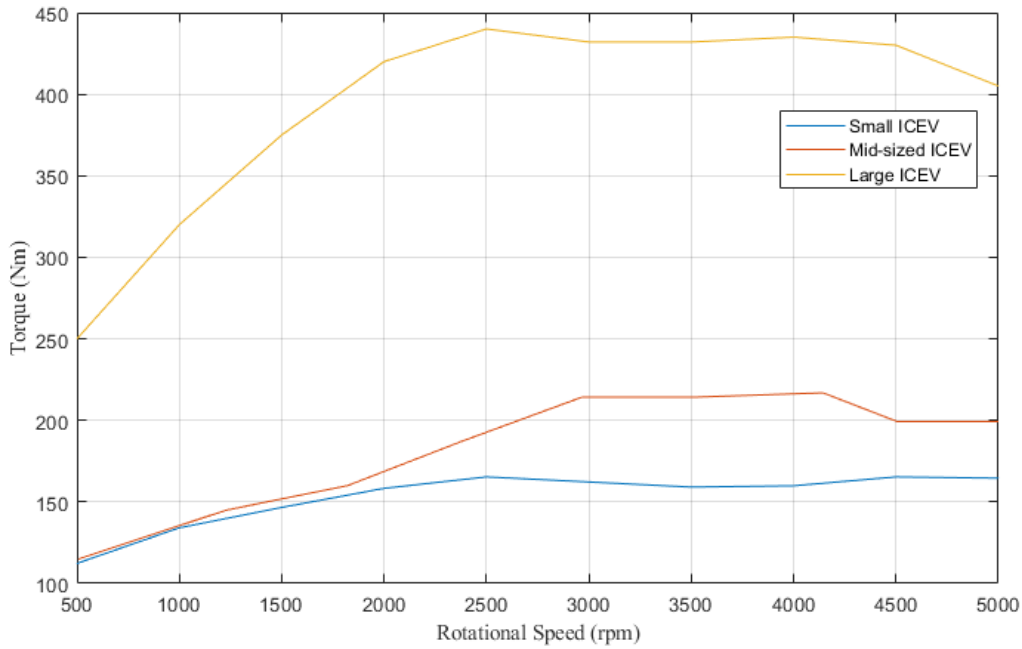

Figure 5.6 ICE torque map of the three sizes of vehicles

5.3.2 Gearbox, Final Drive and Wheel

For the transmission, the TX_5SPD_SI model in ADVISOR was used for all three ICEV models. This is a model of a 5-speed transmission for a gasoline engine. The transmission ratios are listed in Table 5.1.

Table 5.1 Transmission ratio and efficiency

Gear No.	Transmission Ratio i_G	Efficiency η_G
1st	3.46	0.92
2nd	1.94	
3rd	1.29	
4th	0.97	
5th	0.81	

The parameters of the final drive for three ICEV models are also same, transmission ratio i_D = 3.67 and efficiency η_D = 0.95.

For three ICEV models, three different wheel models have been chosen from ADVISOR. The detailed parameters are listed in Table 5.2.

Table 5.2 Parameters of wheel models

Vehicle type	Original model in ADVISOR	Dynamic radius r_{dyn} /m
For small car	185/70R14	0.282
For mid-sized car	P205/60R15	0.304
For large car	P225/60R16	0.33

Since tire deformation and slip are not considered, the wheels are equivalent to non-deformable cylinders whose radius is determined by the dynamic radius of the wheel.

Thus, the traction force on the vehicle, F_T in Equation (5.1), can be obtained by

$$F_T = \frac{T_m i_G i_D \eta_G \eta_D}{r_{dyn}}, \tag{5.7}$$

where i_G is the transmission ratio of the current gear, T_m is the output torque from the engine. T_m is determined by the drive pedal position and engine rotation speed n_{motor}. n_{motor} is obtained by

$$n_{motor} = n_{wheel} i_G i_D, \tag{5.8}$$

$$n_{wheel} = \frac{60 \cdot v}{2\pi r_{dyn}}, \tag{5.9}$$

where n_{wheel} is the rotation speed of wheel in rpm, v is current vehicle speed in m/s.

5.3.3 Shifting Strategy

The function of the gearbox of an ICEV is to extend the range of engine rotation speed and torque, and make engine working at higher efficiency points as much as possible. Figure 5.7 shows the efficiency characteristics of FC_SI95 engine model, which can represent the typical efficiency character of petrol engines. From Figure 5.7 it can be seen that, if torque maintains the same, from about 1,500 rpm to 3,500 rpm the efficiency of engine is relatively high. At about 2,500 rpm engine has the highest efficiency. Therefore, the main target of shifting strategy is to maintain the rotation speed of engine around 2,500 rpm.

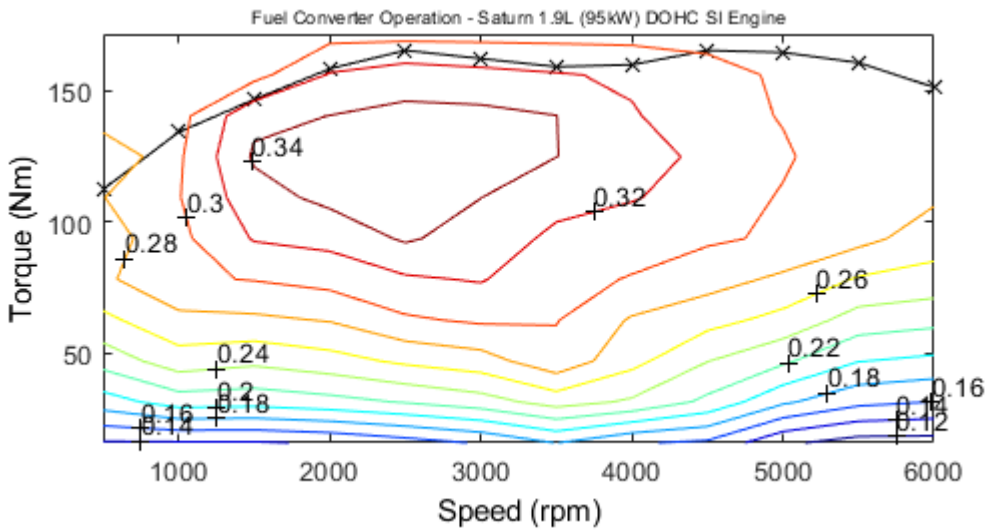

Figure 5.7 Efficiency of FC_SI95 engine model in ADVISOR

As the shifting progress is ignored in the simulation, in each simulation step the gear can be independently selected, without considering the previous gear selection. Then the shifting strategy is to control the engine speed depending on vehicle speed.

The gear distribution of 3 vehicle models is listed in Table 5.3, Table 5.4 and Table 5.5.

Table 5.3 Gear selection and engine speed distribution of small car

Gear No.	Small car	
	Vehicle speed interval /km·h^{-1}	Engine speed interval /rpm
1st	$0 \leq v \leq 19$	500 ~ 2,269
2nd	$19 < v \leq 35$	1,272 ~ 2,343
3rd	$35 < v \leq 53$	1,558 ~ 2,360
4th	$53 < v \leq 70$	1,775 ~ 2,344
5th	> 70	1,957 ~ 6,000

Table 5.4 Gear selection and engine speed distribution of mid-sized car

Gear No.	Mid-sized car	
	Vehicle speed interval /km·h^{-1}	Engine speed interval /rpm
1st	$0 \leq v \leq 19$	1,230 ~ 2,105
2nd	$19 < v \leq 35$	1,180 ~ 2,174
3rd	$35 < v \leq 53$	1,446 ~ 2,189
4th	$53 < v \leq 70$	1,646 ~ 2,174
5th	> 70	1,816 ~ 4,875

Table 5.5 Gear selection and engine speed distribution of large car

Gear No.	Large car	
	Vehicle speed interval /km·h^{-1}	Engine speed interval /rpm
1st	$0 \leq v \leq 23$	1,500 ~ 2,348
2nd	$23 < v \leq 35$	1,316 ~ 2,003
3rd	$35 < v \leq 53$	1,332 ~ 2,017
4th	$53 < v \leq 70$	1,673 ~ 2,003
5th	> 70	1,673 ~ 6,000

5.3.4 Braking System Model

A model of a disk brake system has been implemented in the simulation. When the vehicle model receives the braking pedal position from the driver model, a braking torque T_{brake} is output from the braking model. The relationship between braking pedal position and braking torque can be seen in Figure 5.8.

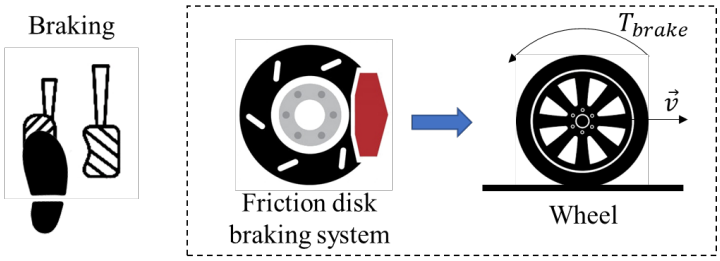

Figure 5.8 Braking system model

The braking force F_b in Equation (5.2) is obtained by

$$F_b = {}^{T_{brake}}/_{r_{dyn}}. \tag{5.10}$$

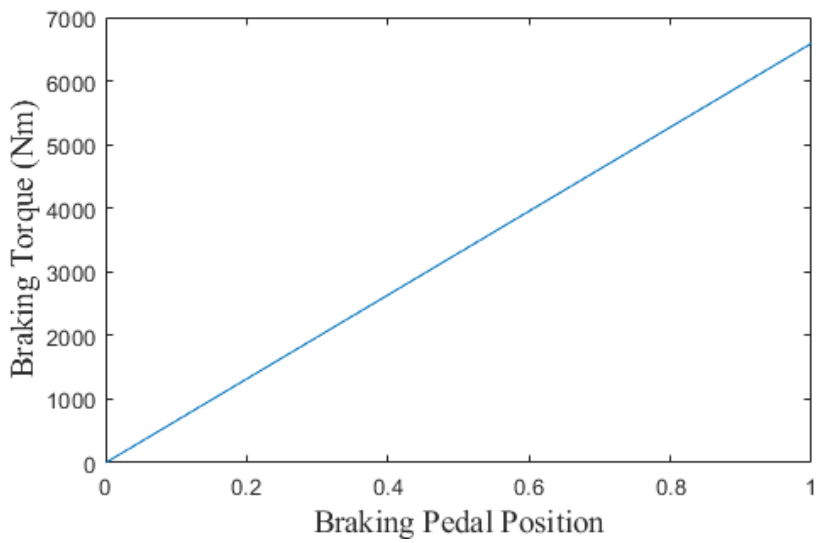

Figure 5.9 Relationship of braking torque and braking pedal position

5.4 Components Modeling for Electric Passenger Vehicles

The main difference between fossil fuel-powered vehicles and an electric vehicle is the structure of the powertrain. Since the electric motor can operate in a wider speed range and still delivers torque even at 0 rpm, a transmission in an electric vehicle is

generally no longer necessary. Thus, when accelerating, the power transmission of an electric powertrain can be represented by Figure 5.10.

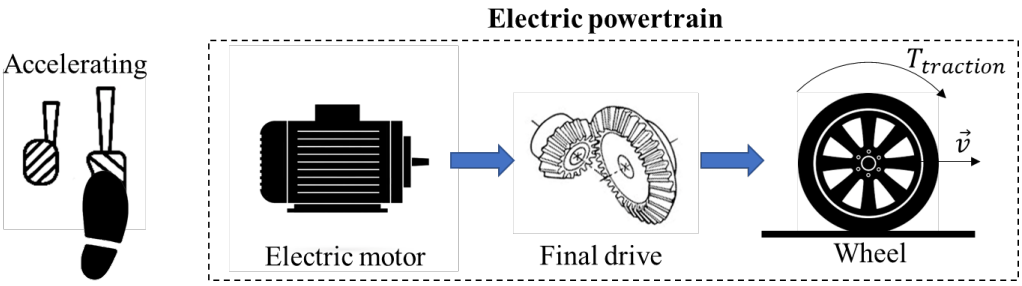

Figure 5.10 Braking system model

For an electric vehicle model, the traction force F_T can be obtained as

$$F_T = \frac{T_m i_D \eta_D}{r_{dyn}}, \tag{5.11}$$

where T_m is the torque of the electric motor.

Similar to the model of the internal combustion engine, the model of the electric motor is described by a look-up table that relates accelerator pedal position, speed and torque. For small car, mid-sized car and large car, electric motor models MC_PM49, MC_AC75 and MC_AC187 in ADVISOR were selected, respectively. MC is the abbreviation for motor/controller, PM means permanent magnet motor, AC represents 3-phase AC induction motor, and the number stands for the continuous power of the corresponding motor in kW. Figure 5.11 shows the maximum torque at different speeds of the electric motors.

From Figure 5.11 it can be seen that electric motors can maintain a constant maximum torque in a certain speed interval. After that the motors operate in constant power mode.

If comparing the electric motor and ICE for a small car, Figure 5.12 shows the result. This Figure shows the dynamic characteristic difference between electric motor and ICE. The speed interval of an electric motor is much wider than as that for an ICE. PM49 is a 49-kW electric motor, while SI95 is 95 kW. However, at lower rotation speeds the electric motor can provide a much higher torque than ICE. This is one reason that electric vehicles are more suitable for urban traffic.

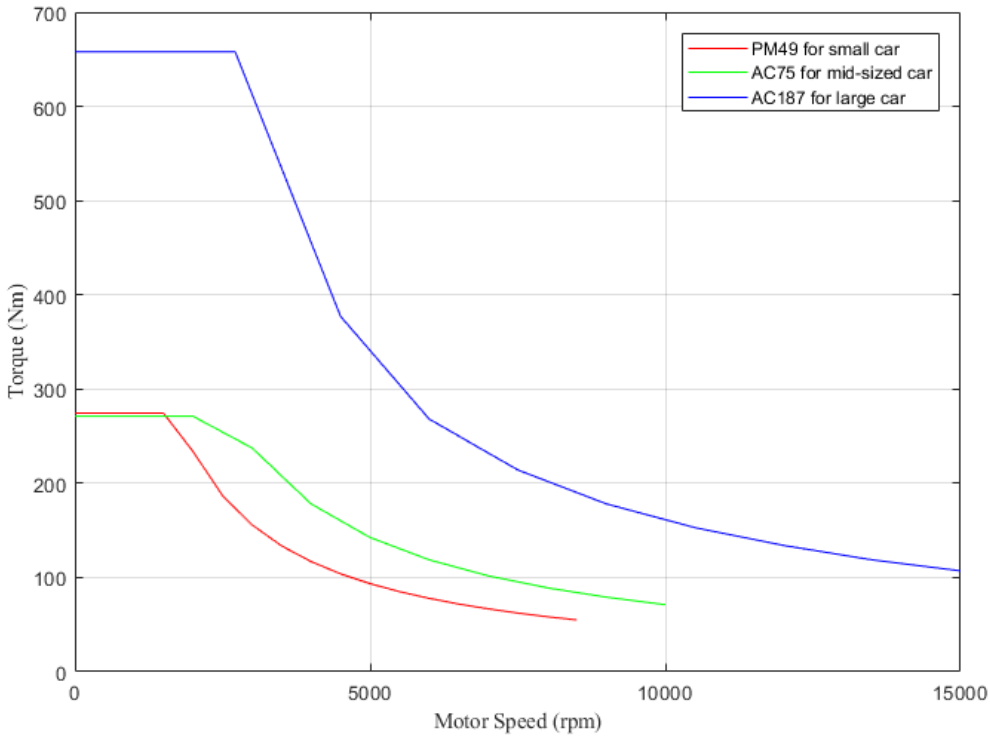

Figure 5.11 Maximum torque of electric motors

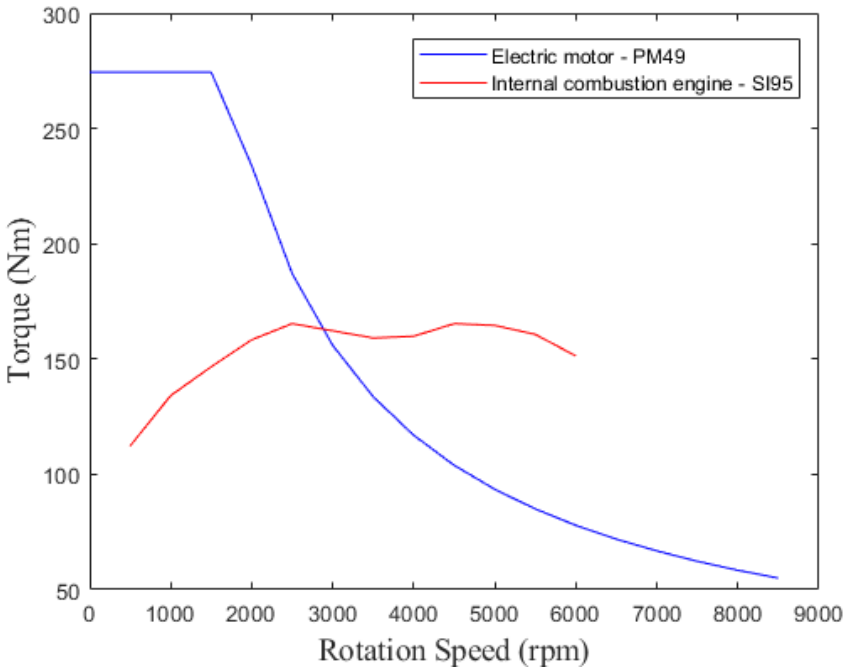

Figure 5.12 Maximum torque of electric motor and internal combustion engine

Electric vehicles have the ability of energy recycling, i.e., converting kinetic energy back into electrical energy during braking. However, most electric vehicles are still equipped with a conventional braking system. When braking, the micro control system distributes the braking torque request to the electric motor and the disk brake

system. The braking pedal position is equivalent to the braking torque request. Therefore, the main difference of the braking systems in EVs and ICEVs is the provision of braking torque, while the relationship of braking pedal position and total braking torque of vehicle in an electric vehicle is not significantly different from the ICEVs. Consequently, the same braking system model was used in the EV model and the ICEV model.

5.5 Vehicle Parameters

The vehicle models in this thesis were divided into three categories according to the size of the vehicle: small car, mid-sized car, and large car. They were based on the vehicle models in ADVISOR, i.e., VEH_SMCAR, VEH_midSizeCar, and VEH_largeCAR, respectively. Therefore, most of the vehicle parameters are from these three models in ADVISOR.

Table 5.6 Parameters of fossil fuel-powered vehicle models

Parameter	Symbol	Fossil fuel-powered vehicle		
		Small car	Mid-sized car	Large car
Mass / kg	m	1,146	1,650	1,961
Projected frontal area /m^3	A_f	2	2	2.1
Drag coefficient /-	C_d	0.335	0.304	0.3
Rolling resistance coefficient /-	f	0.009		
Air density /$kg \cdot m^{-3}$	ρ_{air}	1.2		

The parameters of fossil fuel-powered vehicle models are listed in Table 5.6. Mass consists of vehicle kerb weight and 136 kg cargo mass. The acceleration resistance of the ICEV model was calculated with the rotational inertias of the corresponding component models in ADVISOR. The acceleration resistance coefficient λ is hence not applicable for the ICEV models.

Since ADVISOR does not provide information about the mass of the battery, the mass of electric vehicles was derived from real vehicles. For the electric small car, the mass of Smart EQ fortwo was used here. For the electric mid-sized car and the large car, the mass of a Nissan Leaf and the Tesla Model S has been considered,

respectively. The detailed parameters of the electric vehicle models are listed in Table 5.7. 136 kg of cargo mass has also been added. The acceleration resistance coefficient λ of an electric passenger car was set to 1.1 in (Tewiele 2020) according to (Haken 2015). The factor λ of all the EV models in this thesis was approximately set to the same value.

Table 5.7 Parameters of electric vehicle models

Parameter	Symbol	Electric vehicle		
		Small car	Mid-sized car	Large car
Mass / kg	m	1,221	1,629	2,244
Projected frontal area /m^3	A_f	2	2	2.1
Drag coefficient /-	C_d	0.335	0.304	0.3
Rolling resistance coefficient /-	f	0.009		
Air density /$kg \cdot m^{-3}$	ρ_{air}	1.2		
Acceleration resistance coefficient /-	λ	1.1		

5.6 Calibration of the Driver Model for Vehicle Models

As many parameters of the vehicle models in this Chapter are different from the simulated vehicle of the driving simulator in Section 4.2, the driver model in Chapter 4 needs calibration for matching with the corresponding vehicle models. This is analogous to the fact that a driver needs some time to get used to a new car.

The fuzzy rule set, which is listed in Table 4.2, can determine how the driver model controls the vehicle model. Adjusting the corresponding fuzzy rules was the method to calibrate the driver model for different vehicle models in this thesis. The fuzzy rule set can be classified into two parts. The first part is the line, where $v_{difference}$ is zero, i.e., the line of Z in Table 4.2. For convenience, this line is called Z-line hereafter. The fuzzy rules in this line determine the pedal position when speed equals desired speed and reflects the control accuracy of driver about the vehicle speed. The drive pedal position only determines the output torque of the engine or the motor. When driving two cars with different engines or motors at the same speed,

the pedal position is most likely different. Therefore, this part of the fuzzy rule set needs to be adjusted for different vehicle model.

The other part is the rest of the fuzzy rules in Table 4.3. This part determines the reaction of the driver in different situations, more precisely, it determines more about the driving style. It can be considered that the driving style of the same driver in different vehicles might change not too much. Therefore, the calibration of the driver model for different vehicle models is mainly about adjusting the fuzzy rules in Z-line.

For finding the relationship between pedal position and speed for each vehicle model, the following test simulations were implemented. Initial speed of vehicle model was set to 0. A pedal position from 0 was given to the vehicle model to accelerate. If the speed of vehicle model in the current step increases less than 0.1 km/h, it means that vehicle model has reached the maximum speed at current pedal position. The corresponding pedal position and speed were recorded. Then the pedal is position increased by 0.01 to find out the next maximum speed, until the pedal position reached 1. Thus, the relationship between pedal position and corresponding maximum speed can be found. As an example, Figure 5.13 shows the corresponding data of conventional small car model.

Then, the corresponding pedal positions at 20 km/h, 40 km/h, 60 km/h, 80 km/h, 100 km/h, 120 km/h and 160 km/h were picked up. The nearest membership functions in fuzzy set of pedal position, i.e., Figure 4.5, were assigned. Consequently, the corresponding fuzzy rules in the Z-line can be determined. The adjusted fuzzy rules are listed in Table 5.8. Except in the Z-line, the rest of fuzzy rules remain the same in all vehicle models.

Thus, the vehicle models with corresponding driver models constitute car-following models for six types of vehicle.

Table 5.8 Calibrated fuzzy rules of driver model for all vehicle models

Vehicle type	Fossil fuel-powered			Electric		
	Small	Mid-sized	Large	Small	Mid-sized	Large
$v_{difference}$ / v	Z	Z	Z	Z	Z	Z
EM	C11	C13	C11	C11	C11	C11
EL	C12	C15	C11	C11	C11	C11
VL	C13	C16	C12	C12	C11	C11
L	C14	C17	C13	C13	C12	C11
MED	C15	C17	C13	C14	C13	C12
H	C16	C18	C14	C15	C14	C13
VH	C17	C18	C14	C17	C15	C14
EH	C17	C18	C14	C19	C17	C14
C	C18	C18	C15	C19	C18	C15

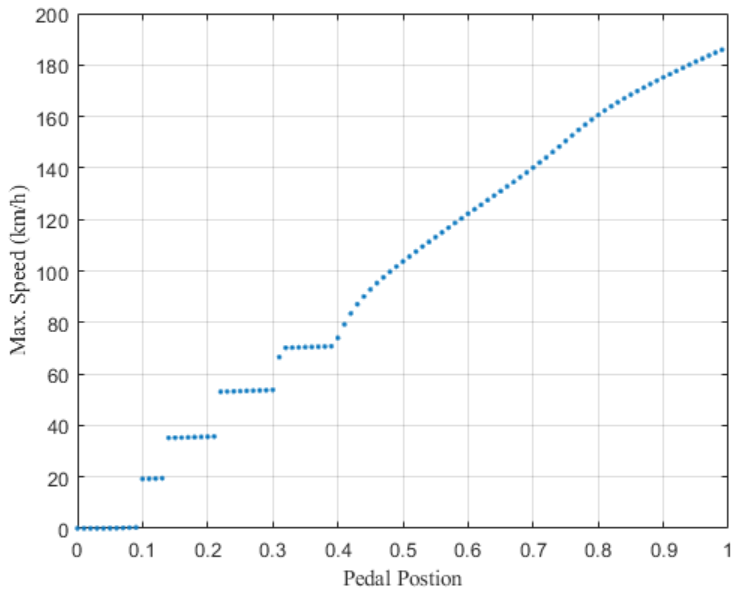

Figure 5.13 Maximum speed at different pedal positions of the conventional small car model

5.7 Comparing with the Default Model in SUMO

The default car-following model in SUMO is a modified Krauß model. A vehicle using this model will always drive with the constant maximum acceleration, especially when there is no leading car and the current speed is much lower than the limit.

However, for a real car it is impossible to always accelerate with a constant acceleration. According to Equation (5.5), the wind drags increase with the square of the speed. For an ICEV, the maximum torque at the wheels also varies at different engine speeds and in different gears. For comparing the characteristics of the car-following models, a scenario of 1 km straight road was built for a test. In the scenario, a vehicle accelerates from 0 km/h at starting point until to the speed limit of 50 km/h. This scenario was simulated with the Krauß model and proposed car-following model, respectively. The speed of the vehicle was tracked and compared with each other.

The speed tracks of the test vehicle using different models are shown in Figure 5.14, Figure 5.15, and Figure 5.16. These Figures do not show the maximum acceleration ability of corresponding vehicle models, but the accelerating progress of a human driver driving a car on a road with 50 km/h speed limit.

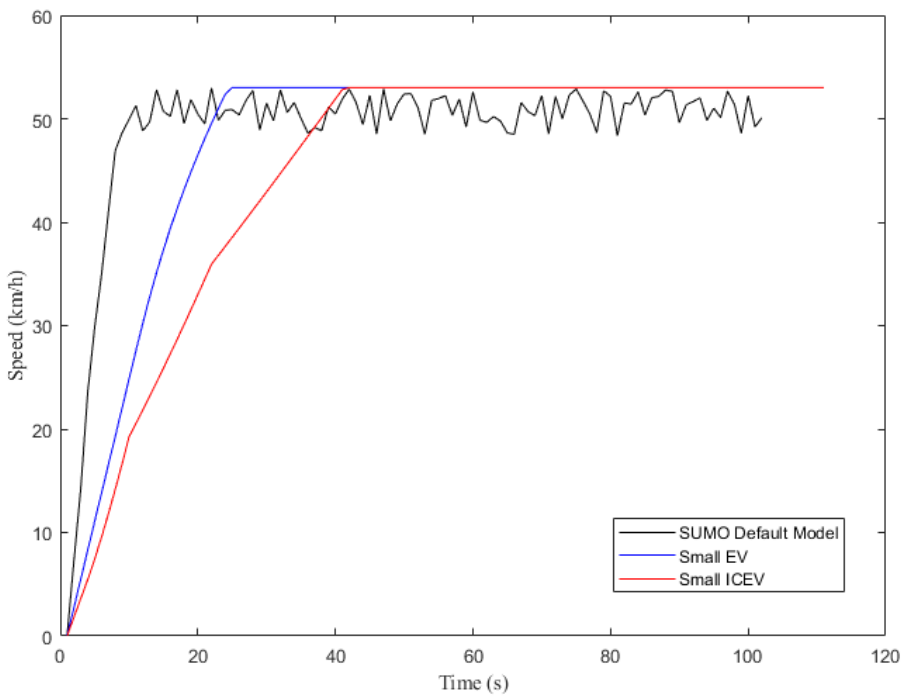

Figure 5.14 Comparing acceleration process of Krauß model and small car model

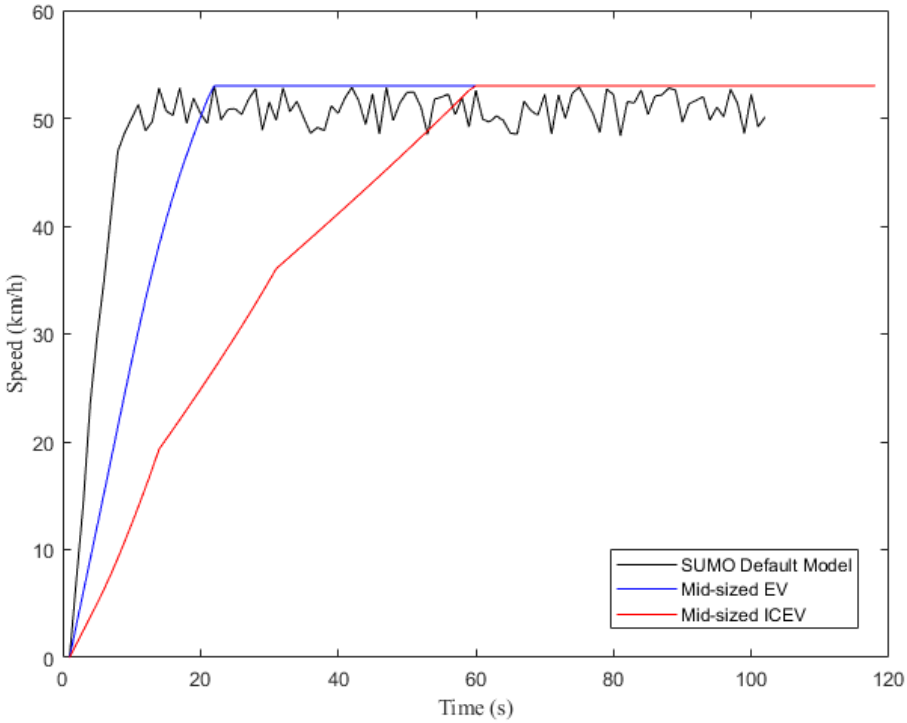

Figure 5.15 Comparing acceleration process of Krauß model and mid-sized car model

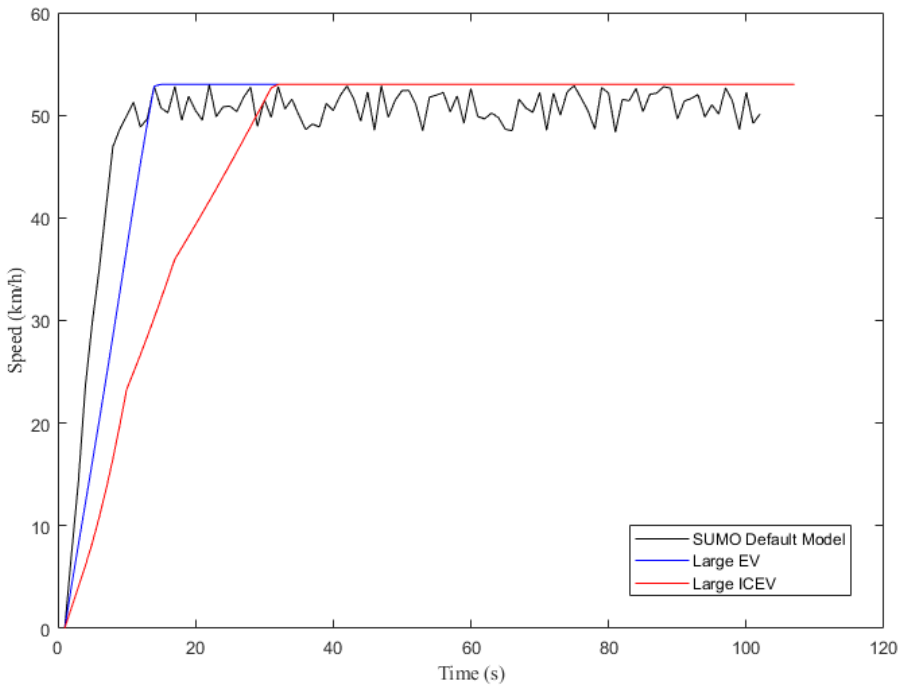

Figure 5.16 Comparing acceleration process of Krauß model and large car model

The comparison shows that according to the Krauß model, the vehicle accelerates with a constant acceleration until the speed limit is reached. Then there is an erratic

trembling in the speed curve after 50 km/h. The reason is that there is a variable called “driver imperfection factor” in the Krauß model. It reflects the imperfection of controlling vehicle speed by a human driver. As in the proposed driver model the imperfection factor was not considered, in the speed curves using proposed car-following model there is not a similar vibration.

In these Figures, the ICEV models always accelerate slower than the EV models. In different gears the acceleration characters of ICEV also vary. Because of higher torque provided from electric motors at low speeds and without gear shift, EVs accelerated faster than ICEVs. When comparing the acceleration process of electric vehicles, it can be seen that the mid-sized and large car can accelerate with a relatively constant acceleration, while the acceleration of the small car decreased after about 30 km/h. From Figure 5.14 it can be seen that the maximal torque of the PM49 motor decreases after 1,500 rpm, the corresponding vehicle speed is after 25.56 km/h. While electric mid-sized and large car were equipped with motors with higher power, they can maintain the constant motor torque in this test.

It can also be seen that the mid-sized ICEV accelerated the slowest, even slightly slower than the small ICEV. The reason is that the maximum torque of the 102-kW engine model in the mid-sized car at low rotation speeds is similar with that of the 95-kW engine model in small car. The conventional mid-sized car is however 504 kg heavier than a small car, which reduces the acceleration capability. However, there are also many compact cars in the automotive market equipped with a small displacement engine. Their acceleration capabilities are no better than the small cars. Moreover, the models in ADVISOR do not exactly describe the newest models in the current automotive market. However, they do reflect the differences between ICEVs and EVs.

6 Simulation Scenario of the City of Duisburg

A scenario of a part of the City of Duisburg has been used and optimized in this thesis. In this Chapter, the scenario is briefly introduced and then calibrated with real traffic data. After the calibration of the scenario, the simulation result with the default car-following model in SUMO is compared with original real data.

6.1 Scenario of Duisburg Inner Ring

This thesis aims to find out the effect of electric vehicles on traffic flow and their energy consumption through traffic simulation. After modeling corresponding drivers and vehicles, a simulation scenario is needed to implement the models. An scenario of Duisburg inner ring (Ma et al. 2020) was used in this thesis.

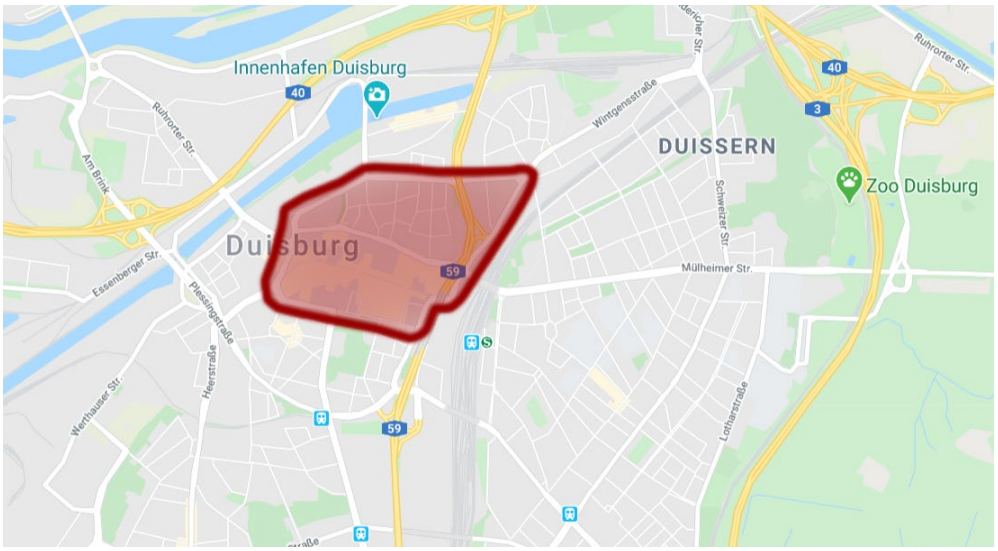

Figure 6.1 Duisburg inner ring in Google Maps

Duisburg inner ring is the center area of the City of Duisburg. Figure 6.1 shows the location of Duisburg inner ring in Google Maps. There is a highway, A59, through this area as an underground tunnel. Since the traffic flow on A59 was ignored in this study, this area can be seen as a purely urban zone. It contains the main business district of Duisburg, and also some residential areas. In the lower right corner, i.e., in the southeastern part, some streets in front of the entrance of the Duisburg train station were also incorporated into the scenario. This area of the city is

regularly used by a large number of road users. It can therefore serve as a basis for answering the research questions dealt with in the thesis.

A traffic scenario that can be simulated in SUMO consists at least of two parts: road network and traffic demand. The road network describes the position, shape, and connection logic of all roads, while traffic demand determines the type, route, and departure time of all vehicles. The road network of the scenario used in this thesis was exported from OSM (Haklay and Weber 2008; OpenStreetMap). The connection errors in the road network has been corrected based on the street view of Google Maps (Ma et al. 2020). Figure 6.2 shows the road network used in this study.

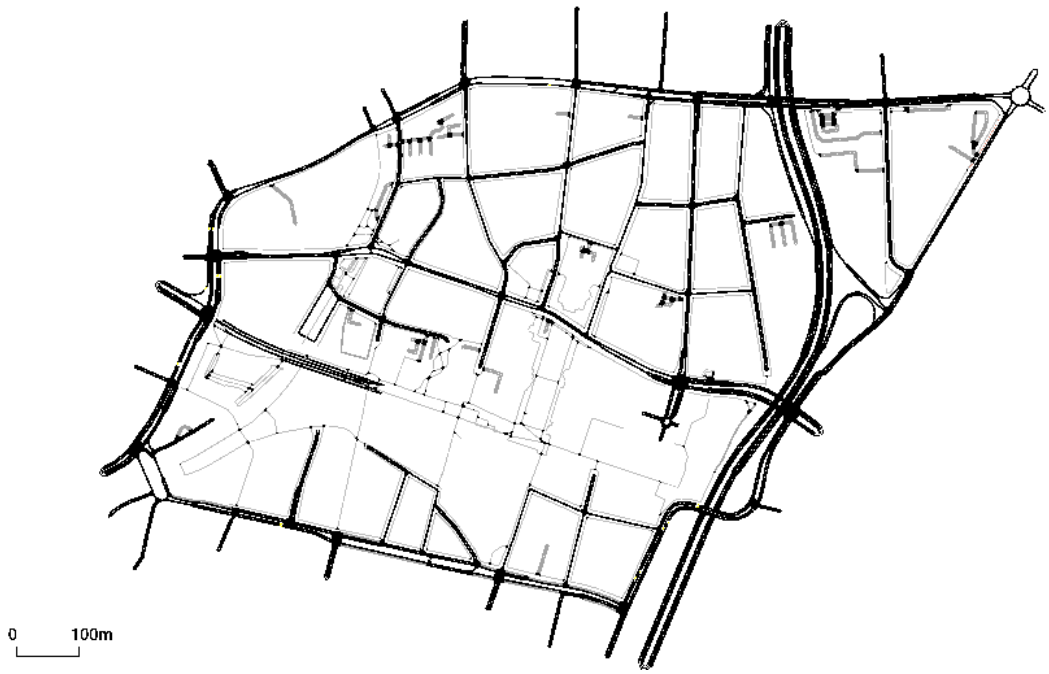

Figure 6.2 Road network of Duisburg inner ring in SUMO

The traffic demand is defined in such a way that for all vehicles of the traffic scenario the corresponding routes are determined in a traffic system. It therefore represents a travel plan for each traffic participant. The traffic demand contains as data e.g., the respective vehicle type, the respective departure and destination position as well as departure time and route. In traffic simulation, especially in SUMO, trip event and route are two typical characteristics of a road user. Trip defines the departure time, departure, and destination position of the road user. On the other hand, the route defines all edges, i.e., roads, thus defining the detailed route of the respective road user. Except in specific studies, the route of a vehicle in traffic sim-

ulation is therefore defined in the traffic demand and is not changed during the simulation. Even if a road is completely congested, the vehicles still retain the routes originally planned for them. During the simulation, the vehicles can only choose their lanes on their defined route. In the scenario of Duisburg inner ring, the real traffic data provided by WBD (Wirtschaftsbetriebe Duisburg) has been used for generating the traffic demand (Ma et al. 2020). Unlike in (Ma et al. 2020), no OD-Matrix (Origin-Destination Matrix) was used here because it cannot optimally reproduce the real traffic demand for the restricted area. An alternative approach was therefore chosen. The 24-hour data from 54 traffic counters that locate around 11 intersections, on 25th Sep. 2019, which is a Wednesday, were utilized for the generation of the traffic demand. The traffic counts data were collected by automatic counter equipment, e.g., induction loops and counter cameras. When a car passes by a detected position of a certain lane, it is automatically detected by the traffic counter and its velocity is also temporarily recorded. Per minute, traffic counter records the quantity of the vehicles detected during simulation and their mean velocity during this time interval.

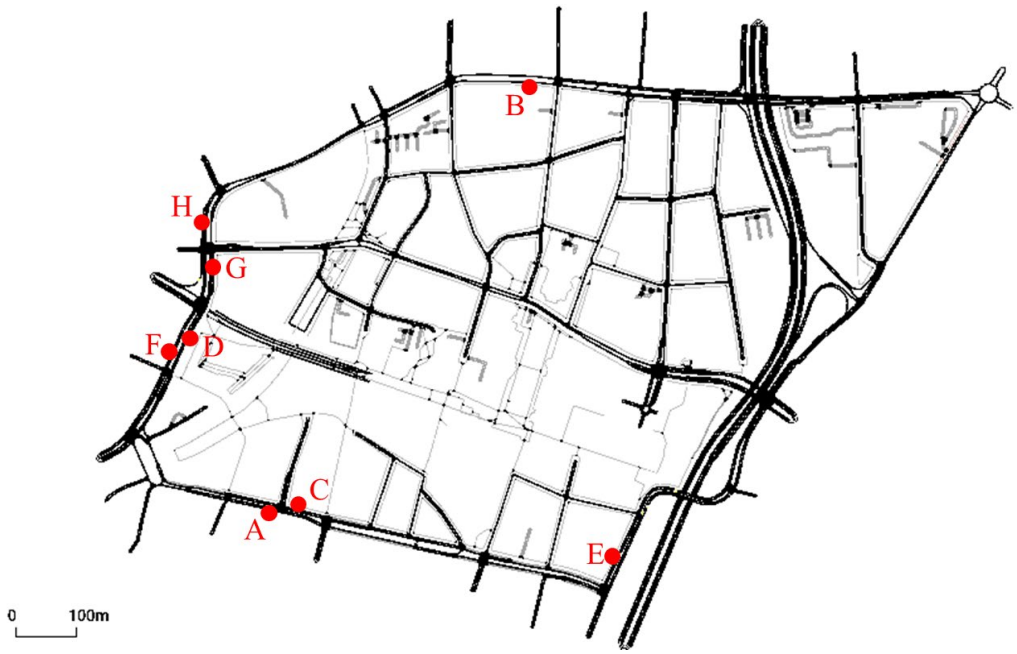

Figure 6.3 Location of validation points

For calibrating and validating the generated traffic flow, 16 vehicle detectors in 8 groups were set into the scenario. Each detector has a corresponding real traffic counter. Thus, the traffic flow and average speed at the 8 points in simulation can

be compared with original data. Figure 6.3 shows the location of the 8 groups of vehicle detectors.

6.2 Calibration and Validation of the Scenario

Although the scenario of Duisburg inner ring has been used for studying about scenario modelling and about self-driving vehicles, the scenario itself still has some defects. Therefore, this thesis focuses on the improvement of the scenario, including the generation of the traffic demand and the adjusting of the road network.

In SUMO, there are several methods to generate traffic demand from different data. The most direct method is to define the trip and route of each vehicle in the scenario manually. In this way, if only the original data are correct, the most accurate traffic demand can be generated. However, this method is obviously unpractical for a scenario in this thesis. It is quite impossible to obtain the detailed routes of each vehicle in this area.

As traffic counts belong to the common forms of traffic data, SUMO provides several tools for handling this data form. These tools were developed for solving different kinds of problems. As an example, DFROUTER algorithm is based on the assumption that the sum of incoming flow equals the outgoing flow in every time interval. This means all the entrances and exits of the simulated area need to be monitored by traffic counters and the departure/destination position of vehicles can only be these entrances and exits. Therefore, this algorithm is better suited for scenarios that contain predominantly highways. However, in a highly meshed urban road network each edge can be a departure position and a destination at the same time. The traffic counts always cannot cover every intersection and every lane. Then, for the DFROUTER algorithm many data are missing, and the algorithm is no more suitable. If this algorithm is used in meshed urban road network, the generated traffic demand can be completely deviating from reality.

For generating the traffic demand of the scenario of Duisburg inner ring, the tool FLOWROUTER in SUMO has been used (Ma et al. 2020). FLOWROUTER can find a set of routes which can maximize the total flow (Behrisch and Erdmann 2018). Therefore, this algorithm is doing better when dealing with missing data. The

FLOWROUTER is a more suitable tool for generating the traffic demands with traffic observation data in a highly meshed road network. It is however still under continuous development, and might fail to deliver the expected results (Tools/Detector - SUMO Documentation). Therefore, the traffic demand has been generated with the original traffic data using the latest development version, SUMO v1.8.0.

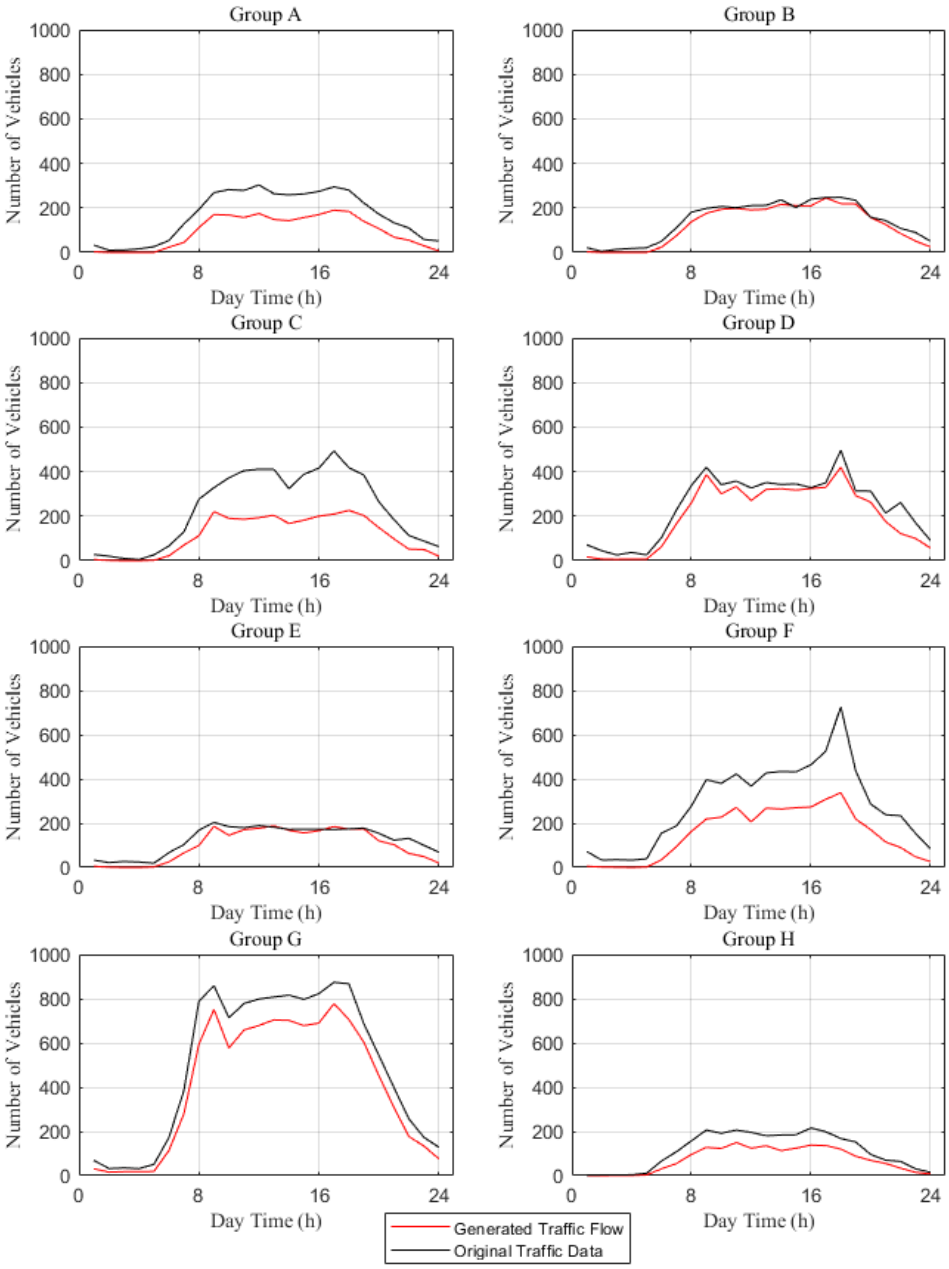

Figure 6.4 Comparison of generated and real hourly traffic flow

For calibration and validation of the generated traffic flow, this scenario was first simulated with the default car-following model in SUMO. Figure 6.4 shows the comparison of generated traffic flow and real traffic flow at each verification point.

Both the original traffic data and the simulation detector data are all minute data. For clearer observation and comparison, as well as for simplifying the later calibration of the traffic flow, the minute data were all converted here into hourly data.

It can be seen that in simulation there is obviously less traffic than the original traffic data, especially at Group C and F. At Group F from 5:00 p.m. to 6:00 p.m., over 387 vehicles were missing when generating the traffic demand. Although the FLOWROUTER is already the most appropriate tool in SUMO for generating the traffic demand for this scenario and the latest version of the software package has been applied, the FLOWROUTER cannot precisely reproduce the real traffic flow at each observation point at present.

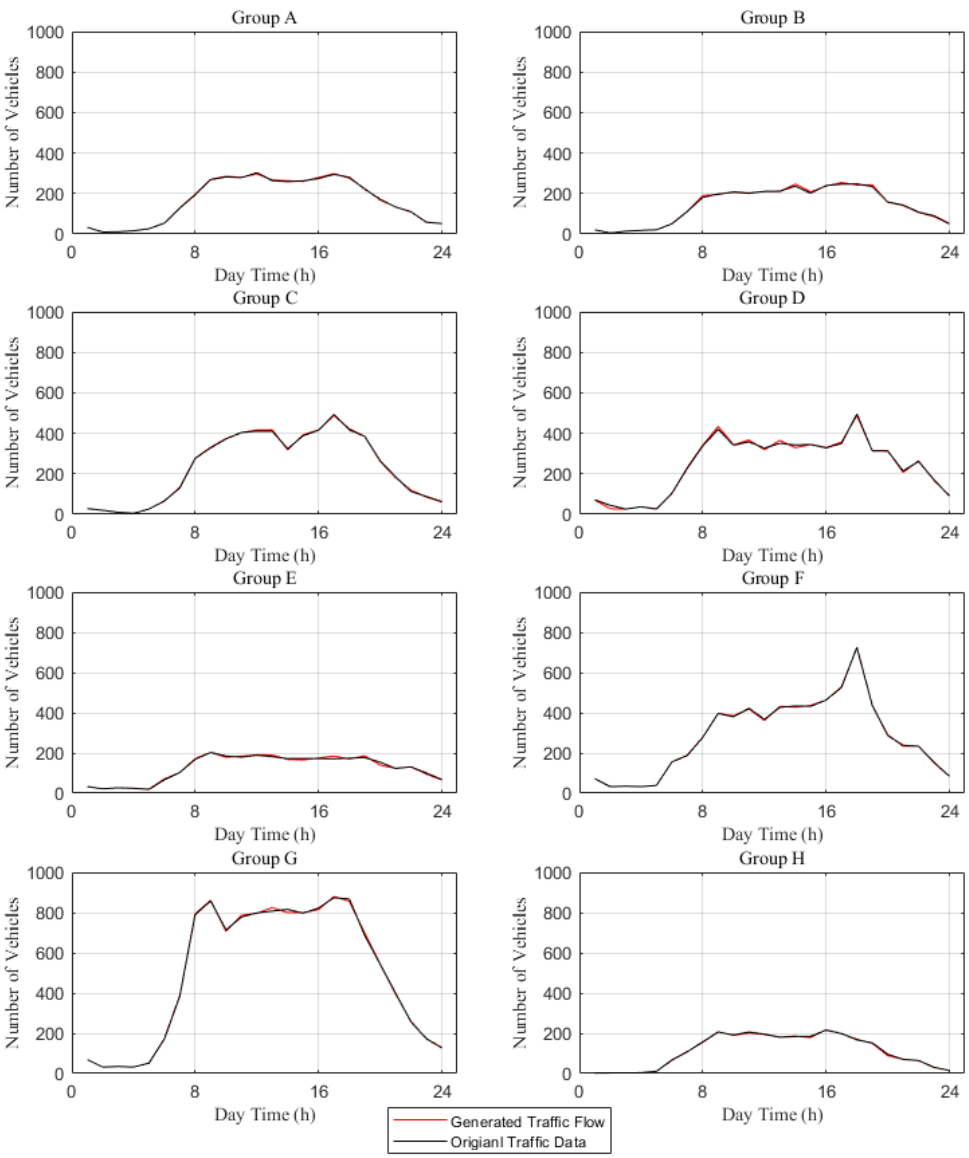

Figure 6.5 Comparison of real hourly traffic flow and calibrated simulation traffic flow

Since the tool FLOWROUTER provides not many options for improving the generating results, the missing traffic demand was manually added based on the traffic flow difference in each hour. Figure 6.5 shows the calibrated traffic flow in simulation. At the 8 groups of verification points, the traffic flow in the simulation is then essentially same with original traffic data.

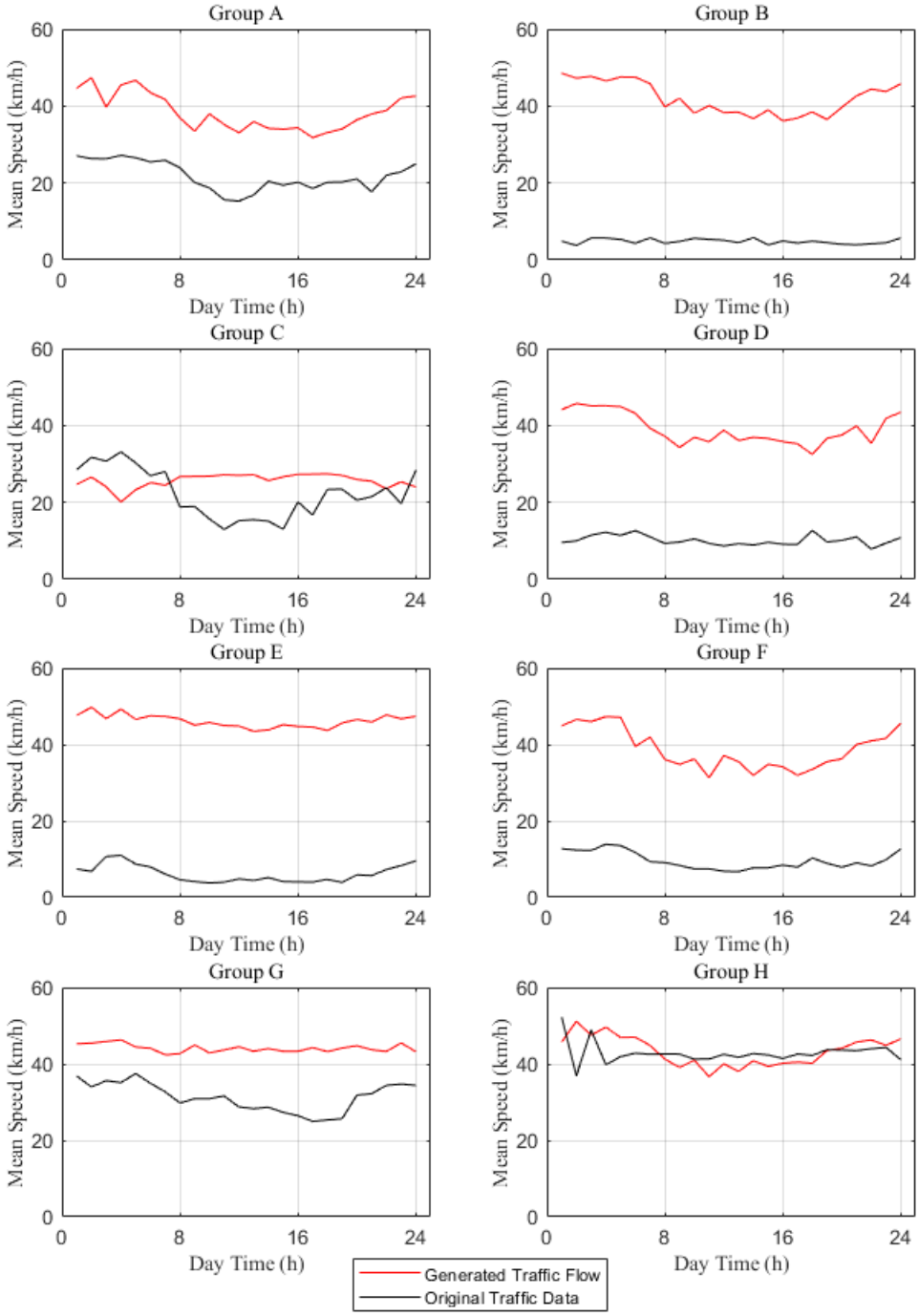

Figure 6.6 Mean speed of the vehicles detected during simulation comparing with original traffic data

After supplementing the missing traffic demand, the average speeds at each observation point in simulation were compared with original data. The improvement about the traffic demand of the scenario has been done. The road network was then adjusted based on the mean speed of the vehicles in the real traffic data.

Figure 6.6 shows the mean speed of the vehicles detected during simulation. It can be seen that the mean speed in simulation was basically always higher than that of the real vehicles. In order to examine this effect and find a solution, the street view of each verification point in Google Maps was investigated.

No additional speed limits were found in the street view around all verification points. This means that the prescribed maximum speed on these roads is 50 km/h throughout, but not that it is always possible to drive this fast. As expected, the average speeds in reality are actually well below 50 km/h in the original traffic data. Therefore, there are other factors, which have impact on the speed of the vehicles.

Figure 6.7 Street view around Group A in Google Maps

Figure 6.7 shows the driving environment around Group A. There are several bus lines on this road. There are also some pedestrians, parking spaces, shops and restaurants on the roadside. The speed of the vehicles on this road can be greatly affected by these other traffic participants and the traffic environment.

Figure 6.8 Street view around Group B in Google Maps

In the street view around Group B, illustrated in Figure 6.8, there are many parking spaces on both sides of the lane. Therefore, the mean speed of the traffic flow might be slowed down because of the vehicles that are parking in and out. Even when there are no vehicles driving into or out from the parking spaces, most drivers will slow down in this driving situation, in order to avoid crashing into any pedestrians or vehicles coming from the side of the road.

Figure 6.9 Street view around Group D and F in Google Maps

Figure 6.9 shows the street view around Group D and F. There are many branch roads to the indoor parking lots of the commercial district, which are not contained in the road network. The vehicles driving into or out from the parking lots will definitely slow down the traffic flow. Another important traffic element is also missing in the road network, i.e., the traffic light for pedestrians on this road.

Figure 6.10 Street view around Group E in Google Maps

The roads around Group E are in a similar condition with that at Group B. This road locates between the biggest commercial district and Duisburg Central Station. Therefore, there are more pedestrians crossing the road and many buses passing by.

Figure 6.11 Street view around Group G in Google Maps

Figure 6.11 illustrates the street view around Group G. There are also some parking spaces on the side of the road, but only for motorcycles. It can be inferred that motorcycles play an important role in the traffic flow on this road.

Therefore, at the verification points there are various factors that are physically or psychologically influencing the driving behavior of the drivers. These factors make the vehicles slow down and cannot reach the speed limit.

In this traffic scenario, only passenger vehicles were simulated, i.e., pedestrians, cyclists, motorcycles, delivery vehicles and busses are all ignored. They are all im-

portant traffic participants and have significant impact on the traffic flow. Additionally, the driver model in Chapter 4 describes only the behavior of the driver when following a driving car. It cannot react to the other driving conditions or anticipate potential danger and slow down the vehicle. Therefore, the speed limits of the corresponding roads were adjusted according to the mean speeds in original traffic data for compensating the mean speed differences in simulation. After adjusting the road speed limits, the scenario was simulated again.

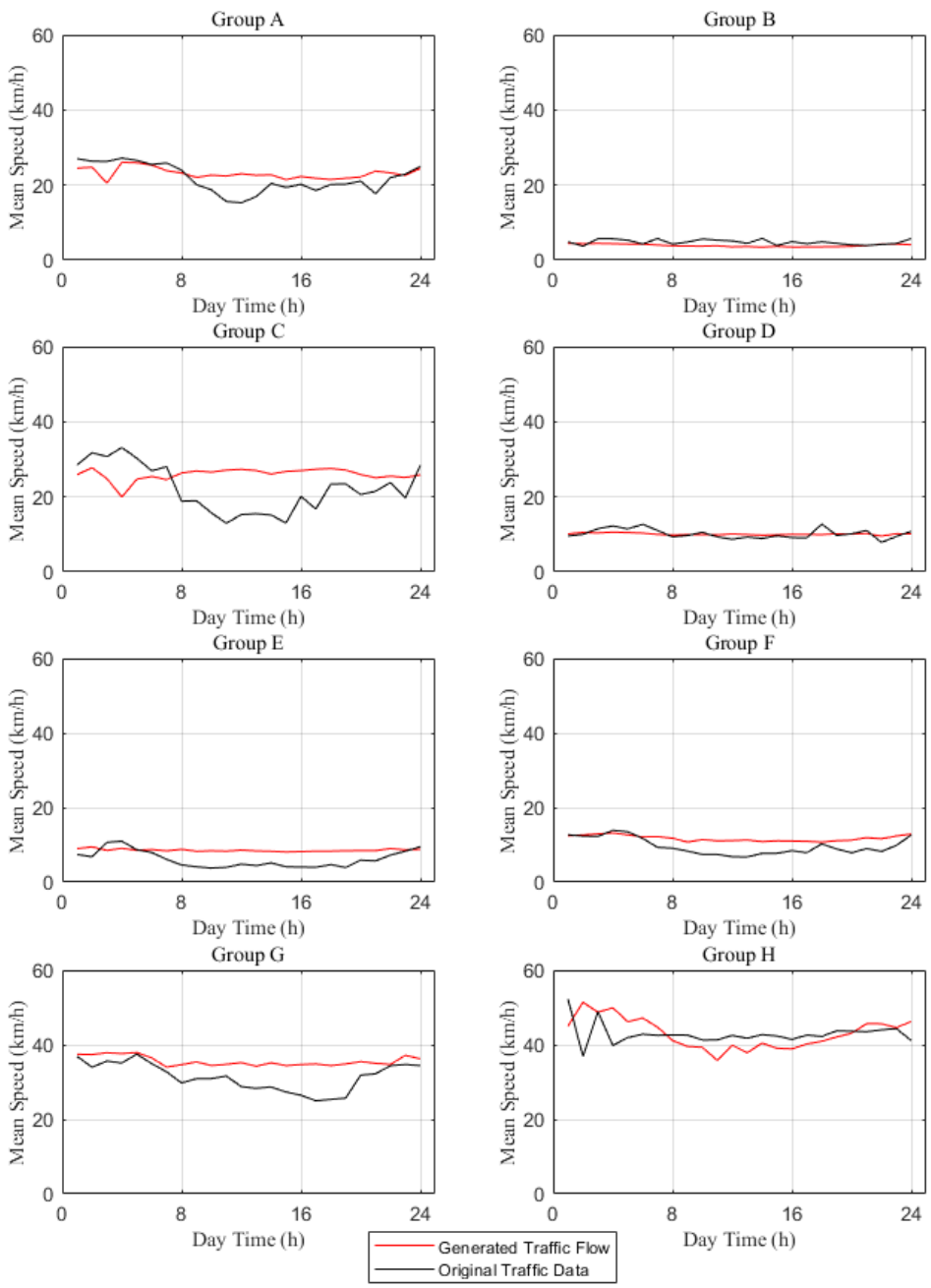

Figure 6.12 Mean speed of the vehicles detected during simulation after adjusting road speed limits

Figure 6.12 shows the simulation results. The decreases of the mean speed in simulation during daytime are less obvious than in the real data. The reason could be that the SUMO default car-following model always drives with the maximal acceleration, as mentioned in Section 5.7. In this case, the vehicles are less impacted by the high traffic density and congestions. On the other hand, the buses and pedestrians were not simulated, which can also belong to the reasons. After adjusting the speed limits of the roads, the mean speed is nevertheless closer to the real data.

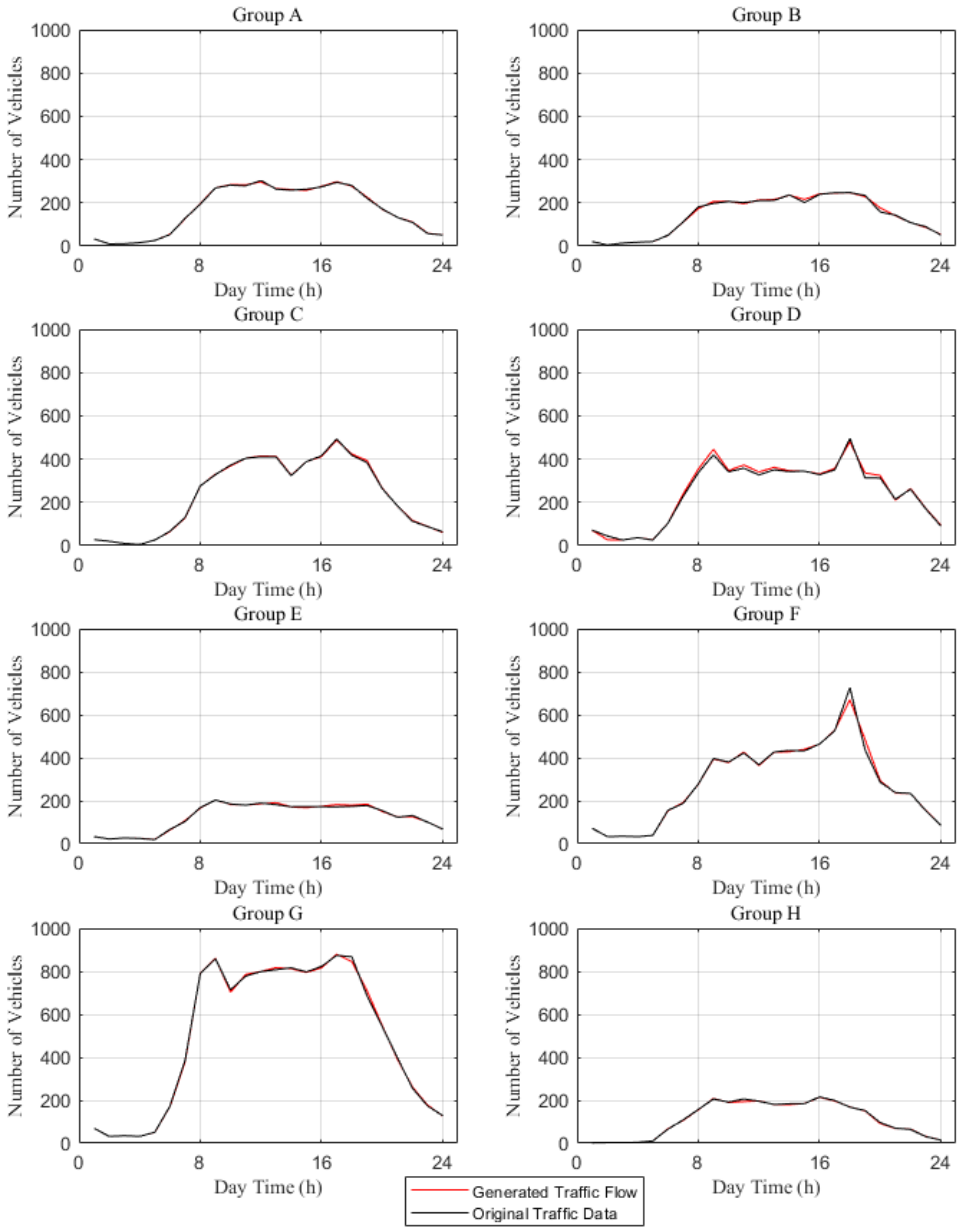

Figure 6.13 Hourly traffic flow in simulation after scenario calibration

Since the speed limits of several roads have been lowered, the passing capacity of these roads has also decreased. The traffic volume over time was also then influenced and different from original traffic data. In (Ma et al. 2020) for the scenario of Duisburg inner ring the default traffic light logic was used, which can also impact on the traffic flow. After adjusting the road speed limit, the traffic light logic at several significant intersections was also calibrated, in order to make both the traffic flow distribution and the mean speed close to real data at the same time. The traffic flow distribution in simulation is illustrated in Figure 6.13. The mean speeds remain the same as in Figure 6.12.

This shows that, especially in heavily frequented urban areas, a careful consideration of the respective local conditions is indispensable. Overall, the adjustment via the road network, as well as the calibration via the traffic scenario of the Duisburg inner ring leads to a solid basis for the effects to be investigated in the work.

In spite of this, the scenario still has some limitations. Although it has been calibrated the traffic volume, other road users, such as pedestrians, cyclists, buses, etc., are not considered. The simulated scenario cannot perfectly reproduce the original traffic situation in the traffic data. After calibration, the traffic volume was however the same as in the original data and the mean speed of the vehicles did not deviate much from the original data. The simulation scenario can therefore serve as an acceptable basis for answering the research questions in this thesis. The following research work was also based on the traffic flows around these eight observation points.

7 Implementation and Validation of the Car-Following Model

In this Chapter the co-simulation of SUMO and MATLAB, and the application method of the proposed car-following model into simulation are introduced. The simulation results using the established car-following model are compared with original traffic data.

7.1 Co-simulation of SUMO and MATLAB

SUMO is an open-source software package using C++. New models can be written in C++ language and embedded into SUMO. As the car-following model in this thesis has a fuzzy control part and most modeling work was done in MATLAB, the calculation of car-following model remains in MATLAB. Therefore, co-simulations with SUMO and MATLAB had to be implemented.

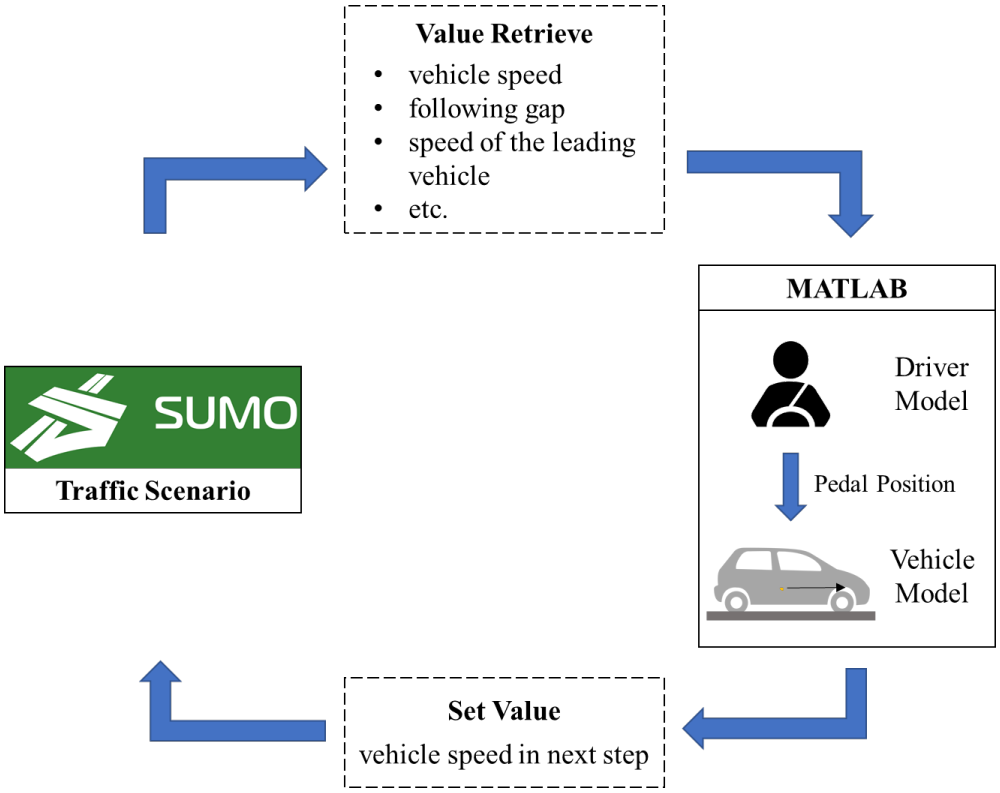

Figure 7.1 Parameter passing process between SUMO and the proposed car-following model

During simulation runtime, SUMO works as a database. Information such as vehicle speed, following gap, speed of the leading vehicle, etc. are retrieved from

SUMO for the purpose of evaluating the vehicle following model. Then the values of variables are sent back to SUMO for updating the state of vehicles. Figure 7.1 shows this parameter passing process.

7.1.1 Communication between SUMO and MATLAB

Since the traffic flow is simulated in SUMO while the calculation of the vehicle following model is performed in MATLAB, data communication between SUMO and MATLAB is mandatory. The co-simulation method in (Hu et al. 2021) has been implemented.

SUMO provides the API (Application Programming Interface), TraCI (Traffic Control Interface), for external communication. At the start of SUMO a TCP connection is established by TraCI (Wegener et al. 2008). Through this TCP connection, data and commands can be transferred in and out of SUMO. According to a request-response protocol defined in TraCI, SUMO can operate as a server. Besides updating the position of vehicles in the traffic scenario, SUMO can also provide retrieved data according to the incoming command. The external software that is connected with SUMO works as a client of SUMO. It can send commands and retrieve various values. It is also possible to set the values of many parameters through the TraCI during simulation. Therefore, the co-simulations with SUMO and MATLAB used in this thesis were based on TraCI.

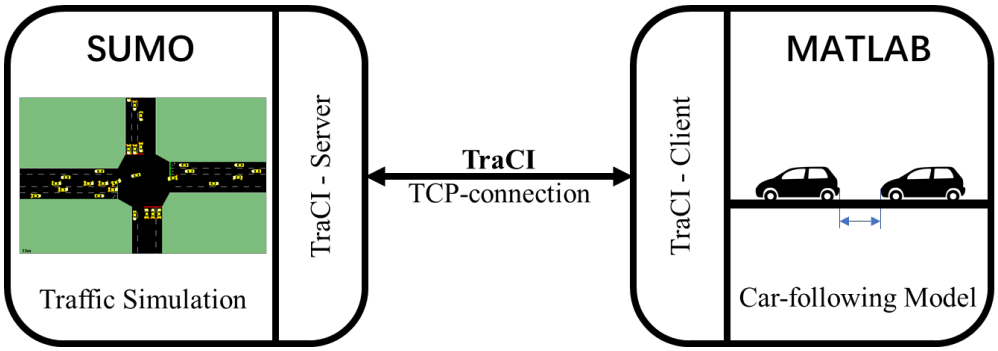

Figure 7.2 Data communication through TraCI

All data and commands need to be encapsulated according to the protocol of TraCI. SUMO also has developed the commands for TraCI using Python, which is a high-level programming language. However, a toolkit for MATLAB called TraCI4Matlab was utilized in this thesis, which is an implementation of the TraCI interface for MATLAB (Acosta et al. 2015). With the help of TraCI4Matlab, most

functions of TraCI can be realized with corresponding commands, which comply with the syntax of MATLAB programming.

7.1.2 Design of the Simulation Program

The program structure of implementing the simulation is introduced in this Section. The main idea is to use program codes in MATLAB controlling the values of necessary variables in SUMO simulation. The flow chart of the main program is illustrated in Figure 7.3.

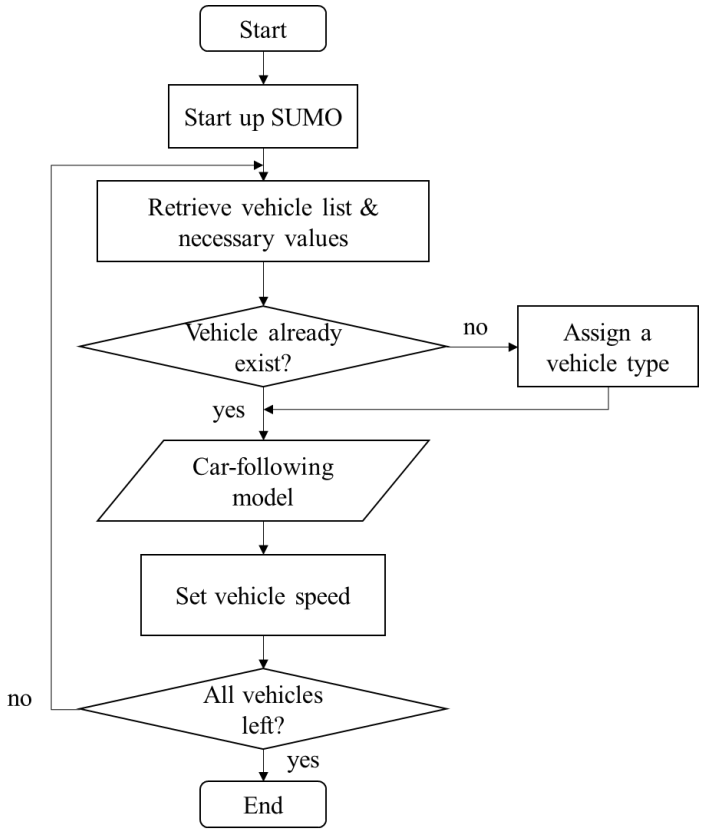

Figure 7.3 Flow chart of the simulation program

The main program was edited in MATLAB. After loading the corresponding files, the SUMO-GUI will be firstly started up through TraCI. Then SUMO loads the network file, traffic demand file, and detector definition file of the scenario. Subsequently, the main loop starts. The ID list of vehicles that are currently driving in the scenario is firstly retrieved into MATLAB. Based on the vehicle ID list, a secondary loop is implemented. In the secondary loop it is initially determined for each vehicle whether the vehicle has already entered the scenario in previous simulation steps. If this is not the case, the vehicle is first assigned a vehicle type. This is done randomly in such a manner that a vehicle is selected with a predetermined probability from

the six vehicle classes defined in Section 5.5. Then, like the other vehicles that already entered the scenario, the values of the necessary variables are retrieved. Based on the retrieved values, the car-following model with a corresponding vehicle type calculates the speed in the next simulation step. The speed is sent back to SUMO through TraCI. After the speeds of all vehicles currently driving in scenario have been calculated, the secondary loop ends, and program jumps back into the main loop. A command is then sent to SUMO to perform the next simulation step. SUMO updates the positions of each vehicle based on the received vehicle speed. Thus, the main loop completes a cycle.

During simulation, SUMO saves the detector data in corresponding files according to the setting in the detector definition file.

7.1.3 Distribution of Vehicle Types

According to the annual report of car ownership published by the Federal Motor Transport Authority of Germany (Kraftfahrt-Bundesamt), until 1st January 2019, among all registered passenger vehicles in Germany, the proportions of small cars, compact cars and mid-size cars are 19%, 25.6% and 13.8%, respectively. If classified by size, there are in total three types of vehicle models established in Chapter 5. Their relative proportions in simulation remain the same with the statistical data. The absolute proportion of small car, mid-sized car and large car in simulation is 32.53%, 43.84%, and 23.63%, respectively.

When the ICEV models are replaced with electric vehicle models, the proportions of three sizes of vehicles are in this thesis assumed to remain the same. As an example, when electric vehicles account for 25% of all vehicles in simulation, the proportion of conventional small car should be 24.40% while electric small car should be 8.13%. The total proportion of conventional and electric small car is still 32.53%. Correspondingly, proportions of conventional mid-sized car, electric mid-sized car, conventional large car, and electric large car should be 32.88%, 10.96%, 17.72% and 5.91%, respectively.

In Chapter 6, based on the real traffic data 26,116 vehicles have been generated in the scenario. It is almost impossible to manually assign the type of every vehicle. Therefore, a vehicle type was randomly assigned to each vehicle as far as possible. Thus, the situation can also be avoided that a certain type of vehicle appears too

concentrated on a road section. As soon as a vehicle was assigned its type, it was registered in the vehicle type list. On one hand this list avoids that a vehicle is assigned a vehicle type more than once during simulation. On the other hand, the list can be used after the simulation to validate whether the distribution of vehicle types meets the expectations or not.

7.2 Validation of the Car-Following Model

For validation of the proposed car-following model, a microscopic traffic simulation with the ICEV models has been implemented. The proportions of each vehicle type are the same as mentioned previously, and the traffic scenario introduced in Chapter 6 was used. Similar with the introduction in Chapter 6, the data of the detectors at the eight verification points in Figure 6.3 were used and compared with real traffic data and traffic flow using the default model in SUMO.

Figure 7.4 shows the detected traffic flows at the verification points. At these, the traffic flow using the SUMO default model along with the ICEV models have a similar trend to the original data. Since the car-following model only determines the speed of the vehicles and does not change their routes, the total traffic volume when using the ICEV models is the same as when using the standard model.

Figure 7.5 shows the mean speed of the vehicles detected during simulation. The curves using the ICEV models are closer to the original data than using the default SUMO models. The mean speed of all the vehicles detected during simulation is 25.08 km/h, while in original data it is 25.03 km/h. The vehicle mean speed of the proposed car-following models can be seen as an acceptable result. At Group A, the hourly mean speed of the vehicles using proposed car-following model decreased with the increase of traffic density. There is the similar trend in the real traffic data. Therefore, it can be inferred that, the proposed car-following model is more impacted by the traffic density than the SUMO default model. Therefore, the proposed car-following model allows a description of the traffic situation that is much closer to the actual characteristic traffic behavior than the SUMO model.

Based on the advance examinations in this Chapter, the ICEV models were replaced by the electric vehicle models. It was studied how the traffic flow changes with the increase of the electric vehicles' proportion.

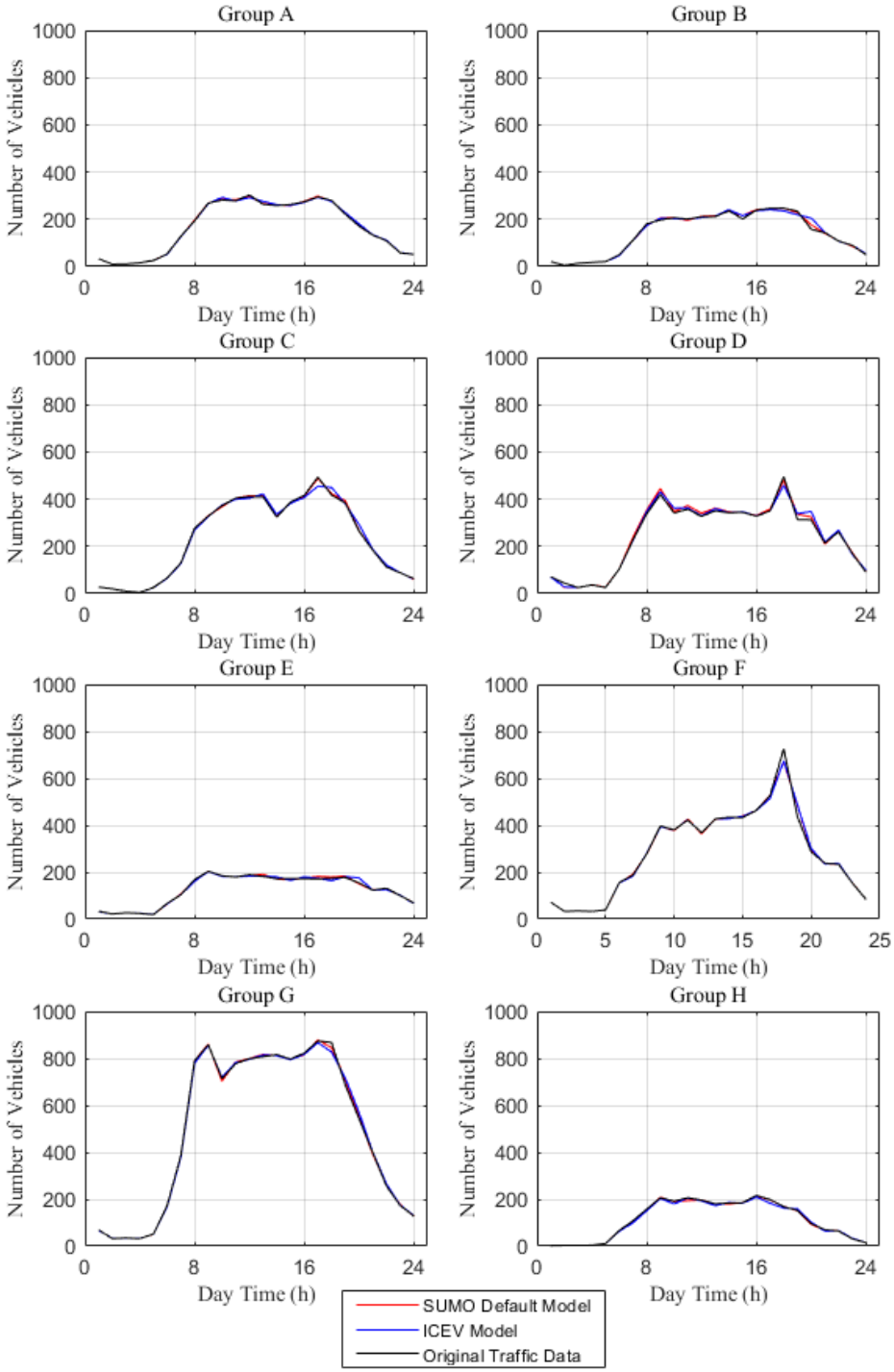

Figure 7.4 Vehicle quantity using the ICEV models, comparing with original data and using the default model

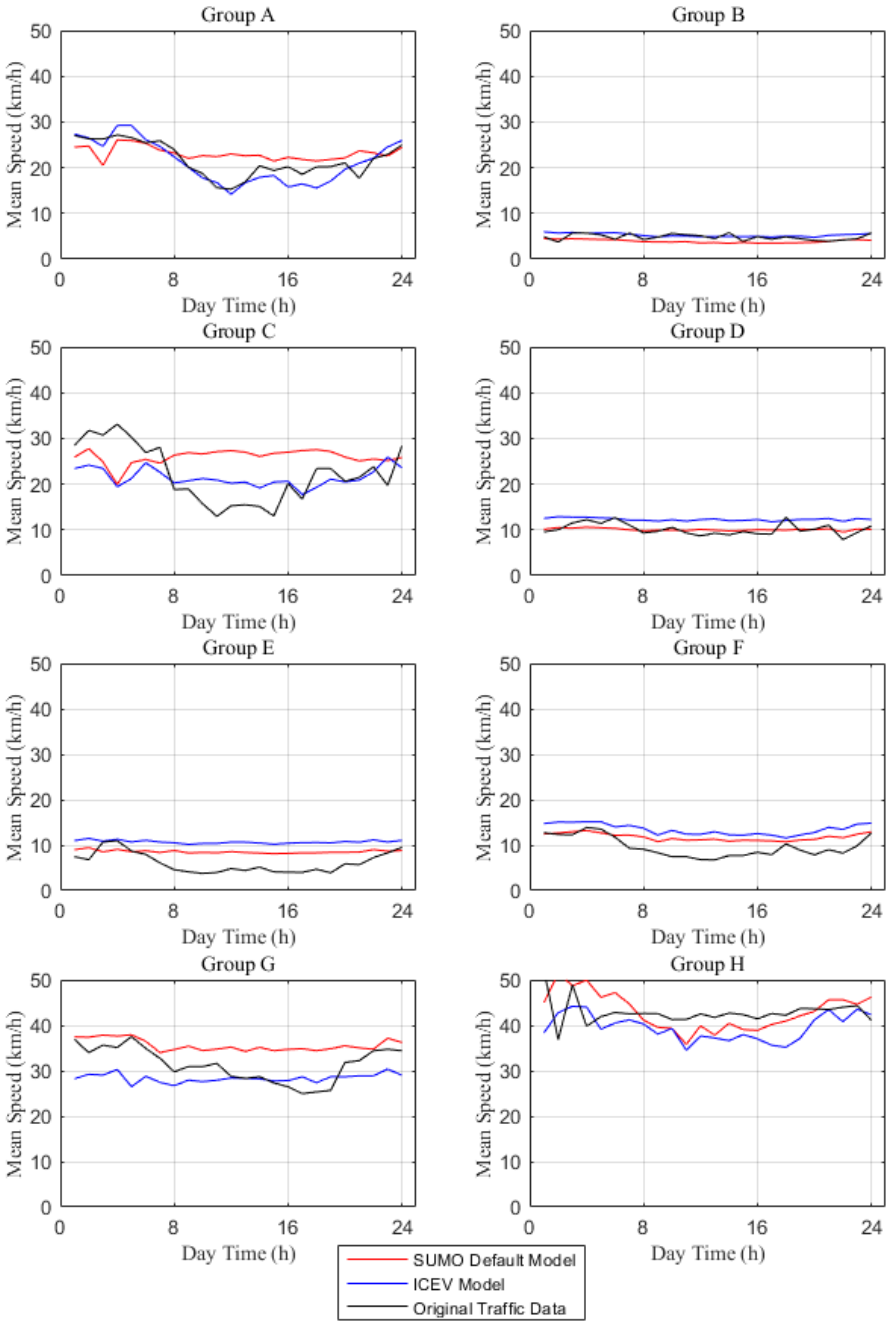

Figure 7.5 Mean speed of the vehicles detected during simulation using the ICEV models

8 Electric Vehicles in Traffic Simulation

Based on the scenario set-up in Chapter 6, traffic simulations with different proportions of electric vehicle models are implemented. Then the simulation results are analyzed and compared.

8.1 Simulation with Different Proportions of EVs

Electric vehicles have outstanding advantages, compared to the vehicles powered by fossil fuels. EVs are more environment friendly, can realize local zero-emission when driving, have excellent dynamic performance at lower speeds, etc. But the disadvantages of EVs are also outstanding. These include, for example, the high price, which is compensated by government subsidies only temporarily and also only to a certain extent. In addition, there are long charging times at most charging stations, since fast-charging stations will not be available everywhere in the near future, and the generally much shorter range compared to ICEVs. The experience of most consumers with electric vehicles is still worse than with internal combustion engine-powered vehicles. The share of all-electric vehicles in the total vehicle population is therefore still almost negligible, with the exception of a few countries such as Norway, even though the governments of many countries have done a great deal to promote the spread of electric vehicles.

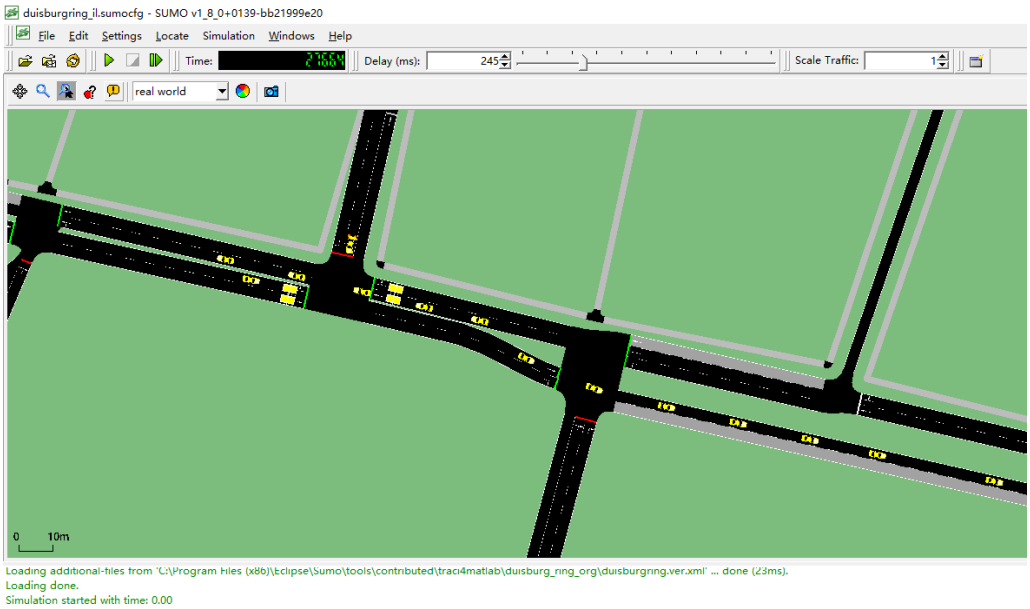

Figure 8.1 Microscopic traffic simulation in SUMO-GUI

As a basic assumption for this work, it is assumed that electric vehicles can become really popular when most of the disadvantages are overcome and this will then lead to the share growing very quickly. Moreover, it is assumed that fossil fuel-powered passenger cars in each classification will then be gradually replaced by electric vehicles in corresponding classification. Therefore, for simulations conducted as part of this work, the shares of electric vehicle models in the three vehicle classes are assumed to remain constant. For example, if the electric small cars constitute 25% of all small cars, the proportion of electric mid-sized car in all mid-sized car is also 25%. Equally, proportion of electric large car is also 25%.

Table 8.1 Number of ICEVs in each simulation

			1st simulation	2nd simulation	3rd simulation	4th simulation	5th simulation
Expected proportion of EVs			0%	25%	50%	75%	100%
Actual proportion of EVs			0%	24.87%	49.64%	74.86%	100%
Fossil fuel-powered vehicle model	**Small car**	**Expected proportion**	32.53%	24.40%	16.27%	8.13%	0%
		Actual proportion	32.80%	24.99%	16.07%	8.02%	0%
		Actual number	8,567	6,527	4,197	2,094	0
	Mid-sized car	**Expected proportion**	43.84%	32.83%	21.92%	10.96%	0%
		Actual proportion	43.79%	32.68%	21.82%	11.13%	0%
		Actual number	11,436	8,573	5,699	2,908	0
	Large car	**Expected proportion**	23.63%	17.72%	11.81%	5.91%	0%
		Actual proportion	23.41%	17.32%	11.75%	5.99%	0%
		Actual number	6,113	4,522	3,069	1,564	0

The traffic scenario of the Duisburg inner ring road was simulated based on five assumptions for shares of electric vehicles. The proportion of all electric vehicles was 0%, 25%, 50%, 75% and 100%, respectively. As the type of each simulated

vehicle was assigned with program codes based on probability, the actual amount of each vehicle type has been recorded. The number of generated vehicles is listed in Table 8.1 and Table 8.2.

Table 8.2 Number of electric vehicles in each simulation

			1st simulation	2nd simulation	3rd simulation	4th simulation	5th simulation
Expected proportion of EVs			0%	25%	50%	75%	100%
Actual proportion of EVs			0%	24.87%	49.64%	74.86%	100%
Electric vehicle model	**Small car**	**Expected proportion**	0%	8.13%	16.27%	24.42%	32.52%
		Actual proportion	0%	8.03%	16.60%	24.35%	32.49%
		Actual number	0	2,096	4,336	6,358	8,484
	Mid-sized car	**Expected proportion**	0%	10.96%	21.92%	32.88%	43.84%
		Actual proportion	0%	10.84%	21.87%	33.07%	43.73%
		Actual number	0	2,830	5,712	8,636	11,421
	Large car	**Expected proportion**	0%	5.91%	11.81%	17.72%	23.63%
		Actual proportion	0%	6.00%	11.88%	17.45%	23.78%
		Actual number	0	1,568	3,103	4,556	6,211

From Table 8.1 and Table 8.2, it can be seen that the vehicle type assigning program successfully distributed the vehicle type according to the expected proportions. The data collected by traffic detectors during simulation are introduced in following.

8.2 Simulation Results and Analysis

The vehicle detectors used in the traffic scenario record traffic data with a time interval of 1 minute. The traffic volume within this time interval, the average speed of the vehicles detected during simulation and the road occupancy are recorded. The road occupancy describes the percentage, 0 to 100%, of the time a vehicle was at

the detector within a time interval. These data were used for analyzing the simulation results.

Figure 8.2 shows the quantities of the vehicles detected during simulation. In the simulation, the hourly traffic flow changed not much by the same group of detectors.

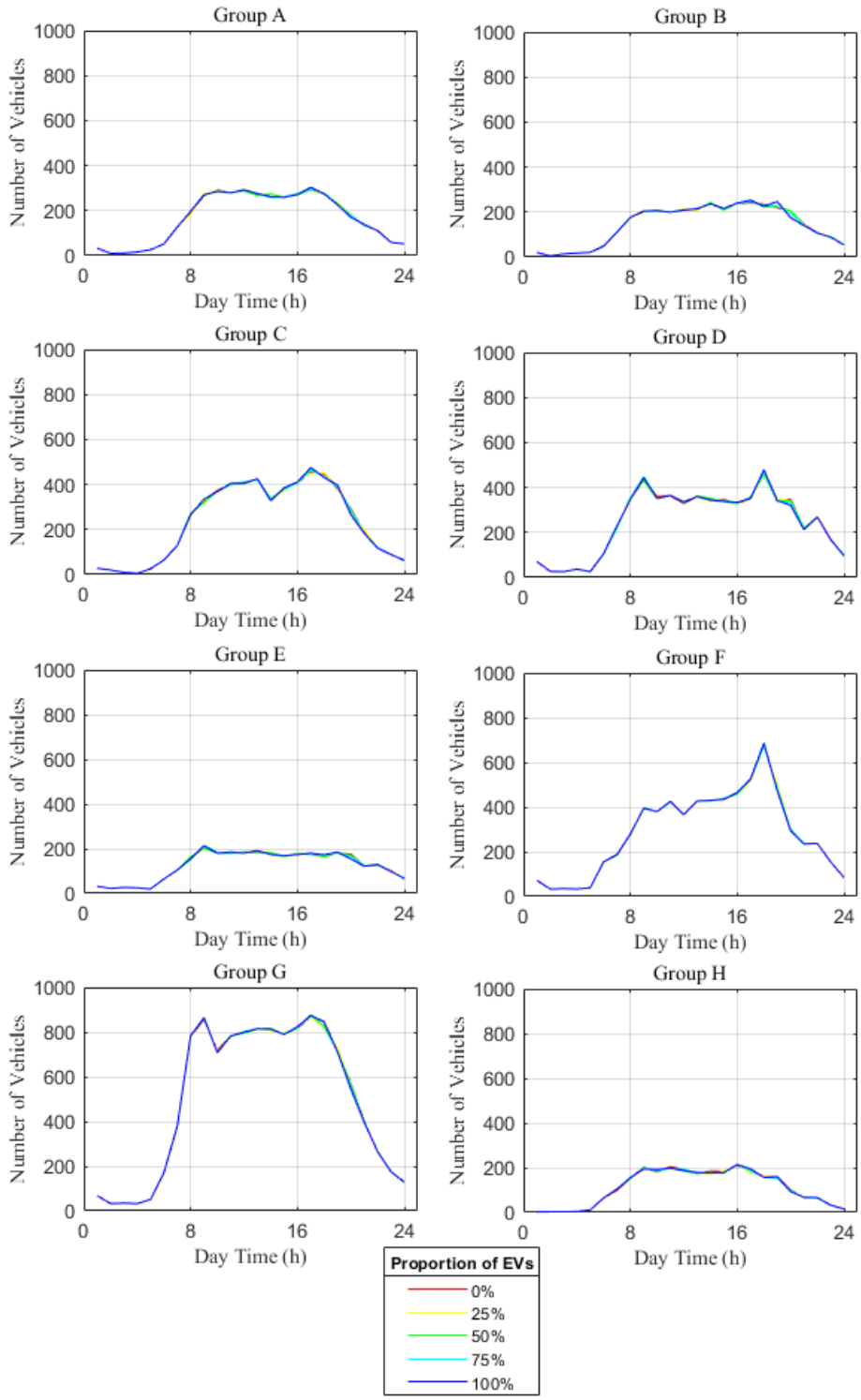

Figure 8.2 Detected traffic flow at verification points

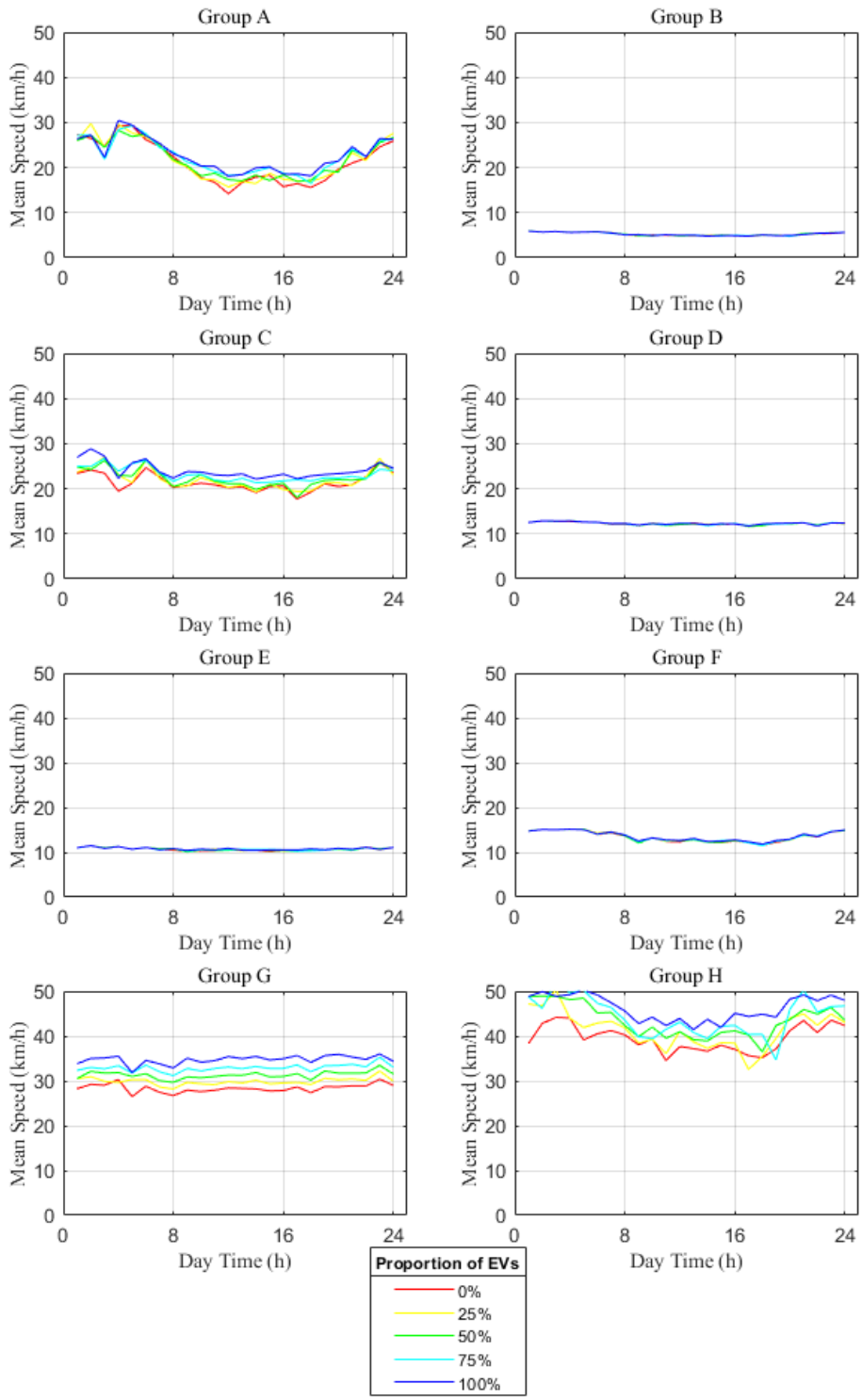

Figure 8.3 Arithmetic mean speed of the vehicles detected during simulation

Figure 8.3 shows the hourly mean speed of the vehicles detected during simulation. At Group A, C, G and H, the mean speed curves with higher proportion of EVs are basically higher than the curves with lower EV proportion. The better dynamic performance of EVs makes that EVs in urban network, where cars always need to

stop and start up, can drive with higher mean speed. Therefore, it is possible for more vehicles driving through the intersection in a traffic light cycle. Under some conditions, it can avoid the accumulation of vehicles on a road or at an intersection. The mean speed at Groups B, D, E and F did however not change with the increase of the EVs' proportion. In Chapter 6, the speed limit of the corresponding roads has been manually reduced for many reasons. On these roads, the vehicles do not have to frequently stop and start up but drive through with a relatively constant and slow speed. In this case, the advantages of the EVs in dynamic performances cannot help much in improving the traffic efficiency. In other words, the speed of the vehicles on these roads are not mostly impacted by the vehicle dynamics, but by the local conditions.

The collected road occupancy is shown in Figure 8.4. The road occupancy in the 24-hour simulation at the verification points has never been higher than 50%. This means that in the 24-hour traffic scenario there were no extremely severe traffic congestions. Most of the vehicles can depart from their origins as originally planned. This also explains why the curves of the traffic flows in Figure 8.2 hardly changed with the increase of the EVs' proportion. When there is too much traffic and they have caused extremely severe traffic congestions, the departure of many vehicles has to be delayed because there is no space for inserting more cars. In that case, the curve of the electric traffic flow can be different from the ICEV flow. In the case of current traffic demand, the impact of the EVs is mainly on the mean speed of traffic flow.

In both, Figure 8.3 and Figure 8.4, the traffic flow with 100% EVs has not always the highest mean speed or lowest road occupancy. This is the result of the randomly distributed vehicle size. The dynamic performances of the vehicle models in Chapter 5 are determined not only by the type of energy source, but also by the vehicle size. For the same vehicular flow, its mean speed is quite determined by the dynamic performance of the first car. Therefore, the randomly distributed vehicle size brings some randomness to the simulation results.

For more clearly estimating the effect of the EVs on traffic, the mean speed and the road occupancy were also discussed from a holistic perspective. The 24-hour

mean speed and the road occupancy of all the eight verification points in each simulation were calculated. The results are illustrated in Figure 8.5 and Figure 8.6.

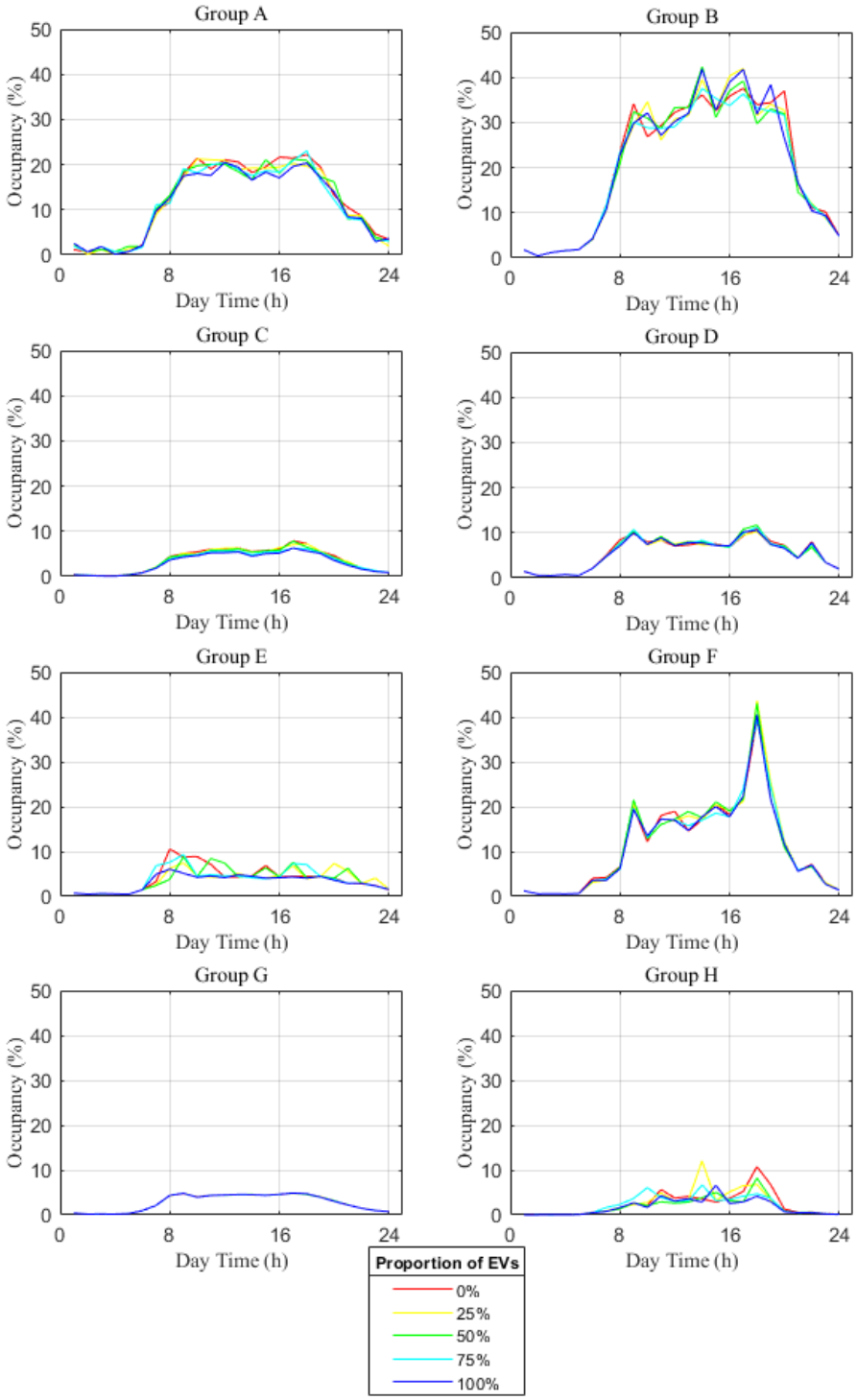

Figure 8.4 Road occupancy at the detected points

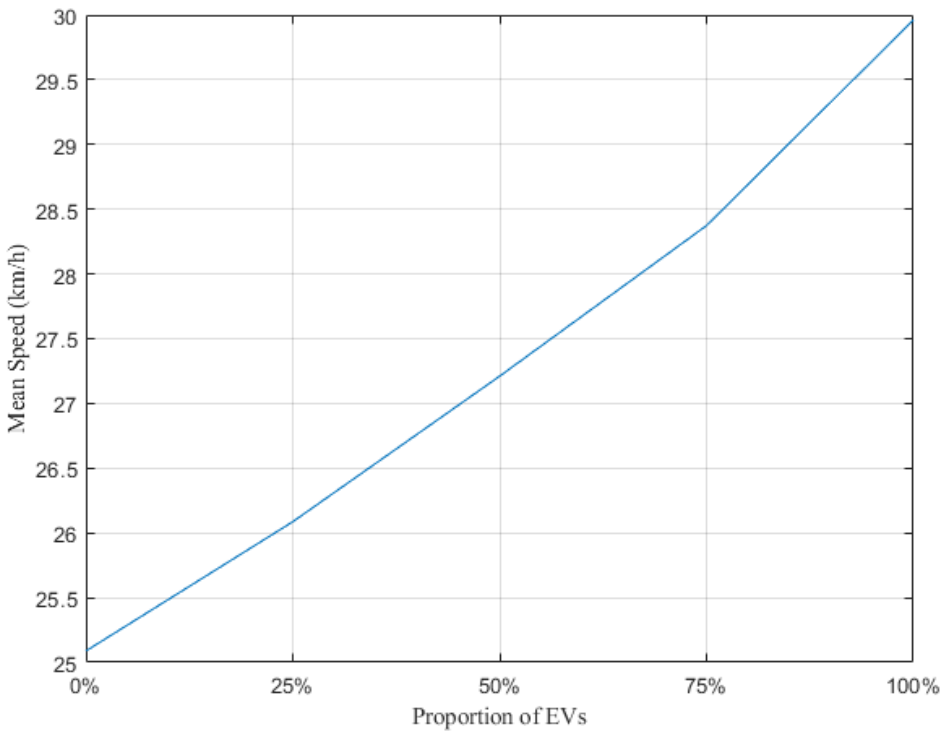

Figure 8.5 Mean speed of all the vehicles detected during simulation in each simulation

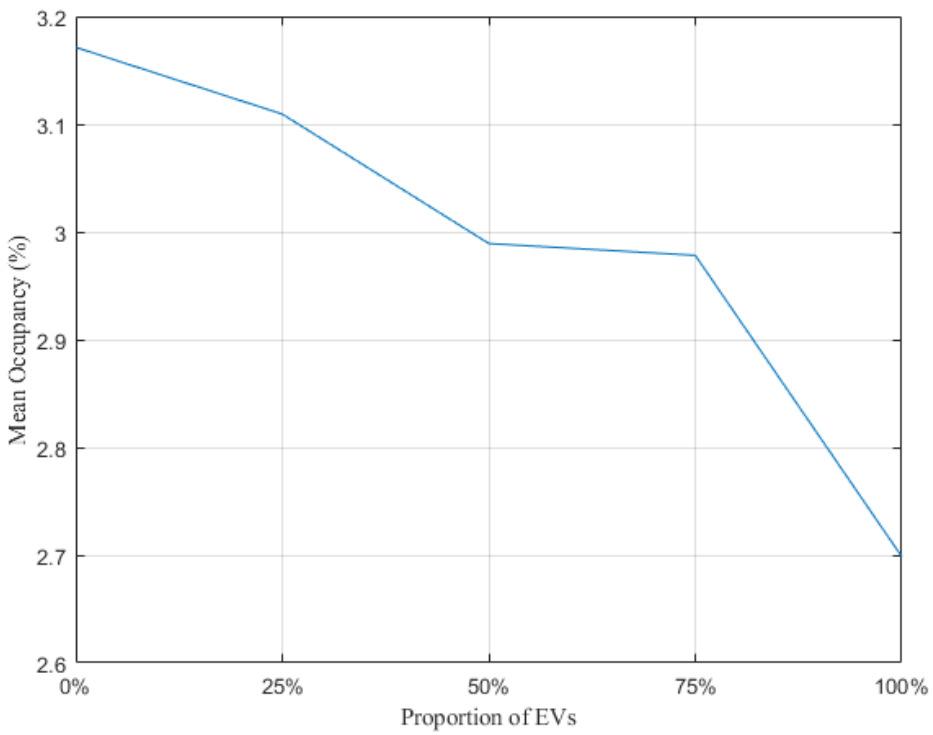

Figure 8.6 Mean occupancy at detectors in each simulation

When the proportion of the EVs increased from 0 to 100%, the mean speed of all the vehicles detected during simulation increased by 4.87 km/h, i.e., increased by 19.43% relatively. Meanwhile, the road occupancy decreased by 0.47%.

Based on the traffic data collected by the eight groups of vehicle detectors, the mean speed of all the vehicles detected during simulation and mean occupancy at the detectors were calculated. From the results, it can be confirmed that electric vehicles relying on their dynamic characteristics can improve the traffic efficiency to a certain degree. When drivers keep their driving styles, with electric vehicles they can drive with higher mean speed in some driving conditions.

Both, the increase of the vehicles' mean speed and the decline of road occupancy, indicate the increase of the traffic efficiency. With higher traffic efficiency, a road network can accommodate more traffic and traffic congestions will also appear less frequently.

9 Fuel/Energy Consumption of the Vehicles in Simulation

This Chapter uses traffic flow simulation to determine the energy savings potential that would result from replacing ICEVs with EVs in the city area under study. First of all, the energy consumption model is presented, followed by a simulation of the consumption and the influence of the traffic situation on the fuel and energy consumption is discussed.

9.1 Fuel/Energy Consumption Modeling

In this thesis a backward method similar to (Tewiele et al. 2017) was used to analyze the fuel/energy consumption of vehicles in the simulation. Thereby only the longitudinal movement of the vehicle is considered.

9.1.1 Fuel Consumption Calculation for ICEVs

In the case of an ICEV, the chemical energy of the fuel is first converted into mechanical energy in the combustion engine. The mechanical energy is then transferred to the driven wheels by means of the clutch, transmission and differential. The energy available at the wheels serves on the one hand to overcome the driving resistances in order to accelerate the vehicle or to maintain a speed once reached. According to conservation of energy, the energy at wheels $W_{at\ wheel}$ equals the work of driving resistance $W_{resistance}$, which also accounts for the energy required to accelerate the vehicle. The converted energy can be determined by a time integration from the converted power:

$$\int P_{at\ wheel}(t)\ dt = \int P_{resistance}(t)\ dt, \tag{9.1}$$

where $P_{at\ wheel}(t)$ is the function of driving power at the wheels, $P_{resistance}(t)$ is the function of power of driving resistance. As in time-discrete simulation, the differential time dt can be expressed by the time step T, Equation (9.1) can then be converted to

$$\sum_{i=1}^{n} P_{at\ wheel}(i) \cdot T = \sum_{i=1}^{n} P_{resistance}(i) \cdot T, \tag{9.2}$$

where i is the simulation step index, n is the total number of steps.

The wheel driving power of an ICEV is provided by the internal combustion engine. Based on the efficiency of each component in powertrain, the output power of the engine P_{engine} can be backwards calculated from $P_{at\ wheel}$:

$$P_{engine}(i) = \frac{P_{at\ wheel}(i) \cdot T}{\eta_{powertrain}}, \tag{9.3}$$

where $\eta_{powertrain}$ is the transmission efficiency of the powertrain.

Then the chemical energy of consumed fuel during step i can be calculated as

$$E_{fuel}(i) = \frac{P_{engine}(i) \cdot T}{\eta_{engine}(i)}, \tag{9.4}$$

where E_{fuel} is chemical energy of consumed fuel, η_{engine} is the efficiency of engine. The volume of consumed fuel V_{fuel} can then be calculated with fuel calorific value q_{fuel} and density ρ_{fuel}.

$$V_{fuel}(i) = \frac{E_{fuel}(i)}{q_{fuel} \cdot \rho_{fuel}}. \tag{9.5}$$

In summary, the volume of consumed fuel in each simulation step can be expressed as

$$V_{fuel}(i) = \frac{P_{resistance}(i) \cdot T}{q_{fuel} \cdot \rho_{fuel} \cdot \eta_{powertrain} \cdot \eta_{engine}(i)}. \tag{9.6}$$

$P_{resistance}$ is determined by the driving resistance and vehicle speed, i.e.

$$P_{resistance}(i) = \left(F_f + F_{grav} + F_w + F_{acc}\right) v(i). \tag{9.7}$$

As V_{fuel} cannot be negative, when $P_{resistance}$ is positive, V_{fuel} is calculated and accumulated. Additionally, an internal combustion engine always needs fuel for maintaining the minimal stable rotate speed.

In traffic congestions, the internal combustion engine operates in idling mode and consumes fuel. The idling fuel consumption can greatly influence the average fuel consumption of the vehicle in real driving conditions. Therefore, a parameter V_{idling} was used here in the fuel consumption model, which describes the volume of consumed fuel in time T when engine is idling. Thus, Equation (9.6) needs to be updated.

$$V_{fuel}(i) = \begin{cases} \dfrac{\left(F_f + F_{grav} + F_w + F_{acc}\right) \cdot v(i) \cdot T}{q_{fuel} \cdot \rho_{fuel} \cdot \eta_{powertrain} \cdot \eta_{engine}(i)}, & P_{resistance}(i) > 0 \\ V_{idling} & , v(i) = 0. \end{cases} \tag{9.8}$$

The average fuel consumption of vehicle in the whole trip V_{100km} is

$$V_{100km} = \frac{\sum_{i=1}^{n} V_{fuel}(i)}{s/1000} \times 100, \tag{9.9}$$

In Equation (9.8), fuel calorific value, fuel density, and powertrain efficiency can all be seen as constant values. The efficiency of an engine varies with the operating point. The engine efficiency map of the 95-kW engine in ADVISOR was used here, shown as in Figure 9.1. The speed and acceleration of vehicle along with gear number determine the operation point of the engine.

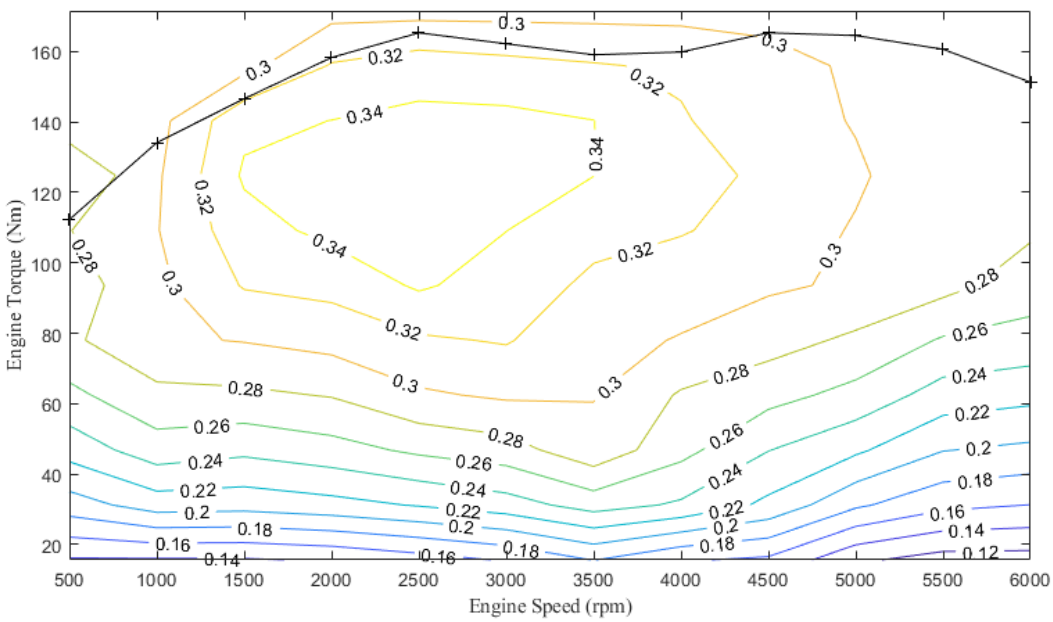

Figure 9.1 Efficiency of a 95-kW internal combustion engine in ADVISOR (Reilly et al. 1991)

Thus, with the speed profiles of vehicle in simulation, the average fuel consumption of each vehicle can be calculated with this efficiency-based model.

9.1.2 Energy Consumption Calculation for EVs

Energy consumption of EVs was calculated in this thesis using a similar method as for the ICEV. The calculation of energy consumption of EVs is however a bit more complicated because of regenerative brake. For ICEVs, only the simulation steps that $P_{resistance}$ is positive were minded. The energy consumption of this situation is firstly introduced.

When $P_{resistance} > 0$, the energy consumption from the battery is

$$W_{output}(\mathrm{i}) = \frac{P_{resistance}(i) \cdot T}{\eta_{discharge} \cdot \eta_{powertrain} \cdot \eta_{motor}}, \tag{9.10}$$

where W_{output} is battery output energy, $\eta_{discharge}$ is the discharging efficiency of battery, η_{motor} is the energy conversion efficiency of electric motor. As the efficiency of electric motor varies with operating point not quite much as internal combustion engine, η_{motor} was used here as constant value.

When $P_{resistance} < 0$, the electric motor can regenerate electric energy from braking energy and charge the battery. The energy fed back into the battery is

$$W_{recycle}(\mathrm{i}) = \frac{P_{resistance}(i) \cdot T}{\eta_{recycle} \cdot \eta_{powertrain} \cdot \eta_{motor}}, \tag{9.11}$$

where $\eta_{recycle}$ is the charging efficiency of the battery delivered from regenerative brake. When $W_{recycle} > 0$, obviously $W_{output} = 0$, and vice versa.

Then, the total energy consumption of single vehicle during a complete trip is

$$E_{total} = 3.6 \times 10^6 \times \sum_{i=1}^{n} \left(W_{output}(\mathrm{i}) - W_{recycle}(\mathrm{i}) \right). \tag{9.12}$$

There is not a general guideline for the calculation method of energy consumption per 100km for EVs. Manufactures prefer to calculate average energy consumption with the energy, which has been charged and stored in batteries. Thus, the energy consumption per 100km of their products looks more pretty. In the tests of some

institutes and organizations, the energy loss during charging is also considered, e.g. ADAC EcoTest (ADAC). As consumers indeed need to pay for the lost electric energy by charging, the charging energy loss was also considered the calculation of energy consumption in following parts. The average energy consumption is

$$E_{100km} = \frac{E_{total}}{\eta_{charge}\, s/1000} \times 100, \tag{9.13}$$

where η_{charge} is the battery charging efficiency when charging from electric grid.

9.1.3 Validation of Consumption Models

Driving cycle tests are the most widely used methods for estimating the fuel consumption of vehicles. Similarly, driving cycles can also be used in simulation for calibrating and validating the previously proposed consumption models.

In this study, the NEDC and the WLTP were both simulated. Since the NEDC has been widely used in Europe for accessing fuel economy of passenger cars for years, the fuel consumption of many vehicles in NEDC-test is easy to find. As the successor of NEDC, the WLTP has also been used for estimating the fuel economy of the vehicles in recent years. NEDC and WLTP are both speed profiles and can be directly used as the input of fuel and energy consumption models.

As lack of necessary parameters, passenger cars were not further classified in fuel and energy consumption modeling. All ICEVs used a fuel consumption model based on VW Golf VII 1.2 TSI, while EVs used a fuel consumption model based on BMW i3 60Ah version.

According to the description in the ADVISOR M-file, the 95-kW spark-ignition engine model was based on (Reilly et al. 1991). With the development of related technologies, the efficiency of the internal combustion engine has been improved in these years. Therefore, the efficiency model of the engine was calibrated based on the NEDC and WLTP simulation results. Figure 9.2 shows the calibrated efficiency model of the internal combustion engine.

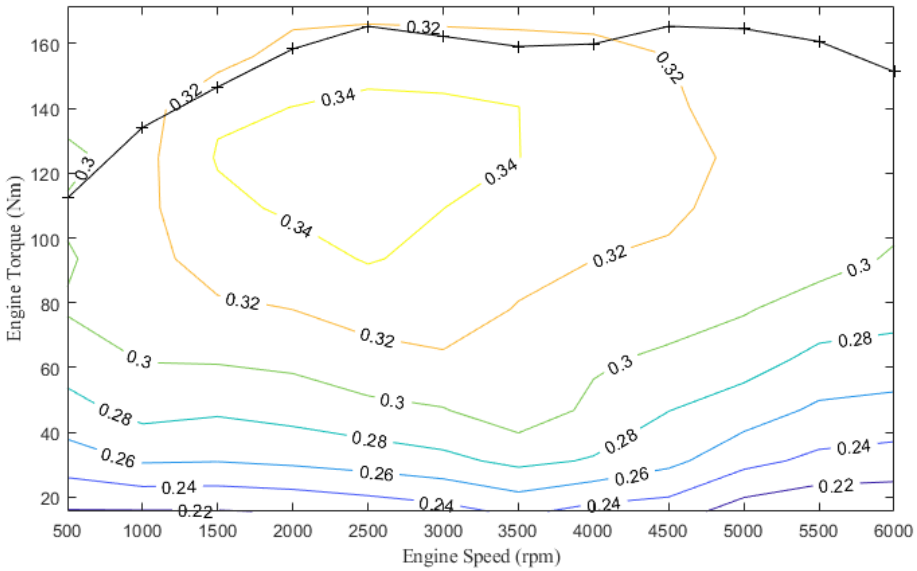

Figure 9.2 Modified efficiency of the internal combustion engine

According to the experiment results from Argonne National Laboratory, the idle fuel consumption of a gasoline compact sedan with a 2.0 L engine is 0.16 Gal/hour, i.e. about 0.61 l/hour, with no load (Energy.gov 2015). The idle fuel consumption of an engine is however related to the engine displacement, number of cylinders, warm idle or cold idle, environment temperature and many other conditions. After calibrating with the NEDC and WLTP simulation results, a 0.5 l/hour of idle fuel consumption was used in this study.

Figure 9.3 shows the comparison of simulated fuel and energy consumption with public data of corresponding real vehicles. The fuel consumption of ICEV from manufacturer is the official fuel consumption of a VW Golf VII 1.2 TSI based on the NEDC. Energy consumption of EV from manufacturer is the official energy consumption of a BMW i3 based on the NEDC, charging loss not considered here. In ADAC EcoTest and simulated WLTP-test, charging loss was taken into consideration. After calibrating the key parameters in consumption models, the proposed models can provide fuel and energy consumption results similar with corresponding real tests.

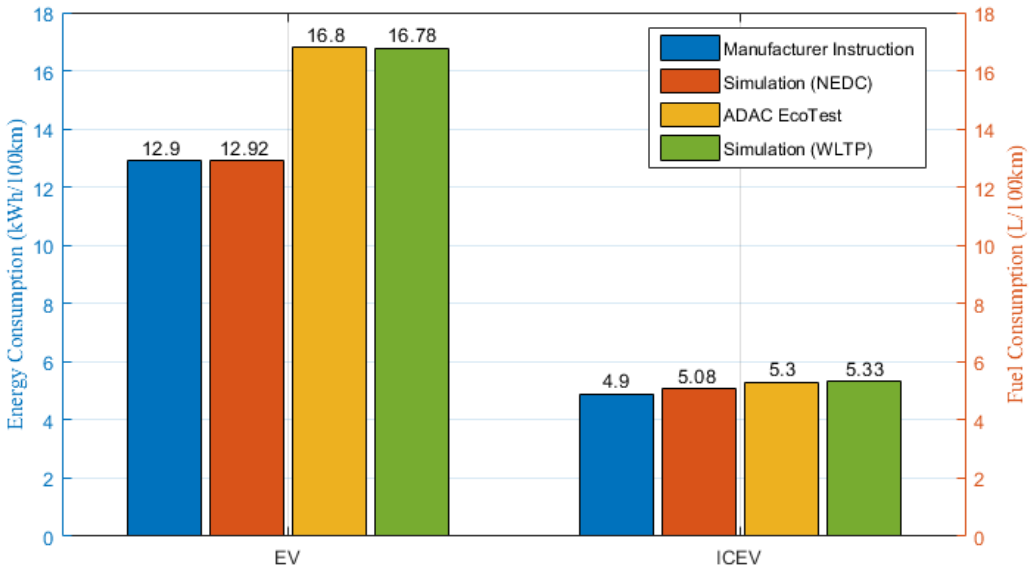

Figure 9.3 Fuel/energy consumption of real and simulated NEDC-/WLTP-tests

9.2 Fuel/Energy Consumption of Scenario Duisburg

Using the proposed fuel consumption model of ICEV and energy consumption model of EV, the 24-hour average fuel/energy consumption of vehicles in Duisburg inner ring scenario was calculated. Since SUMO can calculate the fuel consumption of the ICEVs based on HBEFA during simulation, the average fuel consumption calculated by SUMO was also taken into the comparison. The results are shown in Table 9.1. For better comparing, the fuel consumption has been also converted into energy consumption.

Table 9.1 Average fuel/energy consumption of vehicles in 24-hour Duisburg inner ring scenario

Vehicle Type	Calculation Method	Fuel Consumption	Energy Consumption
EV	Backward Energy Calculation	-	15.07 kWh/100km
ICEV	Backward Energy Calculation	7.52 l/100km	67.60 kWh/100km
	SUMO Output (HBEFA)	31.96 l/100km	287.26 kWh/100km

From Table 9.1 it can be noticed that the average fuel consumption of ICEV using the fuel calculating method in Section 9.1 is higher than the fuel consumption in

NEDC and WLTP. As the traffic scenario is based on the center of the City of Duisburg, which is a typical urban road network, the vehicles usually drive at low speeds and stop&go conditions. In these conditions, the internal combustion engine operates always in the lower efficiency areas. As a result, average fuel consumption in this situation is higher than in NEDC and WLTP, which include both urban and extra-urban traffic situations, while electric motors are similarly efficient at both high and low speeds. Since the vehicle consumes more energy to overcome air resistance at higher speeds, the average energy consumption of an EV in urban traffic can be lower than in interurban traffic. Therefore, the average energy consumption of EVs in this scenario is slightly lower than in WLTP traffic. Since the energy loss during recharging was taken into account when calculating the energy consumption, the average energy consumption is higher than the NEDC result.

It can also be seen that the average fuel consumption outputted from SUMO was absurdly high. HBEFA provides the comprehensive fuel consumption factor of vehicles, which includes both urban traffic situations and road traffic situations. When HBEFA is used to estimate the fuel consumption of a specific scenario, e.g., the urban network in this study, the results may differ significantly from reality. Although the fuel/energy calculation method introduced in Section 9.1 is more complicated, it considers the detailed driving situation of the vehicle and can provide more reliable results in various of traffic scenarios.

9.3 Effect of Traffic Situation on Fuel/Energy Consumption

In the efficiency system of an ICEV, the internal combustion engine is the most important part and decisively determines the overall efficiency of the energy conversion of a vehicle. The efficiency of the internal combustion engine can vary between 15% and 35% according to the operating point. The operating points of an engine are however limited by the driving condition, e.g., speed limits of the road and the traffic situation. Therefore, the traffic situation is also one of the factors which determines the fuel consumption of vehicle. This is also the reason why the development of a suitable driving cycle is important for estimating the fuel consumption of vehicles. With the popularity and steady increase of private cars, traffic congestion has become a major problem for urban life. Poorer traffic flow conditions

could reduce the overall efficiency of vehicles, which will lead to an increase in vehicle emissions and fuel consumption.

Because energy can flow bidirectionally in an electric powertrain, EVs can convert a significant part of kinetic energy of the vehicle back into electrical energy when braking. The efficiency of electric motors even at lower speeds is still higher than internal combustion engines. These characteristics might make EVs less affected by traffic situation. Therefore, the change of fuel consumption in different traffic situations was observed in simulation and the different effects of traffic situation on ICEVs and EVs were compared.

9.3.1 Test Scenario

For this test, several traffic simulation scenes were generated. The road network was still the area of Duisburg inner ring. For this test, traffic demand between 4:00 p.m. and 6:00 p.m. was taken from the 24-hour traffic demand. As shown in Figure 7.4 , the traffic in this time interval is at the peak of day.

For comparison purposes, the traffic density was increased by 125%, 150%, 175% and 200%, respectively, in the 2-hour time frame considered. This also means that, with appropriate simulation, the traffic density would be correspondingly higher. The numbers of simulated vehicles in the five simulations are shown in Figure 9.4.

At each traffic demand level, the scenario was simulated with the ICEV model and the EV model, respectively. Figure 9.5 shows the average speed of all vehicles in the corresponding simulation. When the traffic demand was enlarged to 150%, the traffic has reached a critical point of the road network capacity. Extremely severe traffic congestions occurred in the simulation and the average speed dropped dramatically. For the same traffic demand level, the average speed of EVs was always higher than ICEVs, which is consistent with the conclusion in Chapter 8.

9.3 Effect of Traffic Situation on Fuel/Energy Consumption

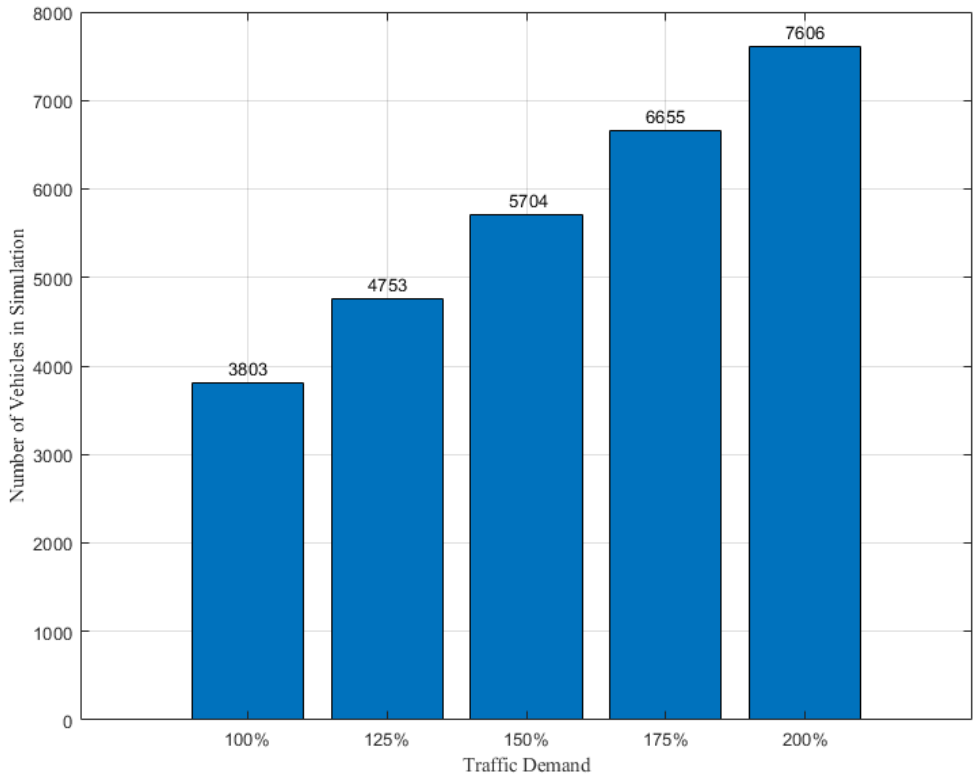

Figure 9.4 Total number of vehicles in the corresponding simulation

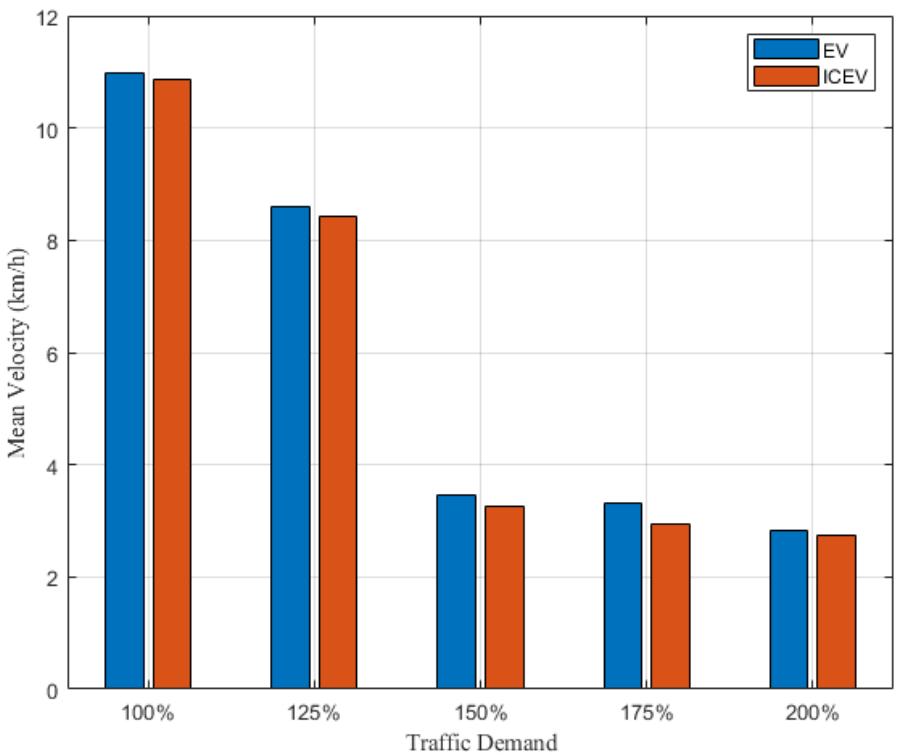

Figure 9.5 Mean speed of all vehicles in the corresponding simulation

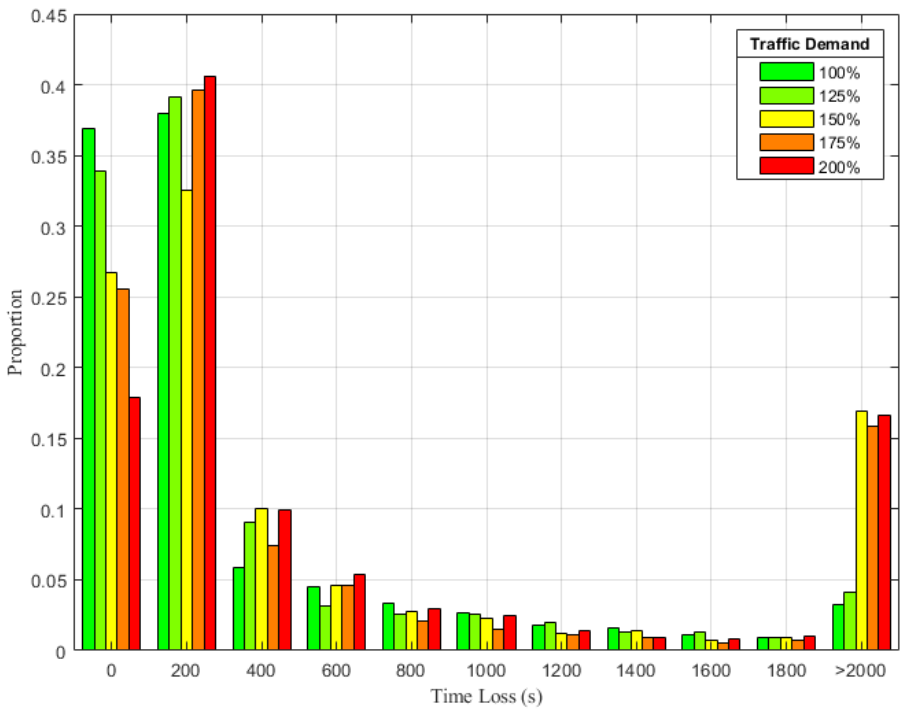

Figure 9.6 Time loss level in corresponding simulation

Time loss is one of the outputs of SUMO, which indicates the time lost by each vehicle on the entire trip due to driving below the ideal speed. Time loss also reflects the traffic situation. Figure 9.6 shows the time loss of EVs in different traffic situations. With the increase of traffic demand, the proportion of vehicles with higher time loss increased. The time loss of ICEVs was almost the same as with EVs and showed the same trend. From Figure 9.5 and Figure 9.6 it can be seen that, with the increase of traffic demand, the traffic situation and driving condition of vehicles were obviously affected and changed.

9.3.2 Test Results and Discussion

The fuel consumption and the equivalent energy consumption of ICEVs and average energy consumption of EVs in each simulation are listed in Table 9.2. With the increase of traffic density, the fuel consumption of ICEV increased dramatically. In traffic congestion, vehicles have to frequently stop and go. At this time, the internal combustion engine always operates in state of low speed and high torque, i.e., in state of low efficiency. On the other hand, the idling fuel consumption was also considered in fuel consumption modeling. Waiting in line will also raise the fuel

consumption. When traffic congestion occurs, the total fuel consumption for accomplishing the same trip will hence increase. These two reasons led to the high average fuel consumption of ICEVs with higher traffic volumes.

Table 9.2 Fuel/energy consumption of the ICEVs and the EVs

Traffic Demand	Vehicle Type	Fuel Consumption	Energy Consumption
100%	EV	-	14.55 kWh/100km
	ICEV	7.01 l/100km	63.01 kWh/100km
125%	EV	-	14.52 kWh/100km
	ICEV	7.32 l/100km	65.79 kWh/100km
150%	EV	-	14.24 kWh/100km
	ICEV	12.11 l/100km	108.85 kWh/100km
175%	EV	-	14.30 kWh/100km
	ICEV	12.47 l/100km	112.08 kWh/100km
200%	EV	-	14.33 kWh/100km
	ICEV	12.63 l/100km	113.52 kWh/100km

The average energy consumption of the EVs was basically the same in simulations with different traffic demand. With the increase of traffic demand, the average energy consumption showed however a slightly downward trend. The reason is that with the decrease of average speed, vehicles consumed less energy against wind drag. Thus, the average energy consumption of the EVs in the simulations with 150% and higher traffic demand was slightly slower than that of the EVs in the simulations with 100% and 125% traffic demand.

As in the energy consumption model of EV a constant motor efficiency was used in this thesis, the average energy consumption of EV could deviate from real vehicles. The efficiency of the electric motor is generally lower when the vehicle starts from standstill. Therefore, the energy consumption of EVs should be higher or remain the same when driving in traffic congestions. On the other hand, no auxiliary loads were considered in the simulations. In particular in the case of electric vehicles, the use of auxiliary devices, e.g. air conditioner, heater, radio, etc., has a decisive

influence on the energy consumption and range (Hesse et al. 2012; Tewiele 2020). If the use of radio, air conditioner, etc. were taken into consideration, the average energy consumption of EVs in heavy traffic will definitely increase, however not so dramatical as fuel consumption of ICEVs.

10 Conclusion and Outlook

10.1 Conclusion

This thesis focuses on the effect of electrification of vehicles on the traffic flow, as well as on the vehicles' fuel and energy consumption.

The development status and related research about traffic flow modeling and simulation, electric vehicle, driver, and vehicle modeling have been reviewed. Based on this, SUMO was chosen as the platform of this study. Because the main difference between ICEVs and EVs is the longitudinal dynamics, the car-following behavior modeling is the focal point of this thesis. As typical car-following methods are not applicable here, a modeling method that driver and vehicle were separately modeled was used in this thesis.

A combination of the Krauß model and a fuzzy model, which is based on the data from human drivers, has been used as the driver part of the car-following model in this thesis.

The models of electric cars in three sizes and ICEVs in three sizes were then built. The vehicle models were based on the parameters of models in ADVISOR. The driver model was respectively calibrated with corresponding vehicle models. Then, each vehicle model with the corresponding driver model constituted a car-following model. The driver model was respectively calibrated with the established vehicle models.

A SUMO traffic scenario of Duisburg inner ring was used for implementing the simulations with the proposed car-following model. Eight points in the scenario were selected for calibrating the traffic flow and for further studies. After calibration about the traffic demand and road network with real traffic data, the traffic at the eight verification points have been basically reproduced in the simulation.

Then, a co-simulation program of SUMO and MATLAB was developed. The proposed car-following model was programmed in MATLAB and controlled the movement of vehicles in SUMO. The generated traffic scenario was firstly used for validating the ICEV models. At the 8 validation points, about the number of the

vehicles detected during simulation proposed model got an almost same result with SUMO default model. The mean speed of the traffic flow was also acceptable.

Finally, the 24-hour traffic scenario was simulated for five different shares of electric vehicles. In this approach, the share of electric vehicles was gradually increased by 25% in each case. The simulation results showed that, with the unchanged driving style, increasing the proportion of electric vehicles from 0 to 100% increased the average speed of the traffic flow by 4.87 km/h. With the increase of EV share, the occupancy of the road also decreased slightly. The higher torque output of electric motors at lower speeds and the elimination of transmission influence for EVs are likely the reasons.

In addition, the fuel and energy consumption in simulation was calculated with the proposed method. The fuel consumption of ICEV and energy consumption of EV in different traffic situation was compared. The simulation results indicated that with the increase of traffic density, the average fuel consumption of ICEV dramatically increased. The energy consumption of EV was however less affected by traffic situation.

10.2 Scientific Contribution of the Thesis

In this thesis, the impact of electrified vehicle propulsion systems on traffic flow and energy consumption in a typical urban traffic environment was to be predicted using an exploratory study. For this purpose, in contrast to known studies, it was necessary to model the driver model and the vehicle model separately. In this way, the vehicle part can be more precisely modeled and has more realistic physical characteristics. The vehicle modeling was mainly based on the characteristic parameters of real vehicles. This enables the acquisition of input data also for the simulation of vehicles whose real behavior cannot be identified with the currently available traffic monitoring equipment. This applies, for example, to the EVs considered in this work.

To the author's knowledge, the change in traffic flow due to the replacement of ICEVs with EVs has not been studied before.

Similarly, there are no known studies on the energy saving potential of EVs specifically due to a change in traffic flow caused by their special driving characteristics,

while there are already many studies on the saving potential by EVs with the same driving behavior.

10.3 Limitations and Outlook

There were however still some deficiencies in the modeling and simulations. Firstly, in the vehicle models it was not possible to use actual parameters and component models. Hence, they might have different dynamic performance with the current vehicles. Secondly, the driver model can only react to the leading vehicle, but not to the factors of driving environment. Therefore, if the speed limit of some roads was not additionally adjusted, the mean speed of the vehicular flow greatly deviated from real data.

Nevertheless, this thesis still proposed a traffic flow modeling method, which has met the requirements of this study. The proposed car-following model can distinguish different vehicle types in simulation, while the distinguishing is not based on the traffic observation data of corresponding vehicle types. Comparing with typical car-following models, this modeling method is more suitable for modeling and distinguishing the vehicle types which are difficult to be observed in real traffic flows. Just like in this study, due to various factors it is not possible to get enough traffic data of electric vehicles. Using the proposed modeling method, the models of electric vehicles were established. Their dynamic characteristics were also obviously distinct from the ICEVs. Similarly, this modeling method was also used for predicting the effect of self-driving vehicles on traffic flow.

In future work, the vehicle models should be firstly improved. A more complete vehicle model could be implemented. Component models like wheel and tire, gear shifting process, steering system should be added. Thus, the vehicle model can be closer to real vehicles in kinematics and kinetics. Then, the steering behavior can be added into driver model. Not only steering and lane-changing behaviors, but also lane-keeping behavior of human driver can be simulated with this model.

11 Publication Bibliography

Acosta, Andrés F.; Espinosa, Jorge E.; Espinosa, Jairo (2015): TraCI4Matlab: enabling the integration of the SUMO road traffic simulator and Matlab® Through a Software Re-engineering Process. In : Modeling Mobility with Open Data: Springer, Cham, pp. 155–170.

ADAC: Stromverbrauch Elektroautos & Reichweiten im Vergleich | ADAC. Available online at https://www.adac.de/rund-ums-fahrzeug/tests/elektromobilitaet/stromverbrauch-elektroautos-adac-test/, checked on 11/7/2020.

Barceló, Jaume (2010): Fundamentals of Traffic Simulation: Springer.

Behrisch, Michael; Erdmann, Jakob (2018): Route estimation based on network flow maximization. In *EPiC Series in Engineering* 2.

Bieker-Walz, Laura; Behrisch, Michael; Junghans, Marek (2018): Analysis of the traffic behavior of emergency vehicles in a microscopic traffic simulation. In *EPiC Series in Engineering* 2, pp. 1–13.

Brackstone, Mark; McDonald, Mike (1999): Car-following: a historical review. In *Transportation Research Part F: Traffic Psychology and Behaviour* 2 (4), pp. 181–196.

Burch, Isabella; Gilchrist, Jock (2018): Survey of global activity to phase out internal combustion engine vehicles. In *Center of Climate Protection: Santa Rosa, CA, USA*.

Burghout, Wilco (2004): Hybrid microscopic-mesoscopic traffic simulation. Dissertation. KTH Royal Institute of Technology.

Chen, Chen; Zhao, Xiaohua; Liu, Hao; Ren, Guichao; Zhang, Yunlong; Liu, Xiaoming (2019): Assessing the influence of adverse weather on traffic flow characteristics using a driving simulator and VISSIM. In *Sustainability* 11 (3), p. 830.

Chowdhury, Debashish; Santen, Ludger; Schadschneider, Andreas (2000): Statistical physics of vehicular traffic and some related systems. In *Physics Reports* 329 (4-6), pp. 199–329.

11 Publication Bibliography

Clark, M. A. (1986): Induction loop vehicle detector. U.S. Patent no. 4,568,937.

Codeca, Lara; Frank, Raphaël; Engel, Thomas (2015): LuST: a 24-hour Scenario of Luxembourg City for SUMO Traffic simulations. In : SUMO 2015–Intermodal Simulation for Intermodal Transport.

Codecá, Lara; Frank, Raphaël; Faye, Sébastien; Engel, Thomas (2017): Luxembourg sumo traffic (LuST) scenario: traffic demand evaluation. In *IEEE Intelligent Transportation Systems Magazine* 9 (2), pp. 52–63.

Cottignies, A.; Daley, M.; Newton, E.; Parker, H. (2017): rFpro & SUMO: the road to a complete real-time simulation of urban environments for DIL, ADAS and autonomous testing. In : SUMO 2017–Towards Simulation for Autonomous Mobility, vol. 31.

Dyno-ChiptuningFiles.com: Audi A6 3.0 TFSI Dyno Tested! | Dyno-ChiptuningFiles.com. Available online at https://www.dyno-chiptuningfiles.com/tuning-projects/audi-a6-30-tfsi-dyno-tested/, checked on 12/4/2020.

Ehlert, Anett; Schneck, Arne; Chanchareon, Nate (2017): Junction parameter calibration for mesoscopic simulation in Vissim. In *Transportation Research Procedia* 21, pp. 216–226.

Energy.gov (2015): Fact #861 February 23, 2015 Idle Fuel Consumption for Selected Gasoline and Diesel Vehicles. Available online at https://www.energy.gov/eere/vehicles/fact-861-february-23-2015-idle-fuel-consumption-selected-gasoline-and-diesel-vehicles, checked on 12/1/2020.

Esteves-Booth, A.; Muneer, T.; Kubie, J.; Kirby, H. (2002): A review of vehicular emission models and driving cycles. In *Proceedings of the Institution of Mechanical Engineers, Part C: Journal of Mechanical Engineering Science* 216 (8), pp. 777–797.

Gipps, Peter G. (1981): A behavioural car-following model for computer simulation. In *Transportation Research Part B: Methodological* 15 (2), pp. 105–111.

Greenshields, B. D.; Bibbins, J. R.; Channing, W. S.; Miller, H. H. (1935): A study of traffic capacity. In : Highway Research Board Proceedings: National Research Council (USA), Highway Research Board (Vol. 1935).

11 Publication Bibliography

Hájek, Petr (2013): Metamathematics of Fuzzy Logic: Springer Science & Business Media.

Haken, Karl-Ludwig (2015): Grundlagen der Kraftfahrzeugtechnik: Carl Hanser Verlag GmbH Co KG.

Haklay, Mordechai; Weber, Patrick (2008): Openstreetmap: user-generated street maps. In *IEEE Pervasive Computing* 7 (4), pp. 12–18.

hbefa.net: HBEFA - Handbook Emission Factors for Road Transport. Available online at https://www.hbefa.net/e/index.html, checked on 11/5/2020.

Hesse, Benjamin; Hiesgen, Gregor; Koppers, Martin; Schramm, Dieter (2012): Einfluss verschiedener Nebenverbraucher auf Elektrofahrzeuge. In : Zukünftige Entwicklungen in der Mobilität: Springer, pp. 91–104.

Hu, Xiaowei; Ma, Xiaoyi; Schramm, Dieter (2020): Study on the fuel consumptions using traffic simulation with example of City Duisburg. In : Joint International Conference of the International Conference on Mechanisms and Mechanical Transmissions and the International Conference on Robotics: Springer, Cham, pp. 488–495.

Hu, Xiaowei; Ma, Xiaoyi; Schramm, Dieter (2021): Simulation with car-following model considering vehicle dynamic features. In *International Journal of Advanced Mechatronic Systems*, accepted, in production.

Ivanov, Valentin (2015): A review of fuzzy methods in automotive engineering applications. In *European Transport Research Review* 7 (3), pp. 1–10.

Karle, Anton (2020): Elektromobilität: Grundlagen und Praxis: Carl Hanser Verlag GmbH Co KG.

Koppers, Martin (2019): Ein methodischer Ansatz zur nutzerspezifischen Bewertung von (teil-) elektrischen Fahrzeugkonzepten. Dissertation. Universität Duisburg-Essen, Duisburg.

Kraftfahrt-Bundesamt: Jahresbilanz des Fahrzeugbestandes am 1. Januar 2019. Available online at https://www.kba.de/DE/Statistik/Fahrzeuge/Bestand/b_jahresbilanz.html?nn=644526, checked on 8/12/2020.

11 Publication Bibliography

Krajzewicz, Daniel; Erdmann, Jakob; Behrisch, Michael; Bieker, Laura (2012): Recent development and applications of SUMO-Simulation of Urban MObility. In *International Journal on Advances in Systems and Measurements* 5 (3&4).

Krajzewicz, Daniel; Hertkorn, Georg; Wagner, Peter (2002): SUMO (Simulation of Urban MObility)-an open-source traffic simulation. In : Proceedings of the 4th middle East Symposium on Simulation and Modelling (MESM20002), pp. 183–187.

Kramer, U.; Rohr, G. (1982): A model of driver behaviour. In *Ergonomics* 25 (10), pp. 891–907.

Kramer, Ulrich (1985): On the application of fuzzy sets to the analysis of the system driver-vehicle-environment. In *Automatica* 21 (1), pp. 101–107.

Krauß, Stefan (1998): Microscopic modeling of traffic flow: Investigation of collision free vehicle dynamics. Dissertation. University of Cologne, Köln-Porz. Institute of Transport Research.

Krauß, Stefan; Wagner, Peter; Gawron, Christian (1997): Metastable states in a microscopic model of traffic flow. In *Physical Review E* 55 (5), p. 5597.

Leutzbach, Wilhelm (1988): Introduction to the Theory of Traffic Flow: Springer.

Lixin Situ (Ed.) (2009): Electric Vehicle Development: the Past, Present & Future. 2009 3rd International Conference on Power Electronics Systems and Applications (PESA): IEEE.

Lu, Zhengyang; Fu, Ting; Fu, Liping; Shiravi, Sajad; Jiang, Chaozhe (2016): A video-based approach to calibrating car-following parameters in VISSIM for urban traffic. In *International Journal of Transportation Science and Technology* 5 (1), pp. 1–9.

Ma, Xiaoyi; Hu, Xiaowei; Schweig, Stephan; Pragalathan, Jenitta; Schramm, Dieter (2021): A vehicle guidance model with a close-to-reality driver model and different levels of vehicle automation. In *Applied Sciences* 11, 380. Available online at https://doi.org/10.3390/app11010380.

Ma, Xiaoyi; Hu, Xiaowei; Weber, Thomas; Schramm, Dieter (2020): Traffic simulation of future intelligent vehicles in Duisburg City Inner Ring. In *Applied Sciences* 11 (1), p. 29.

11 Publication Bibliography

Markel, Tony; Brooker, Aaron; Hendricks, Terry; Johnson, Valerie; Kelly, Kenneth; Kramer, Bill et al. (2002): ADVISOR: a systems analysis tool for advanced vehicle modeling. In *Journal of Power Sources* 110 (2), pp. 255–266.

Matzer, C.; Weller, K.; Dippold, M.; Lipp, S.; Röck, M.; Rexeis, M.; Hausberger, S. (2019): Update of emission factors for HBEFA Version 4.1; final report. I-05/19/CM EM-I-16/26/679 from 09.09. 2019, TU Graz.

Miyajima, Chiyomi; Nishiwaki, Yoshihiro; Ozawa, Koji; Wakita, Toshihiro; Itou, Katsunobu; Takeda, Kazuya; Itakura, Fumitada (2007): Driver modeling based on driving behavior and its evaluation in driver identification. In *Proceedings of the IEEE* 95 (2), pp. 427–437.

Moser, Uwe; Harmening, Nick; Schramm, Dieter (2019): A new method for the objective assessment of ADAS based on multivariate time series classification. In : 19. Internationales Stuttgarter Symposium: Springer Vieweg, Wiesbaden, pp. 636–651.

Moser, Uwe Dominik (2020): Multivariate Time Series Clustering and Classification for Objective Assessment of Automated Driving Functions. Dissertation. Universität Duisburg-Essen, Duisburg.

Nagel, Kai; Schreckenberg, Michael (1992): A cellular automaton model for freeway traffic. In *Journal de Physique I* 2 (12), pp. 2221–2229.

Newell, Gordon Frank (2002): A simplified car-following theory: a lower order model. In *Transportation Research Part B: Methodological* 36 (3), pp. 195–205.

OpenStreetMap: OpenStreetMap. Available online at https://www.openstreetmap.org/, checked on 11/24/2020.

Panou, Maria; Bekiaris, Evangelos; Papakostopoulos, Vassilis (2007): Modelling driver behaviour in european union and international projects. In : Modelling Driver Behaviour in Automotive Environments: Springer, pp. 3–25.

Pentland, Alex; Liu, Andrew (1999): Modeling and prediction of human behavior. In *Neural Computation* 11 (1), pp. 229–242.

Ping, Peng; Sheng, Yuan; Qin, Wenhu; Miyajima, Chiyomi; Takeda, Kazuya (2018): Modeling driver risk perception on city roads using deep learning. In *IEEE Access* 6, pp. 68850–68866.

Pipes, Louis A. (1953): An operational analysis of traffic dynamics. In *Journal of Applied Physics* 24 (3), pp. 274–281.

PTV-Group (2020): PTV Vissim new. Available online at https://www.ptvgroup.com/en/solutions/products/ptv-vissim/, checked on 12/25/2020.

Ranney, Thomas A. (1999): Psychological factors that influence car-following and car-following model development. In *Transportation Research Part F: Traffic Psychology and Behaviour* 2 (4), pp. 213–219.

Rehder, Tobias (2020): Learning Lane Change Behavior to Enable Situation Awareness for Automated Driving on Highways. Dissertation. Universität Duisburg-Essen, Duisburg.

Rehder, Tobias; Muenst, Wolfgang; Louis, Lawrence; Schramm, Dieter (2016): Learning lane change intentions through lane contentedness estimation from demonstrated driving. In : IEEE 19th International Conference on Intelligent Transportation Systems (ITSC), pp. 893–898.

Reilly, Donald J.; Andersen, Richard P.; Casparian, Robert J.; Dugdale, Peter H. (1991): Saturn DOHC and SOHC four cylinder engines. In *SAE Transactions*, pp. 1104–1119.

Reuschel, Av (1950): Fahrzeugbewegungen in der Kolonne. In *Osterreichisches Ingenieur Archiv* 4, pp. 193–215.

Schramm, Dieter; Dudenhöffer, Ferdinand; Driesch, Patrick; Kannstätter, Timm (2017a): Plug-In-, Range-Extender-und Elektrofahrzeuge unter realen Mobilitätsumständen: Infrastruktur, Umweltbedingungen und Marktakzeptanz: FuE-Programm" Erneuerbar Mobil" des Bundesministeriums für Umwelt, Naturschutz, Bau und Reaktorsicherheit (BMUB): Schlussbericht: Laufzeit des Vorhabens: vom: 01.01. 2014 bis: 31.05. 2017: Universität Duisburg-Essen.

Schramm, Dieter; Hesse, Benjamin; Maas, Niko; Unterreiner, Michael (2017b): Fahrzeugtechnik: technische Grundlagen aktueller und zukünftiger Kraftfahrzeuge: Walter de Gruyter GmbH & Co KG.

11 Publication Bibliography

Schramm, Dieter; Hesse, Benjamin; Maas, Niko; Unterreiner, Michael (2020): Vehicle Technology: Technical foundations of current and future motor vehicles: Walter de Gruyter GmbH & Co KG.

Schramm, Dieter; Hiller, Manfred; Bardini, Roberto (2018): Modellbildung und Simulation der Dynamik von Kraftfahrzeugen: Springer.

Schramm, Dieter; Koppers, Martin (2013): Das Automobil im Jahr 2025: Vielfalt der Antriebstechnik: Springer-Verlag.

Schüller, Mira (2019): Technisch optimale Auslegung von Elektrofahrzeugen für Nutzergruppen in China und Deutschland: eine vergleichende Untersuchung. Dissertation. Universität Duisburg-Essen, Duisburg.

Schüller, Mira; Tewiele, S.; Schramm, D. (2016): Alternative Antriebe und Kraftstoffe für die nachhaltige Sicherung der Mobilität mit besonderem Fokus auf Ostasien. In : Nationale und internationale Trends in der Mobilität: Springer, pp. 179–200.

Taylor III, Alex; Kano, C.; Levinstein, J. (2006): The birth of the Prius. In *Fortune* 153 (4), pp. 65–72.

Tewiele, Sarah (2020): Generierung von repräsentativen Fahr-und Lastzyklen aus realen Fahrdaten batterieelektrischer Fahrzeuge. Dissertation. Universität Duisburg-Essen, Duisburg.

Tewiele, Sarah; Schüller, Mira; Koppers, Martin; Schramm, Dieter (2017): Driving pattern analysis of hybrid and electric vehicles in a German conurbation including a drive system evaluation. In *International Journal of Advanced Mechatronic Systems* 7 (3), pp. 158–164.

Tools/Detector - SUMO Documentation. Available online at https://sumo.dlr.de/docs/Tools/Detector.html, checked on 12/17/2020.

Treiber, Martin; Hennecke, Ansgar; Helbing, Dirk (2000): Congested traffic states in empirical observations and microscopic simulations. In *Physical Review E* 62 (2), p. 1805.

Treiber, Martin; Kesting, Arne (2013): Traffic Flow Dynamics: Data, Models and Simulation.

11 Publication Bibliography

UNECE: Worldwide harmonized Light vehicles Test Procedure (WLTP) - Transport - Vehicle Regulations - UNECE Wiki. Available online at https://wiki.unece.org/pages/viewpage.action?pageId=2523179, checked on 11/7/2020.

Wegener, A.; Piórkowski, M.; Raya, M.; Hellbrück, H.; Fischer, S.; Hubaux, J. P. (2008): TraCI: an interface for coupling road traffic and network simulators. In : Proceedings of the 11th Communications and Networking Simulation Symposium, pp. 155–163.

Wiedemann, Rainer (1974): Simulation des Strassenverkehrsflusses. In *Schriftenreihe des Instituts für Verkehrswesen der Universität Karlsruhe* 8.

Xu, Xiaodan; Liu, Haobing; Anderson, James M.; Xu, Yanzhi; Hunter, Michael P.; Rodgers, Michael O.; Guensler, Randall L. (2016): Estimating project-level vehicle emissions with Vissim and MOVES-matrix. In *Transportation Research Record* 2570 (1), pp. 107–117.

Yeo, Hwasoo; Skabardonis, Alexander; Halkias, John; Colyar, James; Alexiadis, Vassili (2008): Oversaturated freeway flow algorithm for use in next generation simulation. In *Transportation Research Record* 2088 (1), pp. 68–79.

DOI: 10.17185/duepublico/74086
URN: urn:nbn:de:hbz:464-20210318-121943-2